

NEUROSCIENCE

Third Edition

NEUROSCIENCE

THIRD EDITION

Edited by

DALE PURVES

GEORGE J. AUGUSTINE

DAVID FITZPATRICK

WILLIAM C. HALL

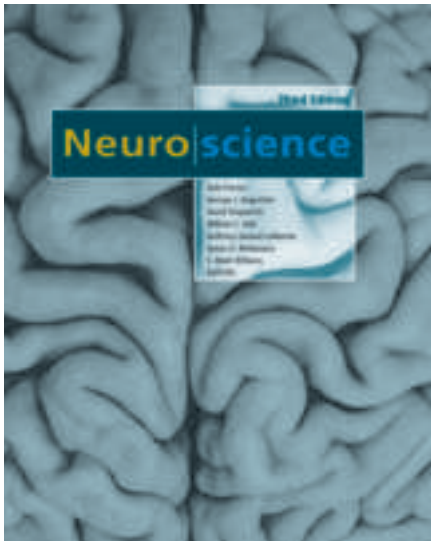
ANTHONY-SAMUEL LAMANTIA

JAMES O. McNAMARA

S. MARK WILLIAMS



Sinauer Associates, Inc. • Publishers
Sunderland, Massachusetts U.S.A.



THE COVER

Dorsal view of the human brain.
(Courtesy of S. Mark Williams.)

NEUROSCIENCE: Third Edition

Copyright © 2004 by Sinauer Associates, Inc. All rights reserved.
This book may not be reproduced in whole or in part without permission.

Address inquiries and orders to
Sinauer Associates, Inc.
23 Plumtree Road
Sunderland, MA 01375 U.S.A.

www.sinauer.com
FAX: 413-549-1118
orders@sinauer.com
publish@sinauer.com

Library of Congress Cataloging-in-Publication Data

Neuroscience / edited by Dale Purves ... [et al.].— 3rd ed.

p. ; cm.

Includes bibliographical references and index.

ISBN 0-87893-725-0 (casebound : alk. paper)

1. Neurosciences.

[DNLM: 1. Nervous System Physiology. 2. Neurochemistry.

WL 102 N50588 2004] I. Purves, Dale.

QP355.2.N487 2004

612.8—dc22

2004003973

Printed in U.S.A.

5 4 3 2 1

Contributors

George J. Augustine, Ph.D.
Dona M. Chikaraishi, Ph.D.
Michael D. Ehlers, M.D., Ph.D.
Gillian Einstein, Ph.D.
David Fitzpatrick, Ph.D.
William C. Hall, Ph.D.
Erich Jarvis, Ph.D.
Lawrence C. Katz, Ph.D.
Julie Kauer, Ph.D.
Anthony-Samuel LaMantia, Ph.D.
James O. McNamara, M.D.
Richard D. Mooney, Ph.D.
Miguel A. L. Nicolelis, M.D., Ph.D.
Dale Purves, M.D.
Peter H. Reinhart, Ph.D.
Sidney A. Simon, Ph.D.
J. H. Pate Skene, Ph.D.
James Voyvodic, Ph.D.
Leonard E. White, Ph.D.
S. Mark Williams, Ph.D.

UNIT EDITORS

UNIT I: George J. Augustine
UNIT II: David Fitzpatrick
UNIT III: William C. Hall
UNIT IV: Anthony-Samuel LaMantia
UNIT V: Dale Purves

Contents in Brief

1. Studying the Nervous Systems of Humans and Other Animals 1

UNIT I NEURAL SIGNALING

2. Electrical Signals of Nerve Cells 31
3. Voltage-Dependent Membrane Permeability 47
4. Channels and Transporters 69
5. Synaptic Transmission 93
6. Neurotransmitters, Receptors, and Their Effects 129
7. Molecular Signaling within Neurons 165

UNIT II SENSATION AND SENSORY PROCESSING

8. The Somatic Sensory System 189
9. Pain 209
10. Vision: The Eye 229
11. Central Visual Pathways 259
12. The Auditory System 283
13. The Vestibular System 315
14. The Chemical Senses 337

UNIT III MOVEMENT AND ITS CENTRAL CONTROL

15. Lower Motor Neuron Circuits and Motor Control 371
16. Upper Motor Neuron Control of the Brainstem and Spinal Cord 393
17. Modulation of Movement by the Basal Ganglia 417
18. Modulation of Movement by the Cerebellum 435
19. Eye Movements and Sensory Motor Integration 453
20. The Visceral Motor System 469

UNIT IV THE CHANGING BRAIN

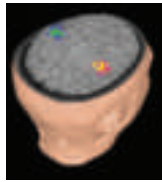
21. Early Brain Development 501
22. Construction of Neural Circuits 521
23. Modification of Brain Circuits as a Result of Experience 557
24. Plasticity of Mature Synapses and Circuits 575

UNIT V COMPLEX BRAIN FUNCTIONS

25. The Association Cortices 613
26. Language and Speech 637
27. Sleep and Wakefulness 659
28. Emotions 687
29. Sex, Sexuality, and the Brain 711
30. Memory 733

APPENDIX A THE BRAINSTEM AND CRANIAL NERVES 755

APPENDIX B VASCULAR SUPPLY, THE MENINGES, AND THE VENTRICULAR SYSTEM 763



Contents

Preface *xvi*

Acknowledgments *xvii*

Supplements to Accompany NEUROSCIENCE *xviii*

Chapter 1 Studying the Nervous Systems of Humans and Other Animals 1

Overview 1

Genetics, Genomics, and the Brain 1

The Cellular Components of the Nervous System 2

Neurons 4

Neuroglial Cells 8

Cellular Diversity in the Nervous System 9

Neural Circuits 11

Overall Organization of the Human Nervous System 14

Neuroanatomical Terminology 16

The Subdivisions of the Central Nervous System 18

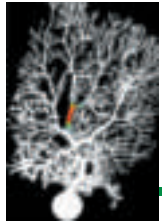
Organizational Principles of Neural Systems 20

Functional Analysis of Neural Systems 23

Analyzing Complex Behavior 24

Box A Brain Imaging Techniques 25

Summary 26



Unit I NEURAL SIGNALING

Chapter 2 Electrical Signals of Nerve Cells 31

Overview 31

Electrical Potentials across Nerve Cell Membranes 31

How Ionic Movements Produce Electrical Signals 34

The Forces That Create Membrane Potentials 36

Electrochemical Equilibrium in an Environment with More Than One Permeant Ion 38

The Ionic Basis of the Resting Membrane Potential 40

Box A The Remarkable Giant Nerve Cells of Squid 41

The Ionic Basis of Action Potentials 43

Box B Action Potential Form and Nomenclature 44

Summary 45

Chapter 3 Voltage-Dependent Membrane Permeability 47

Overview 47

Ionic Currents Across Nerve Cell Membranes 47

Box A The Voltage Clamp Method 48

Two Types of Voltage-Dependent Ionic Current 49

Two Voltage-Dependent Membrane Conductances 52

Reconstruction of the Action Potential 54

Long-Distance Signaling by Means of Action Potentials 56

Box B Threshold 57

Box C Passive Membrane Properties 60

The Refractory Period 61

Increased Conduction Velocity as a Result of Myelination 63

Summary 65

Box D Multiple Sclerosis 66

Chapter 4 Channels and Transporters 69

Overview	69	
Ion Channels Underlying Action Potentials		69
Box A The Patch Clamp Method		70
The Diversity of Ion Channels		73
Box B Expression of Ion Channels in <i>Xenopus</i> Oocytes		75
Voltage-Gated Ion Channels		76
Ligand-Gated Ion Channels		78
Stretch- and Heat-Activated Channels		78
The Molecular Structure of Ion Channels		79
Box C Toxins That Poison Ion Channels		82
Box D Diseases Caused by Altered Ion Channels		84
Active Transporters Create and Maintain Ion Gradients		86
Functional Properties of the Na^+/K^+ Pump		87
The Molecular Structure of the Na^+/K^+ Pump		89
Summary		90

Chapter 5 Synaptic Transmission 93

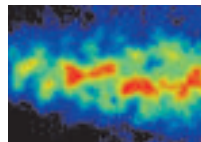
Overview	93	
Electrical Synapses		93
Signal Transmission at Chemical Synapses		96
Properties of Neurotransmitters		96
Box A Criteria That Define a Neurotransmitter		99
Quantal Release of Neurotransmitters		102
Release of Transmitters from Synaptic Vesicles		103
Local Recycling of Synaptic Vesicles		105
The Role of Calcium in Transmitter Secretion		107
Box B Diseases That Affect the Presynaptic Terminal		108
Molecular Mechanisms of Transmitter Secretion		110
Neurotransmitter Receptors		113
Box C Toxins That Affect Transmitter Release		115
Postsynaptic Membrane Permeability Changes during Synaptic Transmission		116
Excitatory and Inhibitory Postsynaptic Potentials		121
Summation of Synaptic Potentials		123
Two Families of Postsynaptic Receptors		124
Summary		126

Chapter 6 Neurotransmitters and Their Receptors 129

Overview	129	
Categories of Neurotransmitters		129
Acetylcholine		129
Box A Addiction		134
Box B Neurotoxins that Act on Postsynaptic Receptors		136
Glutamate		137
Box C Myasthenia Gravis: An Autoimmune Disease of Neuromuscular Synapses		140
GABA and Glycine		143
Box D Excitotoxicity Following Acute Brain Injury		145
The Biogenic Amines		147
Box E Biogenic Amine Neurotransmitters and Psychiatric Disorders		148
ATP and Other Purines		152
Peptide Neurotransmitters		153
Unconventional Neurotransmitters		157
Box F Marijuana and the Brain		160
Summary		161

Chapter 7 Molecular Signaling within Neurons 165

Overview	165	
Strategies of Molecular Signaling		165
The Activation of Signaling Pathways		167
Receptor Types		168
G-Proteins and Their Molecular Targets		170
Second Messengers		172
Second Messenger Targets: Protein Kinases and Phosphatases		175
Nuclear Signaling		178
Examples of Neuronal Signal Transduction		181
Summary		184



Unit II SENSATION AND SENSORY PROCESSING

Chapter 8 The Somatic Sensory System 189

- Overview 189
 Cutaneous and Subcutaneous Somatic Sensory Receptors 189
 Mechanoreceptors Specialized to Receive Tactile Information 192
 Differences in Mechanosensory Discrimination across the Body Surface 193
Box A Receptive Fields and Sensory Maps in the Cricket 195
Box B Dynamic Aspects of Somatic Sensory Receptive Fields 196
 Mechanoreceptors Specialized for Proprioception 197
 Active Tactile Exploration 199
 The Major Afferent Pathway for Mechanosensory Information: The Dorsal Column–Medial Lemniscus System 199
 The Trigeminal Portion of the Mechanosensory System 202
Box C Dermatomes 202
 The Somatic Sensory Components of the Thalamus 203
 The Somatic Sensory Cortex 203
 Higher-Order Cortical Representations 206
Box D Patterns of Organization within the Sensory Cortices: Brain Modules 207
 Summary 208

Chapter 9 Pain 209

- Overview 209
 Nociceptors 209
 Transduction of Nociceptive Signals 211
Box A Capsaicin 212
 Central Pain Pathways 213
Box B Referred Pain 215
Box C A Dorsal Column Pathway for Visceral Pain 218
 Sensitization 220
Box D Phantom Limbs and Phantom Pain 222
 Descending Control of Pain Perception 224
 The Placebo Effect 224
 The Physiological Basis of Pain Modulation 225
 Summary 227

Chapter 10 Vision: The Eye 229

- Overview 229
 Anatomy of the Eye 229
 The Formation of Images on the Retina 231
Box A Myopia and Other Refractive Errors 232
 The Retina 234
 Phototransduction 236
Box B Retinitis Pigmentosa 239
 Functional Specialization of the Rod and Cone Systems 240
Box C Macular Degeneration 243
 Anatomical Distribution of Rods and Cones 244
 Cones and Color Vision 245
Box D The Importance of Context in Color Perception 247
 Retinal Circuits for Detecting Luminance Change 249
Box E The Perception of Light Intensity 250
 Contribution of Retinal Circuits to Light Adaptation 254
 Summary 257

Chapter 11 Central Visual Pathways 259

- Overview 259
 Central Projections of Retinal Ganglion Cells 259
Box A The Blind Spot 262
 The Retinotopic Representation of the Visual Field 263
 Visual Field Deficits 267
 The Functional Organization of the Striate Cortex 269
 The Columnar Organization of the Striate Cortex 271
Box B Random Dot Stereograms and Related Amusements 272
 Division of Labor within the Primary Visual Pathway 275
Box C Optical Imaging of Functional Domains in the Visual Cortex 276
 The Functional Organization of Extrastriate Visual Areas 278
 Summary 281

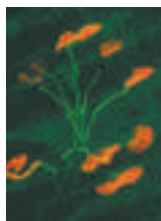
Chapter 12 The Auditory System 283

- Overview 283
 Sound 283
 The Audible Spectrum 284

A Synopsis of Auditory Function	285
Box A Four Causes of Acquired Hearing Loss	285
Box B Music	286
The External Ear	287
The Middle Ear	289
The Inner Ear	289
Box C Sensorineural Hearing Loss and Cochlear Implants	290
Box D The Sweet Sound of Distortion	295
Hair Cells and the Mechanoelectrical Transduction of Sound Waves	294
Two Kinds of Hair Cells in the Cochlea	300
Tuning and Timing in the Auditory Nerve	301
How Information from the Cochlea Reaches Targets in the Brainstem	303
Integrating Information from the Two Ears	303
Monaural Pathways from the Cochlear Nucleus to the Lateral Lemniscus	307
Integration in the Inferior Colliculus	307
The Auditory Thalamus	308
The Auditory Cortex	309
Box E Representing Complex Sounds in the Brains of Bats and Humans	310
Summary	313

Chapter 13 The Vestibular System 315

Overview	315
The Vestibular Labyrinth	315
Vestibular Hair Cells	316
The Otolith Organs: The Utricle and Saccule	317
Box A A Primer on Vestibular Navigation	318
Box B Adaptation and Tuning of Vestibular Hair Cells	320
How Otolith Neurons Sense Linear Forces	322
The Semicircular Canals	324



Unit III MOVEMENT AND ITS CENTRAL CONTROL

Chapter 15 Lower Motor Neuron Circuits and Motor Control 371

Overview	371
Neural Centers Responsible for Movement	371

How Semicircular Canal Neurons Sense Angular Accelerations	325
Box C Throwing Cold Water on the Vestibular System	326
Central Pathways for Stabilizing Gaze, Head, and Posture	328
Vestibular Pathways to the Thalamus and Cortex	331
Box D Mauthner Cells in Fish	332
Summary	333

Chapter 14 The Chemical Senses 337

Overview	337
The Organization of the Olfactory System	337
Olfactory Perception in Humans	339
Physiological and Behavioral Responses to Odorants	341
The Olfactory Epithelium and Olfactory Receptor Neurons	342

Box A Olfaction, Pheromones, and Behavior in the Hawk Moth 344

The Transduction of Olfactory Signals	345
Odorant Receptors	346
Olfactory Coding	348
The Olfactory Bulb	350

Box B Temporal "Coding" of Olfactory Information in Insects 350

Central Projections of the Olfactory Bulb	353
The Organization of the Taste System	354
Taste Perception in Humans	356
Idiosyncratic Responses to Tastants	357
The Organization of the Peripheral Taste System	359
Taste Receptors and the Transduction of Taste Signals	360
Neural Coding in the Taste System	362
Trigeminal Chemoreception	363
Summary	366

Motor Neuron–Muscle Relationships	373
The Motor Unit	375
The Regulation of Muscle Force	377
The Spinal Cord Circuitry Underlying Muscle Stretch Reflexes	379

The Influence of Sensory Activity on Motor Behavior	381
Other Sensory Feedback That Affects Motor Performance	382
Box A Locomotion in the Leech and the Lamprey	
384	
Flexion Reflex Pathways	387
Spinal Cord Circuitry and Locomotion	387
Box B The Autonomy of Central Pattern Generators: Evidence from the Lobster Stomatogastric Ganglion	388
The Lower Motor Neuron Syndrome	389
Box C Amyotrophic Lateral Sclerosis	391
Summary	391

Chapter 16 Upper Motor Neuron Control of the Brainstem and Spinal Cord 393

Overview	393
Descending Control of Spinal Cord Circuitry: General Information	393
Motor Control Centers in the Brainstem: Upper Motor Neurons That Maintain Balance and Posture	397
Box A The Reticular Formation	398
The Corticospinal and Corticobulbar Pathways: Upper Motor Neurons That Initiate Complex Voluntary Movements	402
Box B Descending Projections to Cranial Nerve Motor Nuclei and Their Importance in Diagnosing the Cause of Motor Deficits	404
Functional Organization of the Primary Motor Cortex	405
Box C What Do Motor Maps Represent?	408
The Premotor Cortex	411
Box D Sensory Motor Talents and Cortical Space	410
Damage to Descending Motor Pathways: The Upper Motor Neuron Syndrome	412
Box E Muscle Tone	414
Summary	415

Chapter 17 Modulation of Movement by the Basal Ganglia 417

Overview	417
Projections to the Basal Ganglia	417
Projections from the Basal Ganglia to Other Brain Regions	422
Evidence from Studies of Eye Movements	423

Circuits within the Basal Ganglia System	424
Box A Huntington's Disease	426
Box B Parkinson's Disease: An Opportunity for Novel Therapeutic Approaches	429
Box C Basal Ganglia Loops and Non-Motor Brain Functions	432
Summary	433

Chapter 18 Modulation of Movement by the Cerebellum 435

Overview	435
Organization of the Cerebellum	435
Projections to the Cerebellum	438
Projections from the Cerebellum	440
Circuits within the Cerebellum	441
Box A Prion Diseases	444
Cerebellar Circuitry and the Coordination of Ongoing Movement	445
Futher Consequences of Cerebellar Lesions	448
Summary	449
Box B Genetic Analysis of Cerebellar Function	450

Chapter 19 Eye Movements and Sensory Motor Integration 453

Overview	453
What Eye Movements Accomplish	453
The Actions and Innervation of Extraocular Muscles	454
Box A The Perception of Stabilized Retinal Images	456
Types of Eye Movements and Their Functions	457
Neural Control of Saccadic Eye Movements	458
Box B Sensory Motor Integration in the Superior Colliculus	462
Neural Control of Smooth Pursuit Movements	466
Neural Control of Vergence Movements	466
Summary	467

Chapter 20 The Visceral Motor System 469

Overview	469
Early Studies of the Visceral Motor System	469
Distinctive Features of the Visceral Motor System	470
The Sympathetic Division of the Visceral Motor System	471
The Parasympathetic Division of the Visceral Motor System	476
The Enteric Nervous System	479
Sensory Components of the Visceral Motor System	480

Central Control of Visceral Motor Functions	483
Box A The Hypothalamus	484
Neurotransmission in the Visceral Motor System	487
Box B Horner's Syndrome	488
Box C Obesity and the Brain	490

Visceral Motor Reflex Functions	491
Autonomic Regulation of Cardiovascular Function	491
Autonomic Regulation of the Bladder	493
Autonomic Regulation of Sexual Function	496
Summary	498



Unit IV THE CHANGING BRAIN

Chapter 21 Early Brain Development **501**

Overview	501
The Initial Formation of the Nervous System: Gastrulation and Neurulation	501
The Molecular Basis of Neural Induction	503
Box A Stem Cells: Promise and Perils	504
Box B Retinoic Acid: Teratogen and Inductive Signal	506
Formation of the Major Brain Subdivisions	510
Box C Homeotic Genes and Human Brain Development	513
Box D Rhombomeres	514
Genetic Abnormalities and Altered Human Brain Development	515
The Initial Differentiation of Neurons and Glia	516
Box E Neurogenesis and Neuronal Birthdating	517
The Generation of Neuronal Diversity	518
Neuronal Migration	520
Box F Mixing It Up: Long-Distance Neuronal Migration	524
Summary	525

Chapter 22 Construction of Neural Circuits **527**

Overview	527
The Axonal Growth Cone	527
Non-Diffusible Signals for Axon Guidance	528
Box A Choosing Sides: Axon Guidance at the Optic Chiasm	530
Diffusible Signals for Axon Guidance: Chemoattraction and Repulsion	534
The Formation of Topographic Maps	537
Selective Synapse Formation	539

Box B Molecular Signals That Promote Synapse Formation **542**

Trophic Interactions and the Ultimate Size of Neuronal Populations	543
Further Competitive Interactions in the Formation of Neuronal Connections	545
Molecular Basis of Trophic Interactions	547
Box C Why Do Neurons Have Dendrites?	548
Box D The Discovery of BDNF and the Neurotrophin Family	552
Neurotrophin Signaling	553
Summary	554

Chapter 23 Modification of Brain Circuits as a Result of Experience **557**

Overview	557
Critical Periods	557
Box A Built-In Behaviors	558
The Development of Language: Example of a Human Critical Period	559
Box B Birdsong	560
Critical Periods in Visual System Development	562
Effects of Visual Deprivation on Ocular Dominance	563
Box C Transneuronal Labeling with Radioactive Amino Acids	564
Visual Deprivation and Amblyopia in Humans	568
Mechanisms by which Neuronal Activity Affects the Development of Neural Circuits	569
Cellular and Molecular Correlates of Activity- Dependent Plasticity during Critical Periods	572
Evidence for Critical Periods in Other Sensory Systems	572
Summary	573

Chapter 24 Plasticity of Mature Synapses and Circuits 575

Overview 575

Synaptic Plasticity Underlies Behavioral Modification in Invertebrates 575

Box A Genetics of Learning and Memory in the Fruit Fly 581

Short-Term Synaptic Plasticity in the Mammalian Nervous System 582

Long-Term Synaptic Plasticity in the Mammalian Nervous System 583

Long-Term Potentiation of Hippocampal Synapses 584

Molecular Mechanisms Underlying LTP 587

Box B Dendritic Spines 590

Long-Term Synaptic Depression 592

Box C Silent Synapses 594

Changes in Gene Expression Cause Enduring Changes in Synaptic Function during LTP and LTD 597

Plasticity in the Adult Cerebral Cortex 599

Box D Epilepsy: The Effect of Pathological Activity on Neural Circuitry 600

Recovery from Neural Injury 602

Generation of Neurons in the Adult Brain 605

Box E Why Aren't We More Like Fish and Frogs? 606

Summary 609



Unit V COMPLEX BRAIN FUNCTIONS

Chapter 25 The Association Cortices 613

Overview 613

The Association Cortices 613

An Overview of Cortical Structure 614

Specific Features of the Association Cortices 615

Box A A More Detailed Look at Cortical Lamination 617

Lesions of the Parietal Association Cortex: Deficits of Attention 619

Lesions of the Temporal Association Cortex: Deficits of Recognition 622

Lesions of the Frontal Association Cortex: Deficits of Planning 623

Box B Psychosurgery 625

"Attention Neurons" in the Monkey Parietal Cortex 626

"Recognition Neurons" in the Monkey Temporal Cortex 627

"Planning Neurons" in the Monkey Frontal Cortex 630

Box C Neuropsychological Testing 632

Box D Brain Size and Intelligence 634

Summary 635

Chapter 26 Language and Speech 637

Overview 637

Language Is Both Localized and Lateralized 637

Aphasias 638

Box A Speech 640

Box B Do Other Animals Have Language? 642

Box C Words and Meaning 645

A Dramatic Confirmation of Language Lateralization 646

Anatomical Differences between the Right and Left Hemispheres 648

Mapping Language Functions 649

Box D Language and Handedness 650

The Role of the Right Hemisphere in Language 654

Sign Language 655

Summary 656

Chapter 27 Sleep and Wakefulness 659

Overview 659

Why Do Humans (and Many Other Animals) Sleep? 659

Box A Styles of Sleep in Different Species 661

The Circadian Cycle of Sleep and Wakefulness	662
Stages of Sleep	665
Box B Molecular Mechanisms of Biological Clocks	666
Box C Electroencephalography	668
Physiological Changes in Sleep States	671
The Possible Functions of REM Sleep and Dreaming	671
Neural Circuits Governing Sleep	674
Box D Consciousness	675
Thalamocortical Interactions	679
Sleep Disorders	681
Box E Drugs and Sleep	682
Summary	684

Chapter 28 Emotions 687

Overview	687
Physiological Changes Associated with Emotion	687
The Integration of Emotional Behavior	688
Box A Facial Expressions: Pyramidal and Extrapyramidal Contributions	690
The Limbic System	693
Box B The Anatomy of the Amygdala	696
The Importance of the Amygdala	697
Box C The Reasoning Behind an Important Discovery	698
The Relationship between Neocortex and Amygdala	701
Box D Fear and the Human Amygdala: A Case Study	702
Box E Affective Disorders	704
Cortical Lateralization of Emotional Functions	705
Emotion, Reason, and Social Behavior	707
Summary	708

Chapter 29 Sex, Sexuality, and the Brain 711

Overview	711
Sexually Dimorphic Behavior	711
What Is Sex?	712
Box A The Development of Male and Female Phenotypes	714
Hormonal Influences on Sexual Dimorphism	715
Box B The Case of Bruce/Brenda	716
The Effect of Sex Hormones on Neural Circuitry	718

Box C The Actions of Sex Hormones	718
Other Central Nervous System Dimorphisms	
Specifically Related to Reproductive Behaviors	720
Brain Dimorphisms Related to Cognitive Function	728
Hormone-Sensitive Brain Circuits in Adult Animals	729
Summary	731

Chapter 30 Memory 733

Overview	733
Qualitative Categories of Human Memory	733
Temporal Categories of Memory	734
Box A Phylogenetic Memory	735
The Importance of Association in Information Storage	
736	
Forgetting	738
Box B Savant Syndrome	739
Brain Systems Underlying Declarative Memory Formation	741
Box C Clinical Cases That Reveal the Anatomical Substrate for Declarative Memories	742
Brain Systems Underlying Long-Term Storage of Declarative Memory	746
Brain Systems Underlying Nondeclarative Learning and Memory	748
Memory and Aging	749
Box D Alzheimer's Disease	750
Summary	753

Appendix A The Brainstem and Cranial Nerves 755

Appendix B Vascular Supply, the Meninges, and the Ventricular System 763

The Blood Supply of the Brain and Spinal Cord	763
The Blood-Brain Barrier	766
Box A Stroke	767
The Meninges	768
The Ventricular System	770

Glossary

Illustration Source References

Index

Preface

Whether judged in molecular, cellular, systemic, behavioral, or cognitive terms, the human nervous system is a stupendous piece of biological machinery. Given its accomplishments—all the artifacts of human culture, for instance—there is good reason for wanting to understand how the brain and the rest of the nervous system works. The debilitating and costly effects of neurological and psychiatric disease add a further sense of urgency to this quest. The aim of this book is to highlight the intellectual challenges and excitement—as well as the uncertainties—of what many see as the last great frontier of biological science. The information presented should serve as a starting point for undergraduates, medical students, graduate students in the neurosciences, and others who want to understand how the human nervous system operates. Like any other great challenge, neuroscience should be, and is, full of debate, dissension, and considerable fun. All these ingredients have gone into the construction of the third edition of this book; we hope they will be conveyed in equal measure to readers at all levels.

Acknowledgments

We are grateful to numerous colleagues who provided helpful contributions, criticisms and suggestions to this and previous editions. We particularly wish to thank Ralph Adolphs, David Amaral, Eva Anton, Gary Banker, Bob Barlow, Marlene Behrmann, Ursula Bellugi, Dan Blazer, Bob Burke, Roberto Cabeza, Nell Cant, Jim Cavanaugh, John Chapin, Milt Charlton, Michael Davis, Rob Deaner, Bob Desimone, Allison Doupe, Sasha du Lac, Jen Eilers, Anne Fausto-Sterling, Howard Fields, Elizabeth Finch, Nancy Forger, Jannon Fuchs, Michela Gallagher, Dana Garcia, Steve George, the late Patricia Goldman-Rakic, Mike Haglund, Zach Hall, Kristen Harris, Bill Henson, John Heuser, Jonathan Horton, Ron Hoy, Alan Humphrey, Jon Kaas, Jagmeet Kanwal, Herb Killackey, Len Kitzes, Arthur Lander, Story Landis, Simon LeVay, Darrell Lewis, Jeff Lichtman, Alan Light, Steve Lisberger, Donald Lo, Arthur Loewy, Ron Mangun, Eve Marder, Robert McCarley, Greg McCarthy, Jim McIlwain, Chris Muly, Vic Nadler, Ron Oppenheim, Larysa Pevny, Michael Platt, Franck Polleux, Scott Pomeroy, Rodney Radtke, Louis Reichardt, Marnie Riddle, Jamie Roitman, Steve Roper, John Rubenstein, Ben Rubin, David Rubin, Josh Sanes, Cliff Saper, Lynn Selement, Carla Shatz, Bill Snider, Larry Squire, John Staddon, Peter Strick, Warren Strittmatter, Joe Takahashi, Richard Weinberg, Jonathan Weiner, Christina Williams, Joel Winston, and Fulton Wong. It is understood, of course, that any errors are in no way attributable to our critics and advisors.

We also thank the students at Duke University Medical School as well as many other students and colleagues who provided suggestions for improvement of the last edition. Finally, we owe special thanks to Robert Reynolds and Nate O'Keefe, who labored long and hard to put the third edition together, and to Andy Sinauer, Graig Donini, Carol Wigg, Christopher Small, Janice Holabird, and the rest of the staff at Sinauer Associates for their outstanding work and high standards.

Supplements to Accompany NEUROSCIENCE Third Edition



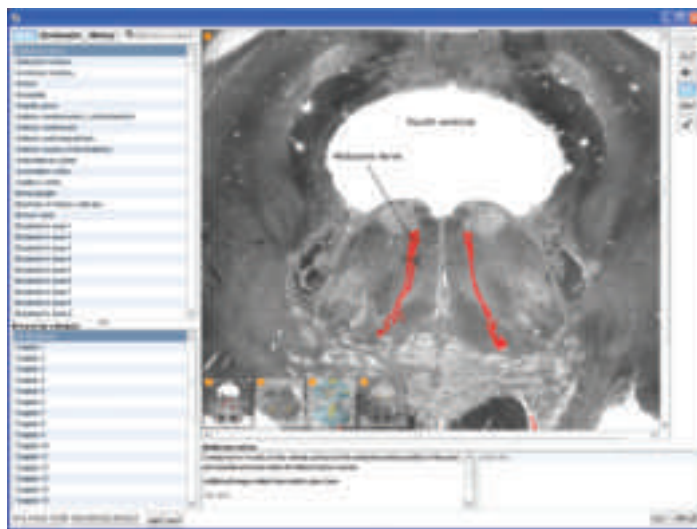
For the Student

Sylvius for Neuroscience:

A Visual Glossary of Human Neuroanatomy (CD-ROM)

S. Mark Williams, Leonard E. White, and Andrew C. Mace

Sylvius for Neuroscience: A Visual Glossary of Human Neuroanatomy, included in every copy of the textbook, is an interactive CD reference guide to the structure of the human nervous system. By entering a corresponding page number from the textbook, students can quickly search the CD for any neuroanatomical structure or term and view corresponding images and animations. Descriptive information is provided with all images and animations. Additionally, students can take notes on the content and share these with other *Sylvius* users. *Sylvius* is an essential study aid for learning basic human neuroanatomy.



Sylvius for Neuroscience features:

- Over 400 neuroanatomical structures and terms.
- High-resolution images.
- Animations of pathways and 3-D reconstructions.
- Definitions and descriptions.
- Audio pronunciations.
- A searchable glossary.
- Categories of anatomical structures and terms (e.g., cranial nerves, spinal cord tracts, lobes, cortical areas, etc.), that can be easily browsed. In addition, structures can be browsed by textbook chapter.

- Images and text relevant to the textbook: Icons in the textbook indicate specific content on the CD. By entering a textbook page number, students can automatically load the relevant images and text.
- A history feature that allows the student to quickly reload recently viewed structures.
- A bookmark feature that adds bookmarks to structures of interest; bookmarks are automatically stored on the student's computer.
- A notes feature that allows students to type notes for any selected structure; notes are automatically saved on the student's computer and can be shared among students and instructors (i.e., imported and exported).
- A self-quiz mode that allows for testing on structure identification and functional information.
- A print feature that formats images and text for printed output.
- An image zoom tool.

For the Instructor

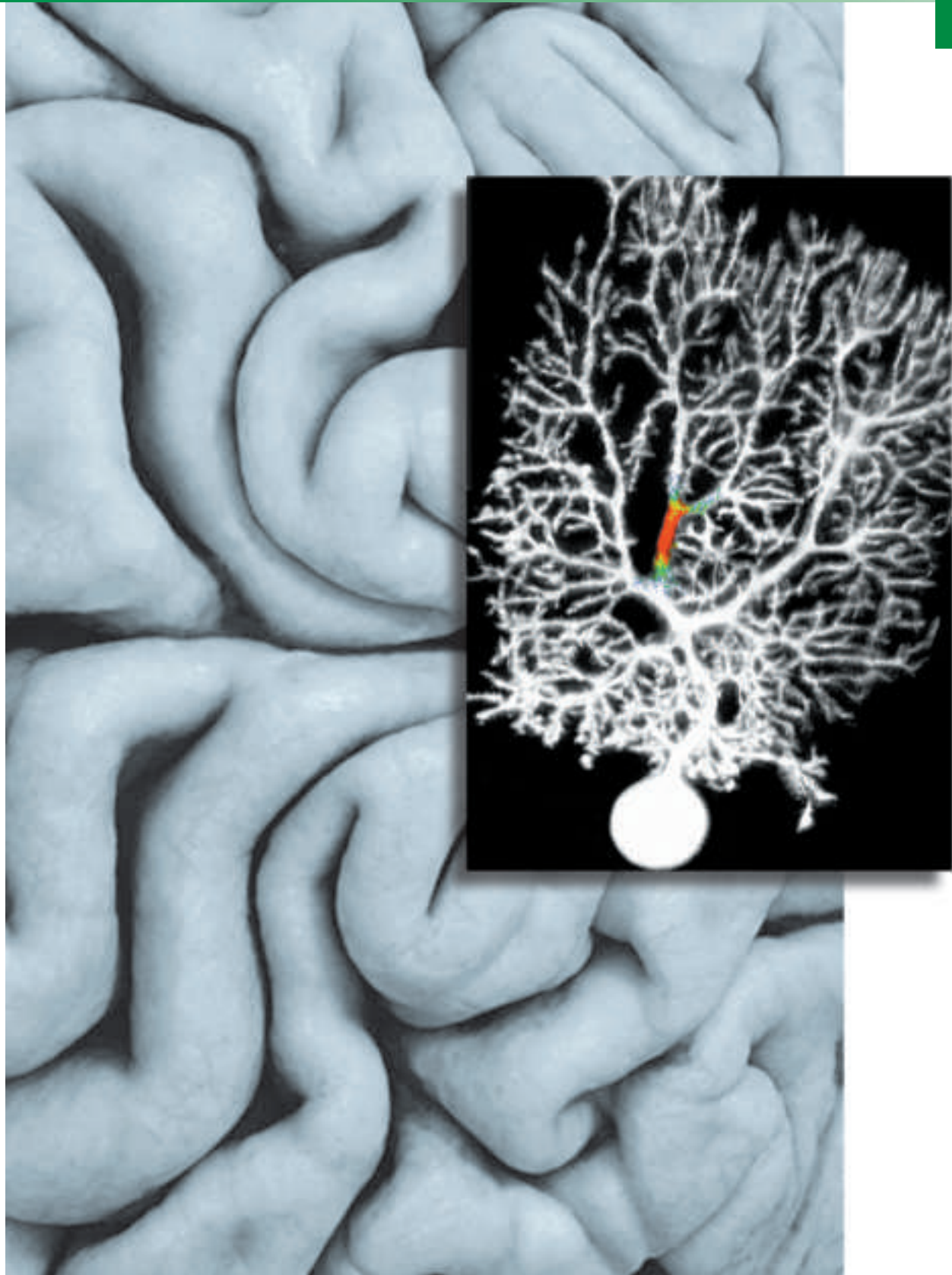
Instructor's Resource CD (ISBN 0-87893-750-1)

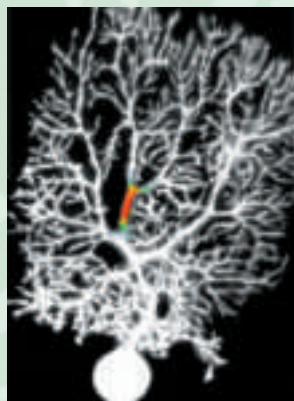
This expanded resource includes all the figures and tables from the textbook in JPEG format, reformatted and relabeled for optimal readability. Also included are ready-to-use PowerPoint® presentations of all figures and tables. In addition, new for the Third Edition, the Instructor's Resource CD includes a set of short-answer study questions for each chapter in Microsoft® Word® format.

Overhead Transparencies (ISBN 0-87893-751-X)

This set includes 100 illustrations (approximately 150 transparencies), selected from throughout the textbook for teaching purposes. These are relabeled and optimized for projection in classrooms.

Neural Signaling





Calcium signaling in a cerebellar Purkinje neuron. An electrode was used to fill the neuron with a fluorescent calcium indicator dye. This dye revealed the release of intracellular calcium ions (color) produced by the actions of the second messenger IP₃. (Courtesy of Elizabeth A. Finch and George J. Augustine.)

UNIT I

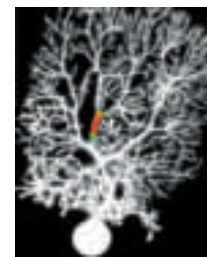
NEURAL SIGNALING

- 2 *Electrical Signals of Nerve Cells*
- 3 *Voltage-Dependent Membrane Permeability*
- 4 *Channels and Transporters*
- 5 *Synaptic Transmission*
- 6 *Neurotransmitters, Receptors, and Their Effects*
- 7 *Molecular Signaling within Neurons*

The brain is remarkably adept at acquiring, coordinating, and disseminating information about the body and its environment. Such information must be processed within milliseconds, yet it also can be stored away as memories that endure for years. Neurons within the central and peripheral nervous systems perform these functions by generating sophisticated electrical and chemical signals. This unit describes these signals and how they are produced. It explains how one type of electrical signal, the action potential, allows information to travel along the length of a nerve cell. It also explains how other types of signals—both electrical and chemical—are generated at synaptic connections between nerve cells. Synapses permit information transfer by interconnecting neurons to form the circuitry on which neural processing depends. Finally, it describes the intricate biochemical signaling events that take place within neurons. Appreciating these fundamental forms of neuronal signaling provides a foundation for appreciating the higher-level functions considered in the rest of the book.

The cellular and molecular mechanisms that give neurons their unique signaling abilities are also targets for disease processes that compromise the function of the nervous system. A working knowledge of the cellular and molecular biology of neurons is therefore fundamental to understanding a variety of brain pathologies, and for developing novel approaches to diagnosing and treating these all too prevalent problems.

Chapter 2



Electrical Signals of Nerve Cells

Overview

Nerve cells generate electrical signals that transmit information. Although neurons are not intrinsically good conductors of electricity, they have evolved elaborate mechanisms for generating these signals based on the flow of ions across their plasma membranes. Ordinarily, neurons generate a negative potential, called the resting membrane potential, that can be measured by recording the voltage between the inside and outside of nerve cells. The action potential transiently abolishes the negative resting potential and makes the transmembrane potential positive. Action potentials are propagated along the length of axons and are the fundamental signal that carries information from one place to another in the nervous system. Still other types of electrical signals are produced by the activation of synaptic contacts between neurons or by the actions of external forms of energy on sensory neurons. All of these electrical signals arise from ion fluxes brought about by nerve cell membranes being selectively permeable to different ions, and from the non-uniform distribution of these ions across the membrane.

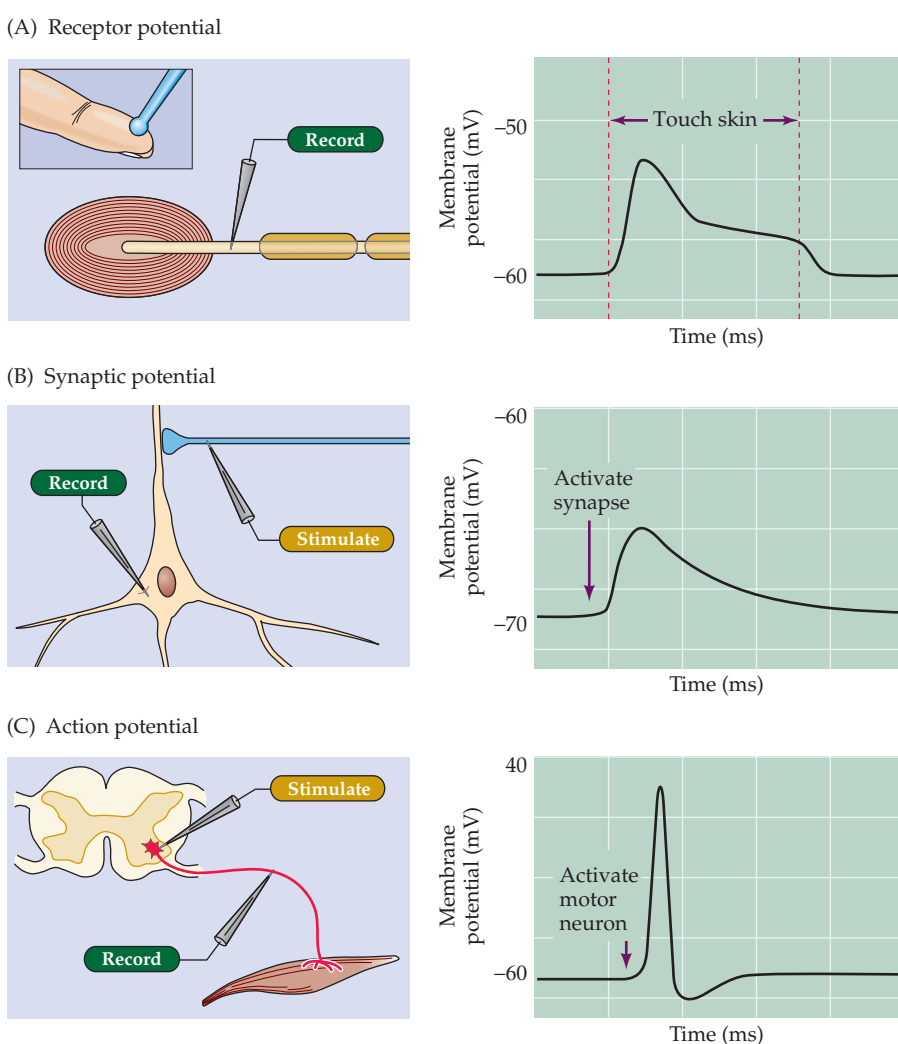
Electrical Potentials across Nerve Cell Membranes

Neurons employ several different types of electrical signal to encode and transfer information. The best way to observe these signals is to use an intracellular microelectrode to measure the electrical potential across the neuronal plasma membrane. A typical microelectrode is a piece of glass tubing pulled to a very fine point (with an opening of less than 1 μm diameter) and filled with a good electrical conductor, such as a concentrated salt solution. This conductive core can then be connected to a voltmeter, such as an oscilloscope, to record the transmembrane voltage of the nerve cell.

The first type of electrical phenomenon can be observed as soon as a microelectrode is inserted through the membrane of the neuron. Upon entering the cell, the microelectrode reports a negative potential, indicating that neurons have a means of generating a constant voltage across their membranes when at rest. This voltage, called the **resting membrane potential**, depends on the type of neuron being examined, but it is always a fraction of a volt (typically -40 to -90 mV).

The electrical signals produced by neurons are caused by responses to stimuli, which then change the resting membrane potential. **Receptor potentials** are due to the activation of sensory neurons by external stimuli, such as light, sound, or heat. For example, touching the skin activates Pacinian corpuscles, receptor neurons that sense mechanical disturbances of the skin. These neurons respond to touch with a receptor potential that changes the resting potential for a fraction of a second (Figure 2.1A). These transient

Figure 2.1 Types of neuronal electrical signals. In all cases, microelectrodes are used to measure changes in the resting membrane potential during the indicated signals. (A) A brief touch causes a receptor potential in a Pacinian corpuscle in the skin. (B) Activation of a synaptic contact onto a hippocampal pyramidal neuron elicits a synaptic potential. (C) Stimulation of a spinal reflex produces an action potential in a spinal motor neuron.



changes in potential are the first step in generating the sensation of vibrations (or “tickles”) of the skin in the somatic sensory system (Chapter 8). Similar sorts of receptor potentials are observed in all other sensory neurons during transduction of sensory signals (Unit II).

Another type of electrical signal is associated with communication between neurons at synaptic contacts. Activation of these synapses generates **synaptic potentials**, which allow transmission of information from one neuron to another. An example of such a signal is shown in Figure 2.1B. In this case, activation of a synaptic terminal innervating a hippocampal pyramidal neuron causes a very brief change in the resting membrane potential in the pyramidal neuron. Synaptic potentials serve as the means of exchanging information in complex neural circuits in both the central and peripheral nervous systems (Chapter 5).

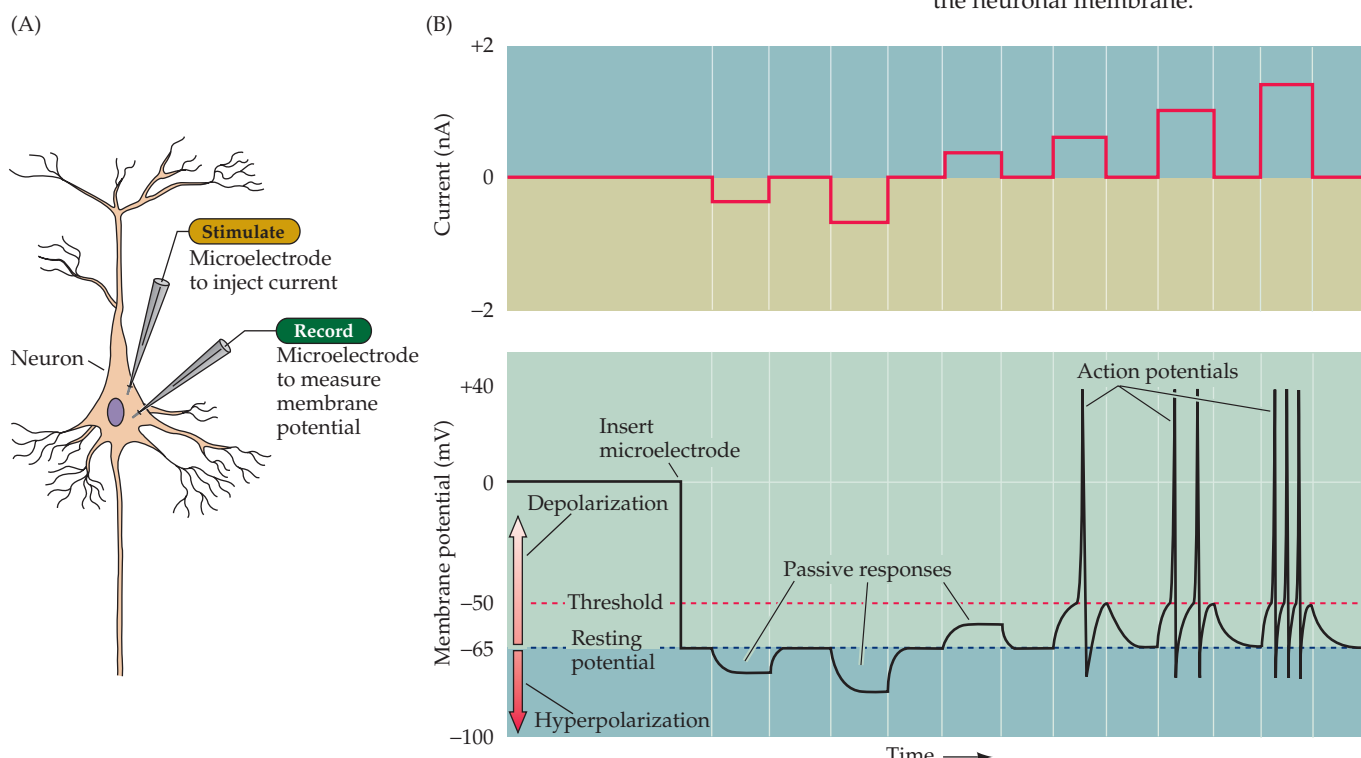
The use of electrical signals—as in sending electricity over wires to provide power or information—presents a series of problems in electrical engineering. A fundamental problem for neurons is that their axons, which can be quite long (remember that a spinal motor neuron can extend for a meter or more), are not good electrical conductors. Although neurons and wires

are both capable of passively conducting electricity, the electrical properties of neurons compare poorly to an ordinary wire. To compensate for this deficiency, neurons have evolved a “booster system” that allows them to conduct electrical signals over great distances despite their intrinsically poor electrical characteristics. The electrical signals produced by this booster system are called **action potentials** (which are also referred to as “spikes” or “impulses”). An example of an action potential recorded from the axon of a spinal motor neuron is shown in Figure 2.1C.

One way to elicit an action potential is to pass electrical current across the membrane of the neuron. In normal circumstances, this current would be generated by receptor potentials or by synaptic potentials. In the laboratory, however, electrical current suitable for initiating an action potential can be readily produced by inserting a second microelectrode into the same neuron and then connecting the electrode to a battery (Figure 2.2A). If the current delivered in this way makes the membrane potential more negative (**hyperpolarization**), nothing very dramatic happens. The membrane potential simply changes in proportion to the magnitude of the injected current (central part of Figure 2.2B). Such hyperpolarizing responses do not require any unique property of neurons and are therefore called passive electrical responses. A much more interesting phenomenon is seen if current of the opposite polarity is delivered, so that the membrane potential of the nerve cell becomes more positive than the resting potential (**depolarization**). In this case, at a certain level of membrane potential, called the **threshold potential**, an action potential occurs (see right side of Figure 2.2B).

The action potential, which is an active response generated by the neuron, is a brief (about 1 ms) change from negative to positive in the transmem-

Figure 2.2 Recording passive and active electrical signals in a nerve cell. (A) Two microelectrodes are inserted into a neuron; one of these measures membrane potential while the other injects current into the neuron. (B) Inserting the voltage-measuring microelectrode into the neuron reveals a negative potential, the resting membrane potential. Injecting current through the current-passing microelectrode alters the neuronal membrane potential. Hyperpolarizing current pulses produce only passive changes in the membrane potential. While small depolarizing currents also elicit only passive responses, depolarizations that cause the membrane potential to meet or exceed threshold additionally evoke action potentials. Action potentials are active responses in the sense that they are generated by changes in the permeability of the neuronal membrane.



brane potential. Importantly, the amplitude of the action potential is independent of the magnitude of the current used to evoke it; that is, larger currents do not elicit larger action potentials. The action potentials of a given neuron are therefore said to be *all-or-none*, because they occur fully or not at all. If the amplitude or duration of the stimulus current is increased sufficiently, multiple action potentials occur, as can be seen in the responses to the three different current intensities shown in Figure 2.2B (right side). It follows, therefore, that the intensity of a stimulus is encoded in the frequency of action potentials rather than in their amplitude. This arrangement differs dramatically from receptor potentials, whose amplitudes are graded in proportion to the magnitude of the sensory stimulus, or synaptic potentials, whose amplitude varies according to the number of synapses activated and the previous amount of synaptic activity.

Because electrical signals are the basis of information transfer in the nervous system, it is essential to understand how these signals arise. Remarkably, all of the neuronal electrical signals described above are produced by similar mechanisms that rely upon the movement of ions across the neuronal membrane. The remainder of this chapter addresses the question of how nerve cells use ions to generate electrical potentials. Chapter 3 explores more specifically the means by which action potentials are produced and how these signals solve the problem of long-distance electrical conduction within nerve cells. Chapter 4 examines the properties of membrane molecules responsible for electrical signaling. Finally, Chapters 5–7 consider how electrical signals are transmitted from one nerve cell to another at synaptic contacts.

How Ionic Movements Produce Electrical Signals

Electrical potentials are generated across the membranes of neurons—and, indeed, all cells—because (1) there are *differences in the concentrations* of specific ions across nerve cell membranes, and (2) the membranes are *selectively permeable* to some of these ions. These two facts depend in turn on two different kinds of proteins in the cell membrane (Figure 2.3). The ion concentration gradients are established by proteins known as **active transporters**, which, as their name suggests, actively move ions into or out of cells against their concentration gradients. The selective permeability of membranes is

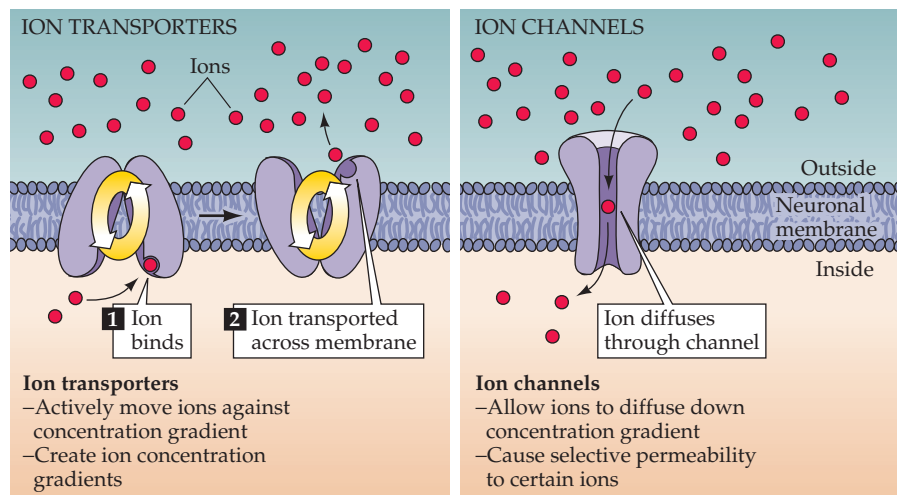


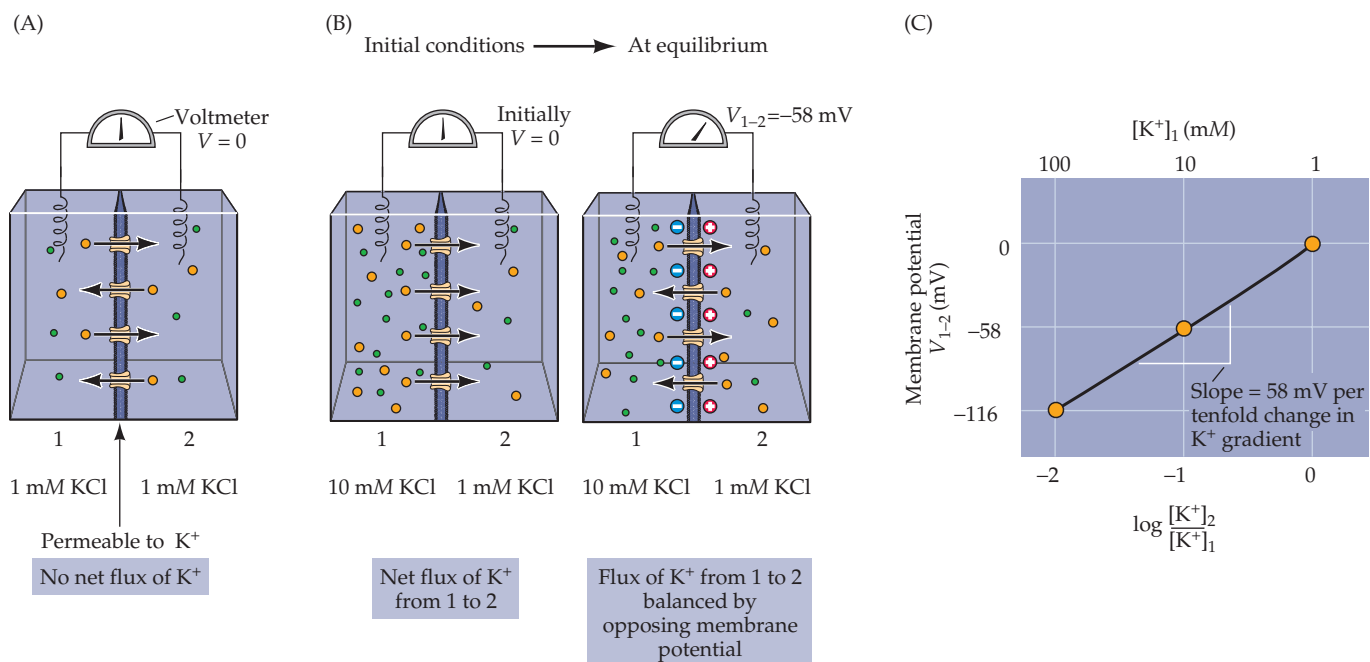
Figure 2.3 Ion transporters and ion channels are responsible for ionic movements across neuronal membranes. Transporters create ion concentration differences by actively transporting ions against their chemical gradients. Channels take advantage of these concentration gradients, allowing selected ions to move, via diffusion, down their chemical gradients.

due largely to **ion channels**, proteins that allow only certain kinds of ions to cross the membrane in the direction of their concentration gradients. Thus, channels and transporters basically work against each other, and in so doing they generate the resting membrane potential, action potentials, and the synaptic potentials and receptor potentials that trigger action potentials. The structure and function of these channels and transporters are described in Chapter 4.

To appreciate the role of ion gradients and selective permeability in generating a membrane potential, consider a simple system in which an artificial membrane separates two compartments containing solutions of ions. In such a system, it is possible to determine the composition of the two solutions and, thereby, control the ion gradients across the membrane. For example, take the case of a membrane that is permeable only to potassium ions (K^+). If the concentration of K^+ on each side of this membrane is equal, then no electrical potential will be measured across it (Figure 2.4A). However, if the concentration of K^+ is not the same on the two sides, then an electrical potential will be generated. For instance, if the concentration of K^+ on one side of the membrane (compartment 1) is 10 times higher than the K^+ concentration on the other side (compartment 2), then the electrical potential of compartment 1 will be negative relative to compartment 2 (Figure 2.4B). This difference in electrical potential is generated because the potassium ions flow down their concentration gradient and take their electrical charge (one positive charge per ion) with them as they go. Because neuronal membranes contain pumps that accumulate K^+ in the cell cytoplasm, and because potassium-permeable channels in the plasma membrane allow a transmembrane flow of K^+ , an analogous situation exists in living nerve cells. A continual resting efflux of K^+ is therefore responsible for the resting membrane potential.

In the hypothetical case just described, an equilibrium will quickly be reached. As K^+ moves from compartment 1 to compartment 2 (the initial conditions on the left of Figure 2.4B), a potential is generated that tends to impede further flow of K^+ . This impediment results from the fact that the

Figure 2.4 Electrochemical equilibrium. (A) A membrane permeable only to K^+ (yellow spheres) separates compartments 1 and 2, which contain the indicated concentrations of KCl. (B) Increasing the KCl concentration in compartment 1 to 10 mM initially causes a small movement of K^+ into compartment 2 (initial conditions) until the electromotive force acting on K^+ balances the concentration gradient, and the net movement of K^+ becomes zero (at equilibrium). (C) The relationship between the transmembrane concentration gradient ($[K^+]_2/[K^+]_1$) and the membrane potential. As predicted by the Nernst equation, this relationship is linear when plotted on semi-logarithmic coordinates, with a slope of 58 mV per tenfold difference in the concentration gradient.



potential gradient across the membrane tends to repel the positive potassium ions that would otherwise move across the membrane. Thus, as compartment 2 becomes positive relative to compartment 1, the increasing positivity makes compartment 2 less attractive to the positively charged K⁺. The net movement (or flux) of K⁺ will stop at the point (at equilibrium on the right of Figure 2.4B) where the potential change across the membrane (the relative positivity of compartment 2) exactly offsets the concentration gradient (the tenfold excess of K⁺ in compartment 1). At this **electrochemical equilibrium**, there is an exact balance between two opposing forces: (1) the concentration gradient that causes K⁺ to move from compartment 1 to compartment 2, taking along positive charge, and (2) an opposing electrical gradient that increasingly tends to stop K⁺ from moving across the membrane (Figure 2.4B). The number of ions that needs to flow to generate this electrical potential is very small (approximately 10⁻¹² moles of K⁺ per cm² of membrane, or 10¹² K⁺ ions). This last fact is significant in two ways. First, it means that the concentrations of permeant ions on each side of the membrane remain essentially constant, even after the flow of ions has generated the potential. Second, the tiny fluxes of ions required to establish the membrane potential do not disrupt chemical electroneutrality because each ion has an oppositely charged counter-ion (chloride ions in the example shown in Figure 2.4) to maintain the neutrality of the solutions on each side of the membrane. The concentration of K⁺ remains equal to the concentration of Cl⁻ in the solutions in compartments 1 and 2, meaning that the separation of charge that creates the potential difference is restricted to the immediate vicinity of the membrane.

The Forces That Create Membrane Potentials

The electrical potential generated across the membrane at electrochemical equilibrium, the **equilibrium potential**, can be predicted by a simple formula called the **Nernst equation**. This relationship is generally expressed as

$$E_X = \frac{RT}{zF} \ln \frac{[X]_2}{[X]_1}$$

where E_X is the equilibrium potential for any ion X, R is the gas constant, T is the absolute temperature (in degrees on the Kelvin scale), z is the valence (electrical charge) of the permeant ion, and F is the Faraday constant (the amount of electrical charge contained in one mole of a univalent ion). The brackets indicate the concentrations of ion X on each side of the membrane and the symbol ln indicates the natural logarithm of the concentration gradient. Because it is easier to perform calculations using base 10 logarithms and to perform experiments at room temperature, this relationship is usually simplified to

$$E_X = \frac{58}{z} \log \frac{[X]_2}{[X]_1}$$

where log indicates the base 10 logarithm of the concentration ratio. Thus, for the example in Figure 2.4B, the potential across the membrane at electrochemical equilibrium is

$$E_K = \frac{58}{z} \log \frac{[K]_2}{[K]_1} = 58 \log \frac{1}{10} = -58 \text{ mV}$$

The equilibrium potential is conventionally defined in terms of the potential difference between the reference compartment, side 2 in Figure 2.4, and the other side. This approach is also applied to biological systems. In this case,

the outside of the cell is the conventional reference point (defined as zero potential). Thus, when the concentration of K^+ is higher inside than out, an inside-negative potential is measured across the K^+ -permeable neuronal membrane.

For a simple hypothetical system with only one permeant ion species, the Nernst equation allows the electrical potential across the membrane at equilibrium to be predicted exactly. For example, if the concentration of K^+ on side 1 is increased to 100 mM, the membrane potential will be -116 mV. More generally, if the membrane potential is plotted against the logarithm of the K^+ concentration gradient ($[K]_2/[K]_1$), the Nernst equation predicts a linear relationship with a slope of 58 mV (actually $58/z$) per tenfold change in the K^+ gradient (Figure 2.4C).

To reinforce and extend the concept of electrochemical equilibrium, consider some additional experiments on the influence of ionic species and ionic permeability that could be performed on the simple model system in Figure 2.4. What would happen to the electrical potential across the membrane (the potential of side 1 relative to side 2) if the potassium on side 2 were replaced with 10 mM sodium (Na^+) and the K^+ in compartment 1 were replaced by 1 mM Na^+ ? No potential would be generated, because no Na^+ could flow across the membrane (which was defined as being permeable only to K^+). However, if under these ionic conditions (10 times more Na^+ in compartment 2) the K^+ -permeable membrane were to be magically replaced by a membrane permeable only to Na^+ , a potential of +58 mV would be measured at equilibrium. If 10 mM calcium (Ca^{2+}) were present in compartment 2 and 1 mM Ca^{2+} in compartment 1, and a Ca^{2+} -selective membrane separated the two sides, what would happen to the membrane potential? A potential of +29 mV would develop, because the valence of calcium is +2. Finally, what would happen to the membrane potential if 10 mM Cl^- were present in compartment 1 and 1 mM Cl^- were present in compartment 2, with the two sides separated by a Cl^- -permeable membrane? Because the valence of this anion is -1, the potential would again be +58 mV.

The balance of chemical and electrical forces at equilibrium means that the electrical potential can determine ionic fluxes across the membrane, just as the ionic gradient can determine the membrane potential. To examine the influence of membrane potential on ionic flux, imagine connecting a battery across the two sides of the membrane to control the electrical potential across the membrane without changing the distribution of ions on the two sides (Figure 2.5). As long as the battery is off, things will be just as in Figure 2.4, with the flow of K^+ from compartment 1 to compartment 2 causing a negative membrane potential (Figure 2.5A, left). However, if the battery is used to make compartment 1 initially more negative relative to compartment 2, there will be less K^+ flux, because the negative potential will tend to keep K^+ in compartment 1. How negative will side 1 need to be before there is no net flux of K^+ ? The answer is -58 mV, the voltage needed to counter the tenfold difference in K^+ concentrations on the two sides of the membrane (Figure 2.5A, center). If compartment 1 is initially made more negative than -58 mV, then K^+ will actually flow from compartment 2 into compartment 1, because the positive ions will be attracted to the more negative potential of compartment 1 (Figure 2.5A, right). This example demonstrates that both the direction and magnitude of ion flux depend on the membrane potential. Thus, in some circumstances the electrical potential can overcome an ionic concentration gradient.

The ability to alter ion flux experimentally by changing either the potential imposed on the membrane (Figure 2.5B) or the transmembrane concen-

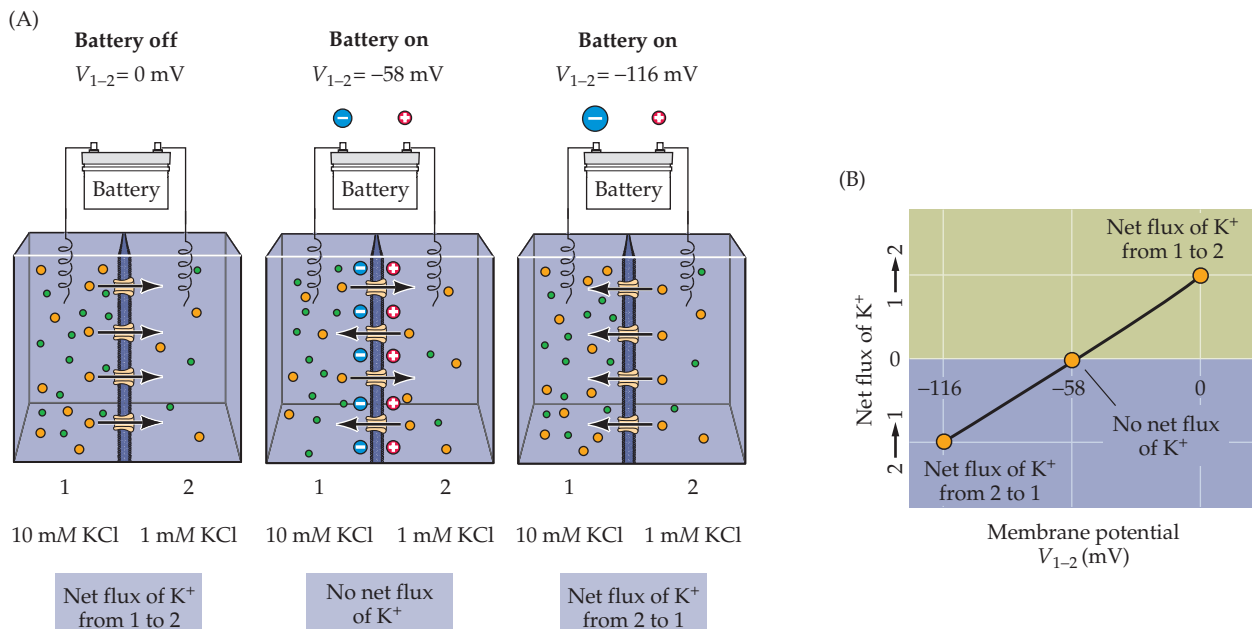


Figure 2.5 Membrane potential influences ion fluxes. (A) Connecting a battery across the K^+ -permeable membrane allows direct control of membrane potential. When the battery is turned off (left), K^+ ions (yellow) flow simply according to their concentration gradient. Setting the initial membrane potential (V_{1-2}) at the equilibrium potential for K^+ (center) yields no net flux of K^+ , while making the membrane potential more negative than the K^+ equilibrium potential (right) causes K^+ to flow against its concentration gradient. (B) Relationship between membrane potential and direction of K^+ flux.

concentration gradient for an ion (see Figure 2.4C) provides convenient tools for studying ion fluxes across the plasma membranes of neurons, as will be evident in many of the experiments described in the following chapters.

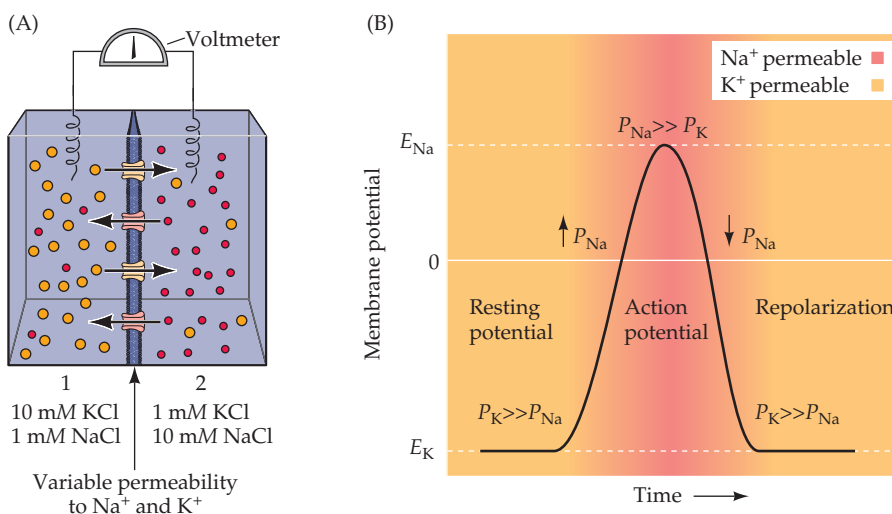
Electrochemical Equilibrium in an Environment with More Than One Permeant Ion

Now consider a somewhat more complex situation in which Na^+ and K^+ are unequally distributed across the membrane, as in Figure 2.6A. What would happen if 10 mM K^+ and 1 mM Na^+ were present in compartment 1, and 1 mM K^+ and 10 mM Na^+ in compartment 2? If the membrane were permeable only to K^+ , the membrane potential would be -58 mV ; if the membrane were permeable only to Na^+ , the potential would be $+58 \text{ mV}$. But what would the potential be if the membrane were permeable to both K^+ and Na^+ ? In this case, the potential would depend on the relative permeability of the membrane to K^+ and Na^+ . If it were more permeable to K^+ , the potential would approach -58 mV , and if it were more permeable to Na^+ , the potential would be closer to $+58 \text{ mV}$. Because there is no permeability term in the Nernst equation, which only considers the simple case of a single permeant ion species, a more elaborate equation is needed that takes into account both the concentration gradients of the permeant ions and the relative permeability of the membrane to each permeant species.

Such an equation was developed by David Goldman in 1943. For the case most relevant to neurons, in which K^+ , Na^+ , and Cl^- are the primary permeant ions, the **Goldman equation** is written

$$V = 58 \log \frac{P_{\text{K}}[\text{K}]_2 + P_{\text{Na}}[\text{Na}]_2 + P_{\text{Cl}}[\text{Cl}]_1}{P_{\text{K}}[\text{K}]_1 + P_{\text{Na}}[\text{Na}]_1 + P_{\text{Cl}}[\text{Cl}]_2}$$

where V is the voltage across the membrane (again, compartment 1 relative to the reference compartment 2) and P indicates the permeability of the



membrane to each ion of interest. The Goldman equation is thus an extended version of the Nernst equation that takes into account the relative permeabilities of each of the ions involved. The relationship between the two equations becomes obvious in the situation where the membrane is permeable only to one ion, say, K^+ ; in this case, the Goldman expression collapses back to the simpler Nernst equation. In this context, it is important to note that the valence factor (z) in the Nernst equation has been eliminated; this is why the concentrations of negatively charged chloride ions, Cl^- , have been inverted relative to the concentrations of the positively charged ions [remember that $-\log(A/B) = \log(B/A)$].

If the membrane in Figure 2.6A is permeable to K^+ and Na^+ only, the terms involving Cl^- drop out because $P_{\text{Cl}} = 0$. In this case, solution of the Goldman equation yields a potential of -58 mV when only K^+ is permeant, $+58 \text{ mV}$ when only Na^+ is permeant, and some intermediate value if both ions are permeant. For example, if K^+ and Na^+ were equally permeant, then the potential would be 0 mV .

With respect to neural signaling, it is particularly pertinent to ask what would happen if the membrane started out being permeable to K^+ , and then temporarily switched to become most permeable to Na^+ . In this circumstance, the membrane potential would start out at a negative level, become positive while the Na^+ permeability remained high, and then fall back to a negative level as the Na^+ permeability decreased again. As it turns out, this last case essentially describes what goes on in a neuron during the generation of an action potential. In the resting state, P_{K} of the neuronal plasma membrane is much higher than P_{Na} ; since, as a result of the action of ion transporters, there is always more K^+ inside the cell than outside (Table 2.1), the resting potential is negative (Figure 2.6B). As the membrane potential is depolarized (by synaptic action, for example), P_{Na} increases. The transient increase in Na^+ permeability causes the membrane potential to become even more positive (red region in Figure 2.6B), because Na^+ rushes in (there is much more Na^+ outside a neuron than inside, again as a result of ion pumps). Because of this positive feedback loop, an action potential occurs. The rise in Na^+ permeability during the action potential is transient, however; as the membrane permeability to K^+ is restored, the membrane potential quickly returns to its resting level.

Figure 2.6 Resting and action potentials entail permeabilities to different ions. (A) Hypothetical situation in which a membrane variably permeable to Na^+ (red) and K^+ (yellow) separates two compartments that contain both ions. For simplicity, Cl^- ions are not shown in the diagram. (B) Schematic representation of the membrane ionic permeabilities associated with resting and action potentials. At rest, neuronal membranes are more permeable to K^+ (yellow) than to Na^+ (red); accordingly, the resting membrane potential is negative and approaches the equilibrium potential for K^+ , E_{K} . During an action potential, the membrane becomes very permeable to Na^+ (red); thus the membrane potential becomes positive and approaches the equilibrium potential for Na^+ , E_{Na} . The rise in Na^+ permeability is transient, however, so that the membrane again becomes primarily permeable to K^+ (yellow), causing the potential to return to its negative resting value. Notice that at the equilibrium potential for a given ion, there is no net flux of that ion across the membrane.

TABLE 2.1
Extracellular and Intracellular Ion Concentrations

<i>Ion</i>	<i>Concentration (mM)</i>	
	<i>Intracellular</i>	<i>Extracellular</i>
Squid neuron		
Potassium (K^+)	400	20
Sodium (Na^+)	50	440
Chloride (Cl^-)	40–150	560
Calcium (Ca^{2+})	0.0001	10
Mammalian neuron		
Potassium (K^+)	140	5
Sodium (Na^+)	5–15	145
Chloride (Cl^-)	4–30	110
Calcium (Ca^{2+})	0.0001	1–2

Armed with an appreciation of these simple electrochemical principles, it will be much easier to understand the following, more detailed account of how neurons generate resting and action potentials.

The Ionic Basis of the Resting Membrane Potential

The action of ion transporters creates substantial transmembrane gradients for most ions. Table 2.1 summarizes the ion concentrations measured directly in an exceptionally large nerve cell found in the nervous system of the squid (Box A). Such measurements are the basis for stating that there is much more K^+ inside the neuron than out, and much more Na^+ outside than in. Similar concentration gradients occur in the neurons of most animals, including humans. However, because the ionic strength of mammalian blood is lower than that of sea-dwelling animals such as squid, in mammals the concentrations of each ion are several times lower. These transporter-dependent concentration gradients are, indirectly, the source of the resting neuronal membrane potential and the action potential.

Once the ion concentration gradients across various neuronal membranes are known, the Nernst equation can be used to calculate the equilibrium potential for K^+ and other major ions. Since the resting membrane potential of the squid neuron is approximately -65 mV , K^+ is the ion that is closest to being in electrochemical equilibrium when the cell is at rest. This fact implies that the resting membrane is more permeable to K^+ than to the other ions listed in Table 2.1, and that this permeability is the source of resting potentials.

It is possible to test this guess, as Alan Hodgkin and Bernard Katz did in 1949, by asking what happens to the resting membrane potential if the concentration of K^+ outside the neuron is altered. If the resting membrane were permeable only to K^+ , then the Goldman equation (or even the simpler Nernst equation) predicts that the membrane potential will vary in proportion to the logarithm of the K^+ concentration gradient across the membrane. Assuming that the internal K^+ concentration is unchanged during the experiment, a plot of membrane potential against the logarithm of the external K^+ concentration should yield a straight line with a slope of 58 mV per tenfold change in external K^+ concentration at room temperature (see Figure 2.4C). (The slope becomes about 61 mV at mammalian body temperatures.)

Box A

The Remarkable Giant Nerve Cells of Squid

Many of the initial insights into how ion concentration gradients and changes in membrane permeability produce electrical signals came from experiments performed on the extraordinarily large nerve cells of the squid. The axons of these nerve cells can be up to 1 mm in diameter—100 to 1000 times larger than mammalian axons. Thus, squid axons are large enough to allow experiments that would be impossible on most other nerve cells. For example, it is not difficult to insert simple wire electrodes inside these giant axons and make reliable electrical measurements. The relative ease of this approach yielded the first intracellular recordings of action potentials from nerve cells and, as discussed in the next chapter, the first experimental measure-

ments of the ion currents that produce action potentials. It also is practical to extrude the cytoplasm from giant axons and measure its ionic composition (see Table 2.1). In addition, some giant nerve cells form synaptic contacts with other giant nerve cells, producing very large synapses that have been extraordinarily valuable in understanding the fundamental mechanisms of synaptic transmission (see Chapter 5).

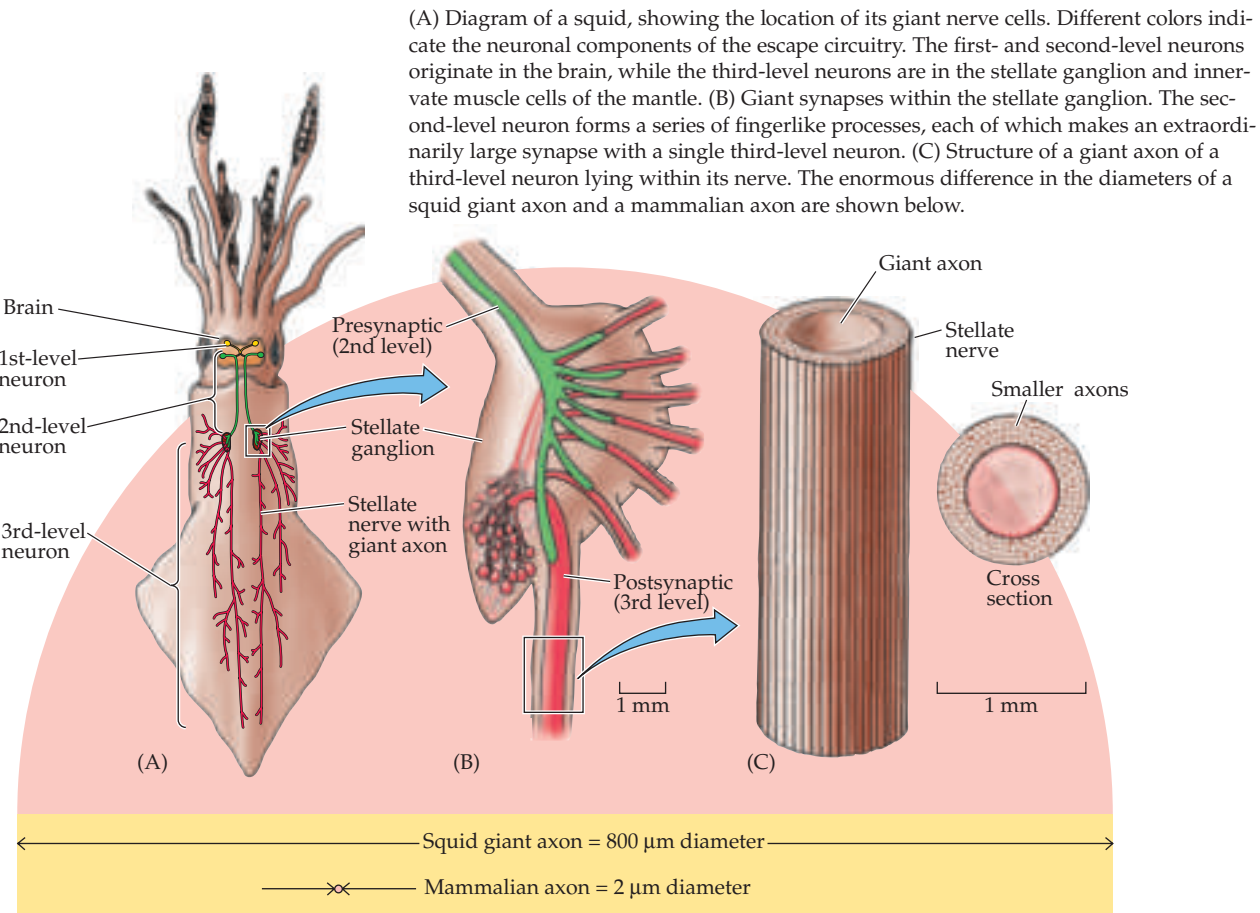
Giant neurons evidently evolved in squid because they enhanced survival. These neurons participate in a simple neural circuit that activates the contraction of the mantle muscle, producing a jet propulsion effect that allows the squid to move away from predators at a remarkably fast speed. As discussed in

Chapter 3, larger axonal diameter allows faster conduction of action potentials. Thus, presumably these huge nerve cells help squid escape more successfully from their numerous enemies.

Today—nearly 70 years after their discovery by John Z. Young at University College London—the giant nerve cells of squid remain useful experimental systems for probing basic neuronal functions.

References

- LLINÁS, R. (1999) *The Squid Synapse: A Model for Chemical Transmission*. Oxford: Oxford University Press.
YOUNG, J. Z. (1939) Fused neurons and synaptic contacts in the giant nerve fibres of cephalopods. Phil. Trans. R. Soc. Lond. 229(B): 465–503.



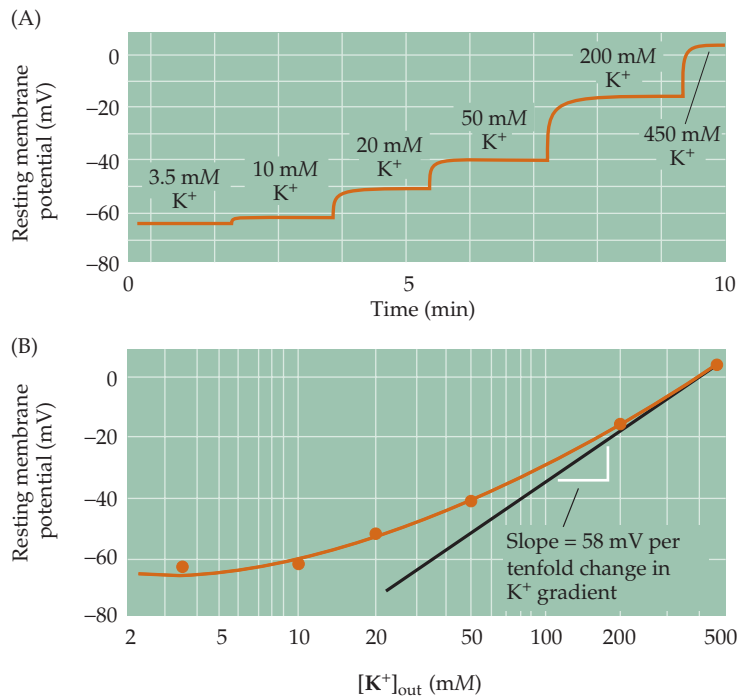


Figure 2.7 Experimental evidence that the resting membrane potential of a squid giant axon is determined by the K⁺ concentration gradient across the membrane. (A) Increasing the external K⁺ concentration makes the resting membrane potential more positive. (B) Relationship between resting membrane potential and external K⁺ concentration, plotted on a semi-logarithmic scale. The straight line represents a slope of 58 mV per tenfold change in concentration, as given by the Nernst equation. (After Hodgkin and Katz, 1949.)

When Hodgkin and Katz carried out this experiment on a living squid neuron, they found that the resting membrane potential did indeed change when the external K⁺ concentration was modified, becoming less negative as external K⁺ concentration was raised (Figure 2.7A). When the external K⁺ concentration was raised high enough to equal the concentration of K⁺ inside the neuron, thus making the K⁺ equilibrium potential 0 mV, the resting membrane potential was also approximately 0 mV. In short, the resting membrane potential varied as predicted with the logarithm of the K⁺ concentration, with a slope that approached 58 mV per tenfold change in K⁺ concentration (Figure 2.7B). The value obtained was not exactly 58 mV because other ions, such as Cl⁻ and Na⁺, are also slightly permeable, and thus influence the resting potential to a small degree. The contribution of these other ions is particularly evident at low external K⁺ levels, again as predicted by the Goldman equation. In general, however, manipulation of the external concentrations of these other ions has only a small effect, emphasizing that K⁺ permeability is indeed the primary source of the resting membrane potential.

In summary, Hodgkin and Katz showed that the inside-negative resting potential arises because (1) the membrane of the resting neuron is more permeable to K⁺ than to any of the other ions present, and (2) there is more K⁺ inside the neuron than outside. The selective permeability to K⁺ is caused by K⁺-permeable membrane channels that are open in resting neurons, and the

large K⁺ concentration gradient is, as noted, produced by membrane transporters that selectively accumulate K⁺ within neurons. Many subsequent studies have confirmed the general validity of these principles.

The Ionic Basis of Action Potentials

What causes the membrane potential of a neuron to depolarize during an action potential? Although a general answer to this question has been given (increased permeability to Na⁺), it is well worth examining some of the experimental support for this concept. Given the data presented in Table 2.1, one can use the Nernst equation to calculate that the equilibrium potential for Na⁺ (E_{Na}) in neurons, and indeed in most cells, is positive. Thus, if the membrane were to become highly permeable to Na⁺, the membrane potential would approach E_{Na} . Based on these considerations, Hodgkin and Katz hypothesized that the action potential arises because the neuronal membrane becomes temporarily permeable to Na⁺.

Taking advantage of the same style of ion substitution experiment they used to assess the resting potential, Hodgkin and Katz tested the role of Na⁺ in generating the action potential by asking what happens to the action potential when Na⁺ is removed from the external medium. They found that lowering the external Na⁺ concentration reduces both the rate of rise of the action potential and its peak amplitude (Figure 2.8A–C). Indeed, when they examined this Na⁺ dependence quantitatively, they found a more-or-less linear relationship between the amplitude of the action potential and the logarithm of the external Na⁺ concentration (Figure 2.8D). The slope of this rela-

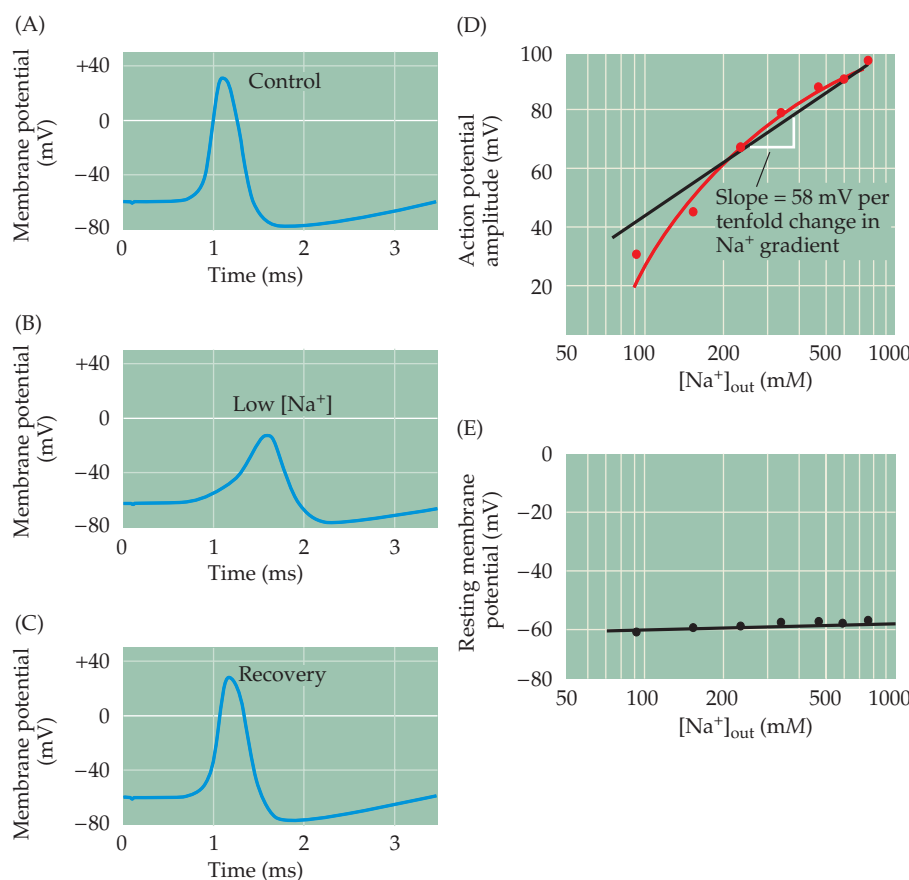


Figure 2.8 The role of sodium in the generation of an action potential in a squid giant axon. (A) An action potential evoked with the normal ion concentrations inside and outside the cell. (B) The amplitude and rate of rise of the action potential diminish when external sodium concentration is reduced to one-third of normal, but (C) recover when the Na⁺ is replaced. (D) While the amplitude of the action potential is quite sensitive to the external concentration of Na⁺, the resting membrane potential (E) is little affected by changing the concentration of this ion. (After Hodgkin and Katz, 1949.)

Box B

Action Potential Form and Nomenclature

The action potential of the squid giant axon has a characteristic shape, or waveform, with a number of different phases (Figure A). During the rising phase, the membrane potential rapidly depolarizes. In fact, action potentials cause the membrane potential to depolarize so much that the membrane potential transiently becomes positive with respect to the external medium, producing an overshoot. The overshoot of the action potential gives way to a falling phase in which the membrane potential rapidly repolarizes. Repolarization takes the membrane potential to levels even more negative than the resting membrane potential for a short time; this brief period of hyperpolarization is called the undershoot.

Although the waveform of the squid action potential is typical, the details of the action potential form vary widely from neuron to neuron in different animals. In myelinated axons of vertebrate motor neurons (Figure B), the action potential is virtually indistinguishable from that of the squid axon. However, the action potential recorded in the cell body of this same motor neuron (Figure

C) looks rather different. Thus, the action potential waveform can vary even within the same neuron. More complex action potentials are seen in other central neurons. For example, action potentials recorded from the cell bodies of neurons in the mammalian inferior olive (a region of the brainstem involved in motor control) last tens of milliseconds (Figure D). These action potentials exhibit a pronounced plateau during their falling phase, and their undershoot lasts even longer than that of the motor neuron. One of the most dramatic types of action potentials occurs in the cell bodies of cerebellar Purkinje neurons (Figure E). These potentials have several complex phases that result from the summation of multiple, discrete action potentials.

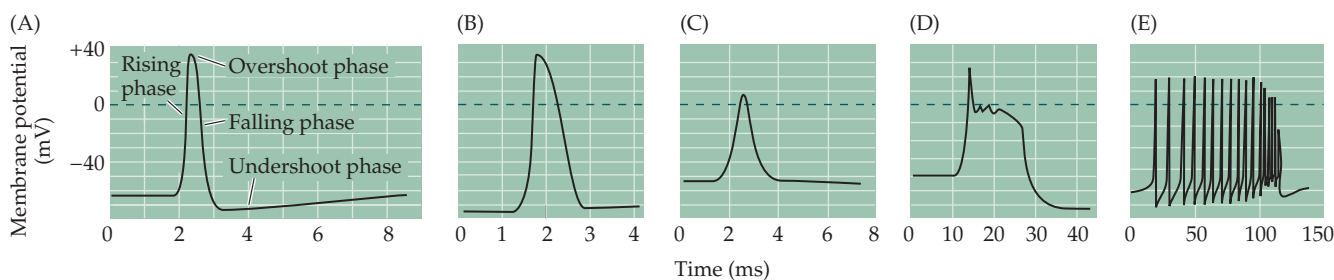
The variety of action potential waveforms could mean that each type of neuron has a different mechanism of action potential production. Fortunately, however, these diverse waveforms all result from relatively minor variations in the scheme used by the squid giant axon. For example, plateaus in the repolarization phase result from the presence of

ion channels that are permeable to Ca^{2+} , and long-lasting undershoots result from the presence of additional types of membrane K^+ channels. The complex action potential of the Purkinje cell results from these extra features plus the fact that different types of action potentials are generated in various parts of the Purkinje neuron—cell body, dendrites, and axons—and are summed together in recordings from the cell body. Thus, the lessons learned from the squid axon are applicable to, and indeed essential for, understanding action potential generation in all neurons.

References

- BARRETT, E. F. AND J. N. BARRETT (1976) Separation of two voltage-sensitive potassium currents, and demonstration of a tetrodotoxin-resistant calcium current in frog motoneurones. *J. Physiol. (Lond.)* 255: 737–774.
- DODGE, F. A. AND B. FRANKENHAEUSER (1958) Membrane currents in isolated frog nerve fibre under voltage clamp conditions. *J. Physiol. (Lond.)* 143: 76–90.
- HODGKIN, A. L. AND A. F. HUXLEY (1939) Action potentials recorded from inside a nerve fibre. *Nature* 144: 710–711.
- LLINÁS, R. AND M. SUGIMORI (1980) Electrophysiological properties of *in vitro* Purkinje cell dendrites in mammalian cerebellar slices. *J. Physiol. (Lond.)* 305: 197–213.
- LLINÁS, R. AND Y. YAROM (1981) Electrophysiology of mammalian inferior olivary neurones *in vitro*. Different types of voltage-dependent ionic conductances. *J. Physiol. (Lond.)* 315: 549–567.

(A) The phases of an action potential of the squid giant axon. (B) Action potential recorded from a myelinated axon of a frog motor neuron. (C) Action potential recorded from the cell body of a frog motor neuron. The action potential is smaller and the undershoot prolonged in comparison to the action potential recorded from the axon of this same neuron (B). (D) Action potential recorded from the cell body of a neuron from the inferior olive of a guinea pig. This action potential has a pronounced plateau during its falling phase. (E) Action potential recorded from the cell body of a Purkinje neuron in the cerebellum of a guinea pig. (A after Hodgkin and Huxley, 1939; B after Dodge and Frankenhaeuser, 1958; C after Barrett and Barrett, 1976; D after Llinás and Yarom, 1981; E after Llinás and Sugimori, 1980.)



tionship approached a value of 58 mV per tenfold change in Na^+ concentration, as expected for a membrane selectively permeable to Na^+ . In contrast, lowering Na^+ concentration had very little effect on the resting membrane potential (Figure 2.8E). Thus, while the resting neuronal membrane is only slightly permeable to Na^+ , the membrane becomes extraordinarily permeable to Na^+ during the **rising phase** and **overshoot phase** of the action potential (see Box B for an explanation of action potential nomenclature). This temporary increase in Na^+ permeability results from the opening of Na^+ -selective channels that are essentially closed in the resting state. Membrane pumps maintain a large electrochemical gradient for Na^+ , which is in much higher concentration outside the neuron than inside. When the Na^+ channels open, Na^+ flows into the neuron, causing the membrane potential to depolarize and approach E_{Na} .

The time that the membrane potential lingers near E_{Na} (about +58 mV) during the overshoot phase of an action potential is brief because the increased membrane permeability to Na^+ itself is short-lived. The membrane potential rapidly repolarizes to resting levels and is actually followed by a transient **undershoot**. As will be described in Chapter 3, these latter events in the action potential are due to an inactivation of the Na^+ permeability and an increase in the K^+ permeability of the membrane. During the undershoot, the membrane potential is transiently hyperpolarized because K^+ permeability becomes even greater than it is at rest. The action potential ends when this phase of enhanced K^+ permeability subsides, and the membrane potential thus returns to its normal resting level.

The ion substitution experiments carried out by Hodgkin and Katz provided convincing evidence that the resting membrane potential results from a high resting membrane permeability to K^+ , and that depolarization during an action potential results from a transient rise in membrane Na^+ permeability. Although these experiments identified the ions that flow during an action potential, they did not establish *how* the neuronal membrane is able to change its ionic permeability to generate the action potential, or what mechanisms trigger this critical change. The next chapter addresses these issues, documenting the surprising conclusion that the neuronal membrane potential itself affects membrane permeability.

Summary

Nerve cells generate electrical signals to convey information over substantial distances and to transmit it to other cells by means of synaptic connections. These signals ultimately depend on changes in the resting electrical potential across the neuronal membrane. A resting potential occurs because nerve cell membranes are permeable to one or more ion species subject to an electrochemical gradient. More specifically, a negative membrane potential at rest results from a net efflux of K^+ across neuronal membranes that are predominantly permeable to K^+ . In contrast, an action potential occurs when a transient rise in Na^+ permeability allows a net flow of Na^+ in the opposite direction across the membrane that is now predominantly permeable to Na^+ . The brief rise in membrane Na^+ permeability is followed by a secondary, transient rise in membrane K^+ permeability that repolarizes the neuronal membrane and produces a brief undershoot of the action potential. As a result of these processes, the membrane is depolarized in an all-or-none fashion during an action potential. When these active permeability changes subside, the membrane potential returns to its resting level because of the high resting membrane permeability to K^+ .

Additional Reading

Reviews

HODGKIN, A. L. (1951) The ionic basis of electrical activity in nerve and muscle. *Biol. Rev.* 26: 339–409.

HODGKIN, A. L. (1958) The Croonian Lecture: Ionic movements and electrical activity in giant nerve fibres. *Proc. R. Soc. Lond. (B)* 148: 1–37.

Important Original Papers

BAKER, P. F., A. L. HODGKIN AND T. I. SHAW (1962) Replacement of the axoplasm of giant nerve fibres with artificial solutions. *J. Physiol. (London)* 164: 330–354.

COLE, K. S. AND H. J. CURTIS (1939) Electric impedance of the squid giant axon during activity. *J. Gen. Physiol.* 22: 649–670.

GOLDMAN, D. E. (1943) Potential, impedance, and rectification in membranes. *J. Gen. Physiol.* 27: 37–60.

HODGKIN, A. L. AND P. HOROWICZ (1959) The influence of potassium and chloride ions on the membrane potential of single muscle fibres. *J. Physiol. (London)* 148: 127–160.

HODGKIN, A. L. AND B. KATZ (1949) The effect of sodium ions on the electrical activity of the giant axon of the squid. *J. Physiol. (London)* 108: 37–77.

HODGKIN, A. L. AND R. D. KEYNES (1953) The mobility and diffusion coefficient of potassium in giant axons from *Sepia*. *J. Physiol. (London)* 119: 513–528.

KEYNES, R. D. (1951) The ionic movements during nervous activity. *J. Physiol. (London)* 114: 119–150.

Books

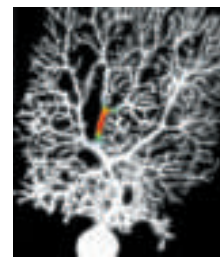
HODGKIN, A. L. (1967) *The Conduction of the Nervous Impulse*. Springfield, IL: Charles C. Thomas.

HODGKIN, A. L. (1992) *Chance and Design*. Cambridge: Cambridge University Press.

JUNGE, D. (1992) *Nerve and Muscle Excitation*, 3rd Ed. Sunderland, MA: Sinauer Associates.

KATZ, B. (1966) *Nerve, Muscle, and Synapse*. New York: McGraw-Hill.

Chapter 3



Voltage-Dependent Membrane Permeability

Overview

The action potential, the primary electrical signal generated by nerve cells, reflects changes in membrane permeability to specific ions. Present understanding of these changes in ionic permeability is based on evidence obtained by the voltage clamp technique, which permits detailed characterization of permeability changes as a function of membrane potential and time. For most types of axons, these changes consist of a rapid and transient rise in sodium (Na^+) permeability, followed by a slower but more prolonged rise in potassium (K^+) permeability. Both permeabilities are voltage-dependent, increasing as the membrane potential depolarizes. The kinetics and voltage dependence of Na^+ and K^+ permeabilities provide a complete explanation of action potential generation. Depolarizing the membrane potential to the threshold level causes a rapid, self-sustaining increase in Na^+ permeability that produces the rising phase of the action potential; however, the Na^+ permeability increase is short-lived and is followed by a slower increase in K^+ permeability that restores the membrane potential to its usual negative resting level. A mathematical model that describes the behavior of these ionic permeabilities predicts virtually all of the observed properties of action potentials. Importantly, this same ionic mechanism permits action potentials to be propagated along the length of neuronal axons, explaining how electrical signals are conveyed throughout the nervous system.

Ionic Currents Across Nerve Cell Membranes

The previous chapter introduced the idea that nerve cells generate electrical signals by virtue of a membrane that is differentially permeable to various ion species. In particular, a transient increase in the permeability of the neuronal membrane to Na^+ initiates the action potential. This chapter considers exactly how this increase in Na^+ permeability occurs. A key to understanding this phenomenon is the observation that action potentials are initiated *only* when the neuronal membrane potential becomes more positive than a threshold level. This observation suggests that the mechanism responsible for the increase in Na^+ permeability is sensitive to the membrane potential. Therefore, if one could understand how a change in membrane potential activates Na^+ permeability, it should be possible to explain how action potentials are generated.

The fact that the Na^+ permeability that generates the membrane potential change is itself sensitive to the membrane potential presents both conceptual and practical obstacles to studying the mechanism of the action potential. A practical problem is the difficulty of systematically varying the membrane

Box A

The Voltage Clamp Method

Breakthroughs in scientific research often rely on the development of new technologies. In the case of the action potential, detailed understanding came only after the invention of the voltage clamp technique by Kenneth Cole in the 1940s. This device is called a voltage clamp because it controls, or clamps, membrane potential (or voltage) at any level desired by the experimenter. The method measures the membrane potential with a microelectrode (or other type of electrode) placed inside the cell (1), and electronically compares this voltage to the voltage to be maintained (called the *command voltage*) (2). The clamp circuitry then passes a current back into the cell through another intracellular elec-

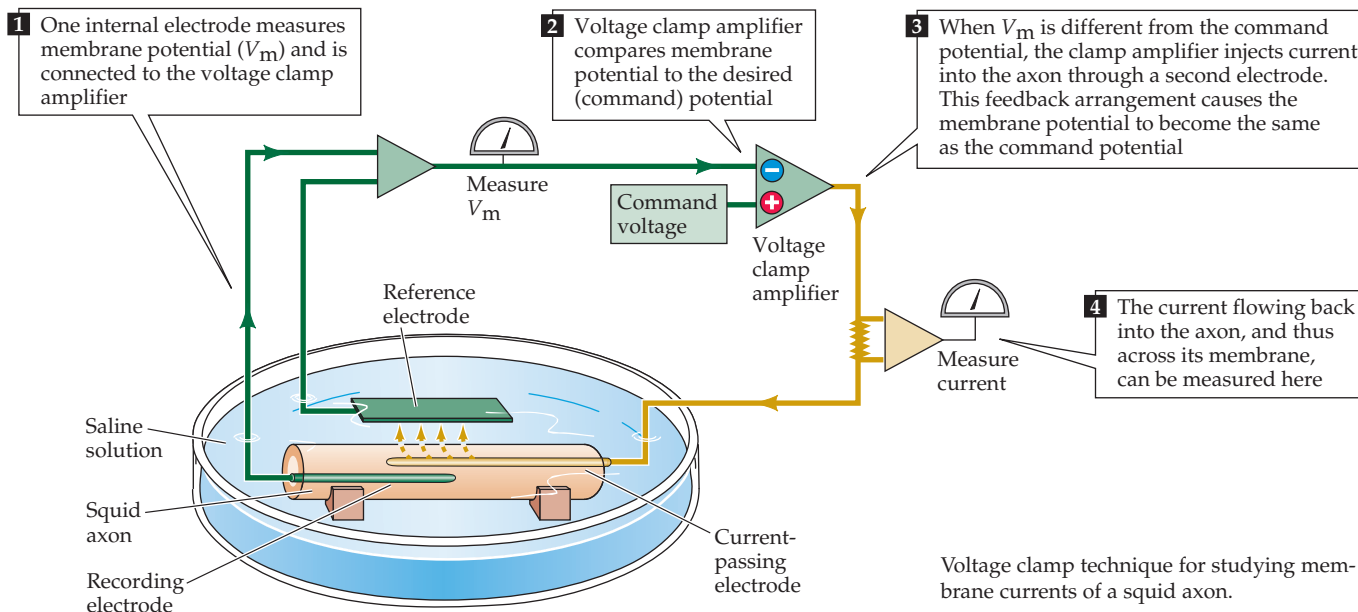
trode (3). This electronic feedback circuit holds the membrane potential at the desired level, even in the face of permeability changes that would normally alter the membrane potential (such as those generated during the action potential). Most importantly, the device permits the simultaneous measurement of the current needed to keep the cell at a given voltage (4). This current is exactly equal to the amount of current flowing across the neuronal membrane, allowing direct measurement of these membrane currents. Therefore, the voltage clamp technique can indicate how membrane potential influences ionic current flow across the membrane. This information gave Hodgkin and Huxley the key

insights that led to their model for action potential generation.

Today, the voltage clamp method remains widely used to study ionic currents in neurons and other cells. The most popular contemporary version of this approach is the patch clamp technique, a method that can be applied to virtually any cell and has a resolution high enough to measure the minute electrical currents flowing through single ion channels (see Box A in Chapter 4).

References

COLE, K. S. (1968) *Membranes, Ions and Impulses: A Chapter of Classical Biophysics*. Berkeley, CA: University of California Press.



Voltage clamp technique for studying membrane currents of a squid axon.

potential to study the permeability change, because such changes in membrane potential will produce an action potential, which causes further, uncontrolled changes in the membrane potential. Historically, then, it was not really possible to understand action potentials until a technique was developed that allowed experimenters to control membrane potential *and* simultaneously measure the underlying permeability changes. This tech-

nique, the **voltage clamp method** (Box A), provides the information needed to define the ionic permeability of the membrane at any level of membrane potential.

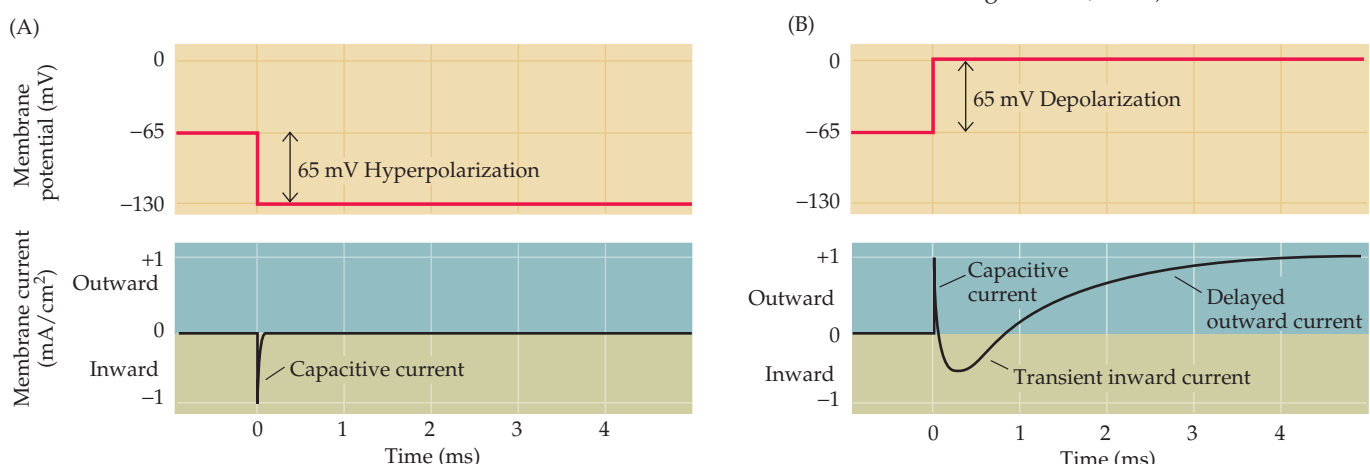
In the late 1940s, Alan Hodgkin and Andrew Huxley working at the University of Cambridge used the voltage clamp technique to work out the permeability changes underlying the action potential. They again chose to use the giant neuron of the squid because its large size (up to 1 mm in diameter; see Box A in Chapter 2) allowed insertion of the electrodes necessary for voltage clamping. They were the first investigators to test directly the hypothesis that potential-sensitive Na^+ and K^+ permeability changes are both necessary and sufficient for the production of action potentials.

Hodgkin and Huxley's first goal was to determine whether neuronal membranes do, in fact, have voltage-dependent permeabilities. To address this issue, they asked whether ionic currents flow across the membrane when its potential is changed. The result of one such experiment is shown in Figure 3.1. Figure 3.1A illustrates the currents produced by a squid axon when its membrane potential, V_m , is hyperpolarized from the resting level of -65 mV to -130 mV . The initial response of the axon results from the redistribution of charge across the axonal membrane. This capacitive current is nearly instantaneous, ending within a fraction of a millisecond. Aside from this brief event, very little current flows when the membrane is hyperpolarized. However, when the membrane potential is depolarized from -65 mV to 0 mV , the response is quite different (Figure 3.1B). Following the capacitive current, the axon produces a rapidly rising inward ionic current (inward refers to a positive charge entering the cell—that is, cations in or anions out), which gives way to a more slowly rising, delayed outward current. The fact that membrane depolarization elicits these ionic currents establishes that the membrane permeability of axons is indeed voltage-dependent.

Two Types of Voltage-Dependent Ionic Current

The results shown in Figure 3.1 demonstrate that the ionic permeability of neuronal membranes is voltage-sensitive, but the experiments do not identify how many types of permeability exist, or which ions are involved. As discussed in Chapter 2 (see Figure 2.5), varying the potential across a membrane makes it possible to deduce the equilibrium potential for the ionic fluxes through the membrane, and thus to identify the ions that are flowing.

Figure 3.1 Current flow across a squid axon membrane during a voltage clamp experiment. (A) A 65 mV hyperpolarization of the membrane potential produces only a very brief capacitive current. (B) A 65 mV depolarization of the membrane potential also produces a brief capacitive current, which is followed by a longer lasting but transient phase of inward current and a delayed but sustained outward current. (After Hodgkin et al., 1952.)



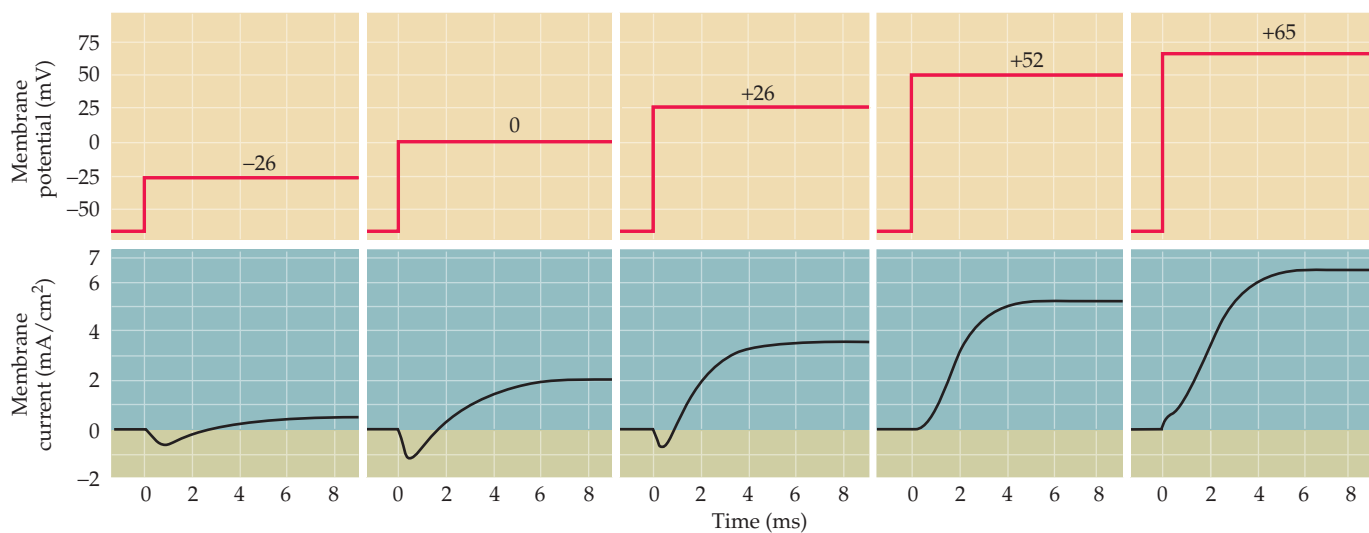


Figure 3.2 Current produced by membrane depolarizations to several different potentials. The early current first increases, then decreases in magnitude as the depolarization increases; note that this current is actually reversed in polarity at potentials more positive than about +55 mV. In contrast, the late current increases monotonically with increasing depolarization. (After Hodgkin et al., 1952.)

Because the voltage clamp method allows the membrane potential to be changed while ionic currents are being measured, it was a straightforward matter for Hodgkin and Huxley to determine ionic permeability by examining how the properties of the early inward and late outward currents changed as the membrane potential was varied (Figure 3.2). As already noted, no appreciable ionic currents flow at membrane potentials more negative than the resting potential. At more positive potentials, however, the currents not only flow but change in magnitude. The early current has a U-shaped dependence on membrane potential, increasing over a range of depolarizations up to approximately 0 mV but decreasing as the potential is depolarized further. In contrast, the late current increases monotonically with increasingly positive membrane potentials. These different responses to membrane potential can be seen more clearly when the magnitudes of the two current components are plotted as a function of membrane potential, as in Figure 3.3.

The voltage sensitivity of the early inward current gives an important clue about the nature of the ions carrying the current, namely, that no current flows when the membrane potential is clamped at +52 mV. For the squid neurons studied by Hodgkin and Huxley, the external Na^+ concentration is 440 mM, and the internal Na^+ concentration is 50 mM. For this concentration gradient, the Nernst equation predicts that the equilibrium poten-

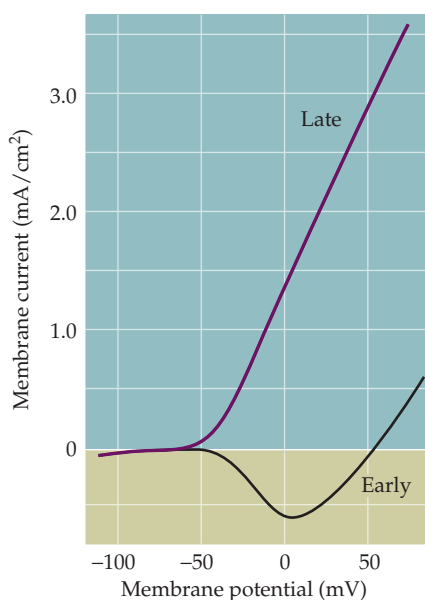


Figure 3.3 Relationship between current amplitude and membrane potential, taken from experiments such as the one shown in Figure 3.2. Whereas the late outward current increases steeply with increasing depolarization, the early inward current first increases in magnitude, but then decreases and reverses to outward current at about +55 mV (the sodium equilibrium potential). (After Hodgkin et al., 1952.)

Figure 3.4 Dependence of the early inward current on sodium. In the presence of normal external concentrations of Na^+ , depolarization of a squid axon to 0 mV produces an inward initial current. However, removal of external Na^+ causes the initial inward current to become outward, an effect that is reversed by restoration of external Na^+ . (After Hodgkin and Huxley, 1952a.)

tial for Na^+ should be +55 mV. Recall further from Chapter 2 that at the Na^+ equilibrium potential there is no net flux of Na^+ across the membrane, even if the membrane is highly permeable to Na^+ . Thus, the experimental observation that no current flows at the membrane potential where Na^+ cannot flow is a strong indication that the early inward current is carried by entry of Na^+ into the axon.

An even more demanding way to test whether Na^+ carries the early inward current is to examine the behavior of this current after removing external Na^+ . Removing the Na^+ outside the axon makes E_{Na} negative; if the permeability to Na^+ is increased under these conditions, current should flow outward as Na^+ leaves the neuron, due to the reversed electrochemical gradient. When Hodgkin and Huxley performed this experiment, they obtained the result shown in Figure 3.4. Removing external Na^+ caused the early inward current to reverse its polarity and become an outward current at a membrane potential that gave rise to an inward current when external Na^+ was present. This result demonstrates convincingly that the early inward current measured when Na^+ is present in the external medium must be due to Na^+ entering the neuron.

Notice that removal of external Na^+ in the experiment shown in Figure 3.4 has little effect on the outward current that flows after the neuron has been kept at a depolarized membrane voltage for several milliseconds. This further result shows that the late outward current must be due to the flow of an ion other than Na^+ . Several lines of evidence presented by Hodgkin, Huxley, and others showed that this late outward current is caused by K^+ exiting the neuron. Perhaps the most compelling demonstration of K^+ involvement is that the amount of K^+ efflux from the neuron, measured by loading the neuron with radioactive K^+ , is closely correlated with the magnitude of the late outward current.

Taken together, these experiments using the voltage clamp show that changing the membrane potential to a level more positive than the resting potential produces two effects: an early influx of Na^+ into the neuron, followed by a delayed efflux of K^+ . The early influx of Na^+ produces a transient inward current, whereas the delayed efflux of K^+ produces a sustained outward current. The differences in the time course and ionic selectivity of the two fluxes suggest that two different ionic permeability mechanisms are activated by changes in membrane potential. Confirmation that there are indeed two distinct mechanisms has come from pharmacological studies of drugs that specifically affect these two currents (Figure 3.5). **Tetrodotoxin**, an alkaloid neurotoxin found in certain puffer fish, tropical frogs, and salamanders, blocks the Na^+ current without affecting the K^+ current. Conversely, **tetraethylammonium ions** block K^+ currents without affecting Na^+ currents. The differential sensitivity of Na^+ and K^+ currents to these drugs provides strong additional evidence that Na^+ and K^+ flow through independent permeability pathways. As discussed in Chapter 4, it is now known that these pathways are ion channels that are selectively permeable to either Na^+ or K^+ . In fact, tetrodotoxin, tetraethylammonium, and other drugs that interact with spe-

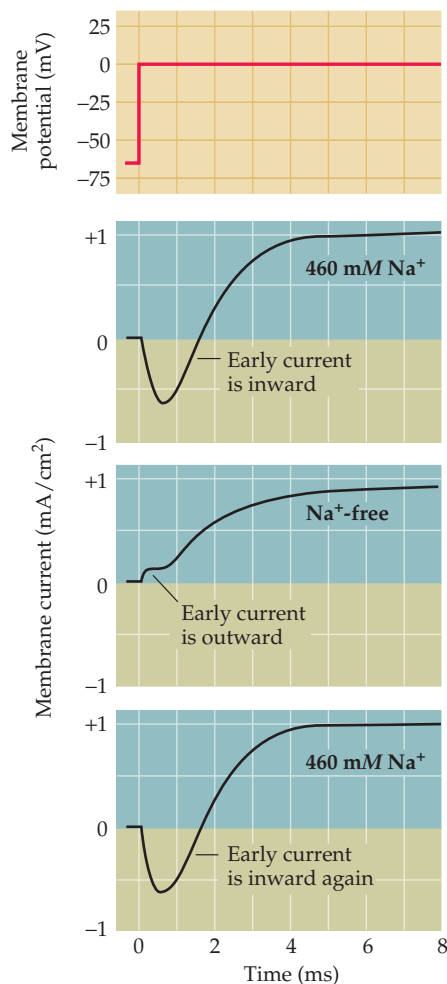
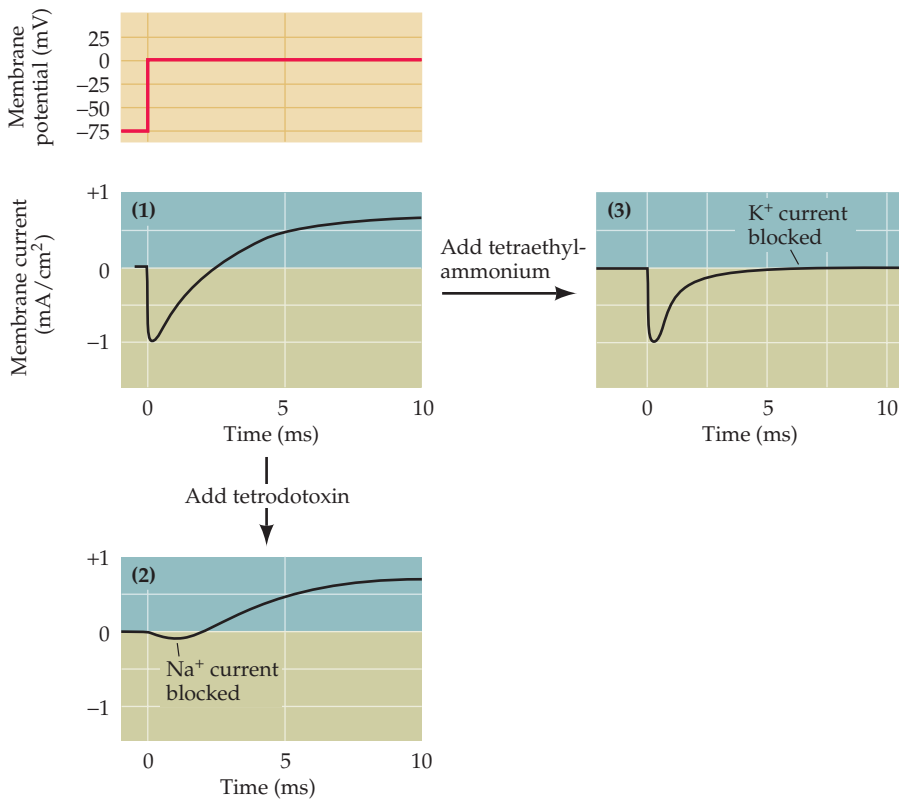


Figure 3.5 Pharmacological separation of Na^+ and K^+ currents into sodium and potassium components. Panel (1) shows the current that flows when the membrane potential of a squid axon is depolarized to 0 mV in control conditions. (2) Treatment with tetrodotoxin causes the early Na^+ currents to disappear but spares the late K^+ currents. (3) Addition of tetraethylammonium blocks the K^+ currents without affecting the Na^+ currents. (After Moore et al., 1967 and Armstrong and Binstock, 1965.)



cific types of ion channels have been extraordinarily useful tools in characterizing these channel molecules (see Chapter 4).

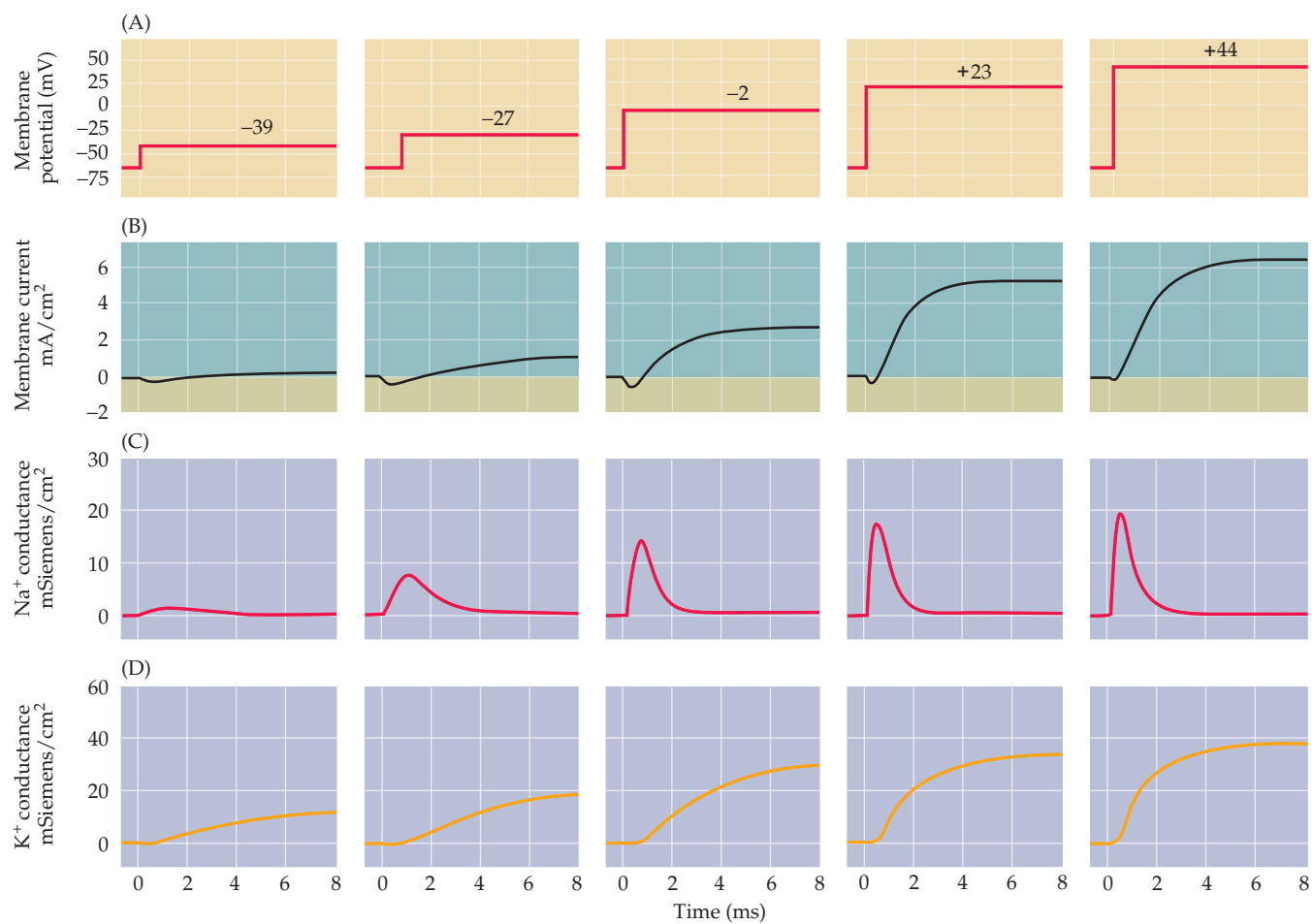
Two Voltage-Dependent Membrane Conductances

The next goal Hodgkin and Huxley set for themselves was to describe Na^+ and K^+ permeability changes mathematically. To do this, they assumed that the ionic currents are due to a change in **membrane conductance**, defined as the reciprocal of the membrane resistance. Membrane conductance is thus closely related, although not identical, to membrane permeability. When evaluating ionic movements from an electrical standpoint, it is convenient to describe them in terms of ionic conductances rather than ionic permeabilities. For present purposes, permeability and conductance can be considered synonymous. If membrane conductance (g) obeys Ohm's Law (which states that voltage is equal to the product of current and resistance), then the ionic current that flows during an increase in membrane conductance is given by

$$I_{\text{ion}} = g_{\text{ion}} (V_m - E_{\text{ion}})$$

where I_{ion} is the ionic current, V_m is the membrane potential, and E_{ion} is the equilibrium potential for the ion flowing through the conductance, g_{ion} . The difference between V_m and E_{ion} is the electrochemical driving force acting on the ion.

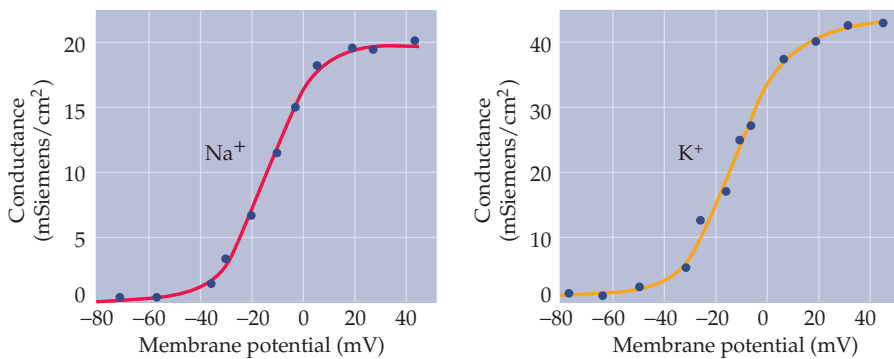
Hodgkin and Huxley used this simple relationship to calculate the dependence of Na^+ and K^+ conductances on time and membrane potential. They knew V_m , which was set by their voltage clamp device (Figure 3.6A), and could determine E_{Na} and E_{K} from the ionic concentrations on the two sides



of the axonal membrane (see Table 2.1). The currents carried by Na^+ and K^+ — I_{Na} and I_{K} —could be determined separately from recordings of the membrane currents resulting from depolarization (Figure 3.6B) by measuring the difference between currents recorded in the presence and absence of external Na^+ (as shown in Figure 3.4). From these measurements, Hodgkin and Huxley were able to calculate g_{Na} and g_{K} (Figure 3.6C,D), from which they drew two fundamental conclusions. The first conclusion is that the Na^+ and K^+ conductances change over time. For example, both Na^+ and K^+ conductances require some time to **activate**, or turn on. In particular, the K^+ conductance has a pronounced delay, requiring several milliseconds to reach its maximum (Figure 3.6D), whereas the Na^+ conductance reaches its maximum more rapidly (Figure 3.6C). The more rapid activation of the Na^+ conductance allows the resulting inward Na^+ current to precede the delayed outward K^+ current (see Figure 3.6B). Although the Na^+ conductance rises rapidly, it quickly declines, even though the membrane potential is kept at a depolarized level. This fact shows that depolarization not only causes the Na^+ conductance to activate, but also causes it to decrease over time, or **inactivate**. The K^+ conductance of the squid axon does not inactivate in this way; thus, while the Na^+ and K^+ conductances share the property of time-dependent activation, only the Na^+ conductance inactivates. (Inactivating K^+ conductances have since been discovered in other types of nerve cells; see Chapter 4.) The time courses of the Na^+ and K^+ conductances are voltage-

Figure 3.6 Membrane conductance changes underlying the action potential are time- and voltage-dependent. Depolarizations to various membrane potentials (A) elicit different membrane currents (B). Below are shown the Na^+ (C) and K^+ (D) conductances calculated from these currents. Both peak Na^+ conductance and steady-state K^+ conductance increase as the membrane potential becomes more positive. In addition, the activation of both conductances, as well as the rate of inactivation of the Na^+ conductance, occur more rapidly with larger depolarizations. (After Hodgkin and Huxley, 1952b.)

Figure 3.7 Depolarization increases Na^+ and K^+ conductances of the squid giant axon. The peak magnitude of Na^+ conductance and steady-state value of K^+ conductance both increase steeply as the membrane potential is depolarized. (After Hodgkin and Huxley, 1952b.)



dependent, with the speed of both activation and inactivation increasing at more depolarized potentials. This finding accounts for more rapid time courses of membrane currents measured at more depolarized potentials.

The second conclusion derived from Hodgkin and Huxley's calculations is that both the Na^+ and K^+ conductances are voltage-dependent—that is, both conductances increase progressively as the neuron is depolarized. Figure 3.7 illustrates this by plotting the relationship between peak value of the conductances (from Figure 3.6C,D) against the membrane potential. Note the similar voltage dependence for each conductance; both conductances are quite small at negative potentials, maximal at very positive potentials, and exquisitely dependent on membrane voltage at intermediate potentials. The observation that these conductances are sensitive to changes in membrane potential shows that the mechanism underlying the conductances somehow “senses” the voltage across the membrane.

All told, the voltage clamp experiments carried out by Hodgkin and Huxley showed that the ionic currents that flow when the neuronal membrane is depolarized are due to three different voltage-sensitive processes: (1) activation of Na^+ conductance, (2) activation of K^+ conductance, and (3) inactivation of Na^+ conductance.

Reconstruction of the Action Potential

From their experimental measurements, Hodgkin and Huxley were able to construct a detailed mathematical model of the Na^+ and K^+ conductance changes. The goal of these modeling efforts was to determine whether the Na^+ and K^+ conductances alone are sufficient to produce an action potential. Using this information, they could in fact generate the form and time course of the action potential with remarkable accuracy (Figure 3.8A). Further, the Hodgkin-Huxley model predicted other features of action potential behavior in the squid axon, such as how the delay before action potential generation changes in response to stimulating currents of different intensities (Figure 3.8B,C). The model also predicted that the axon membrane would become refractory to further excitation for a brief period following an action potential, as was experimentally observed.

The Hodgkin-Huxley model also provided many insights into how action potentials are generated. Figure 3.8A shows a reconstructed action potential, together with the time courses of the underlying Na^+ and K^+ conductances. The coincidence of the initial increase in Na^+ conductance with the rapid rising phase of the action potential demonstrates that a selective increase in

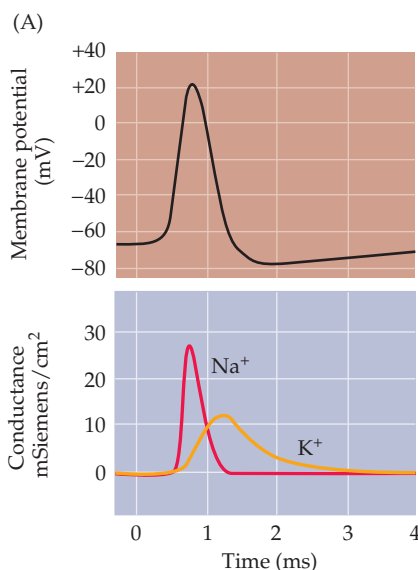
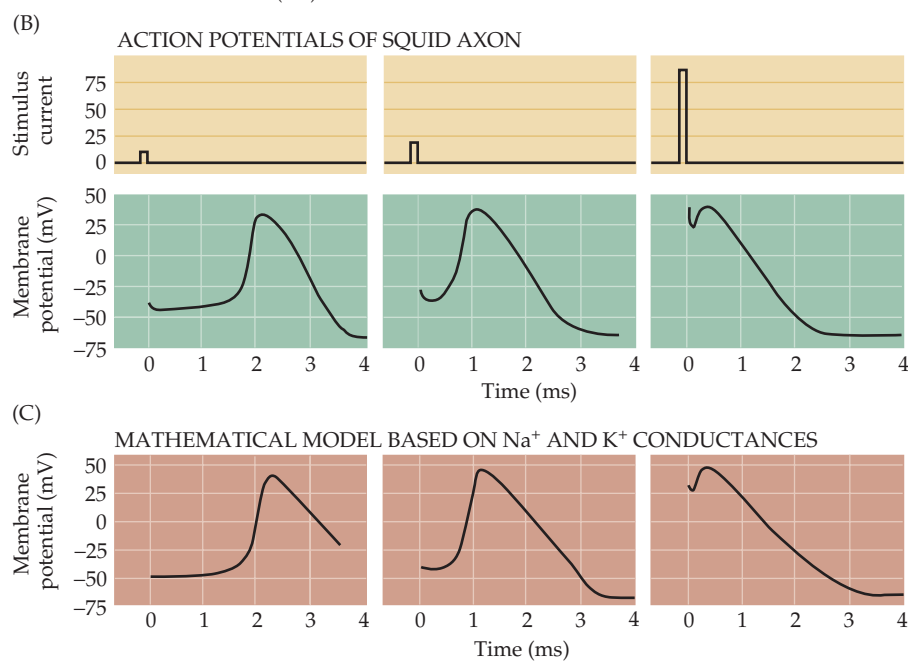


Figure 3.8 Mathematical reconstruction of the action potential. (A) Reconstruction of an action potential (black curve) together with the underlying changes in Na^+ (red curve) and K^+ (yellow curve) conductance. The size and time course of the action potential were calculated using only the properties of g_{Na} and g_{K} measured in voltage clamp experiments. Real action potentials evoked by brief current pulses of different intensities (B) are remarkably similar to those generated by the mathematical model (C). The reconstructed action potentials shown in (A) and (C) differ in duration because (A) simulates an action potential at 19°C, whereas (C) simulates an action potential at 6°C. (After Hodgkin and Huxley, 1952d.)



Na^+ conductance is responsible for action potential initiation. The increase in Na^+ conductance causes Na^+ to enter the neuron, thus depolarizing the membrane potential, which approaches E_{Na} . The rate of depolarization subsequently falls both because the electrochemical driving force on Na^+ decreases and because the Na^+ conductance inactivates. At the same time, depolarization slowly activates the voltage-dependent K^+ conductance, causing K^+ to leave the cell and repolarizing the membrane potential toward E_{K} . Because the K^+ conductance becomes temporarily higher than it is in the resting condition, the membrane potential actually becomes briefly more negative than the normal resting potential (the **undershoot**). The hyperpolarization of the membrane potential causes the voltage-dependent K^+ conductance (and any Na^+ conductance not inactivated) to turn off, allowing the membrane potential to return to its resting level.

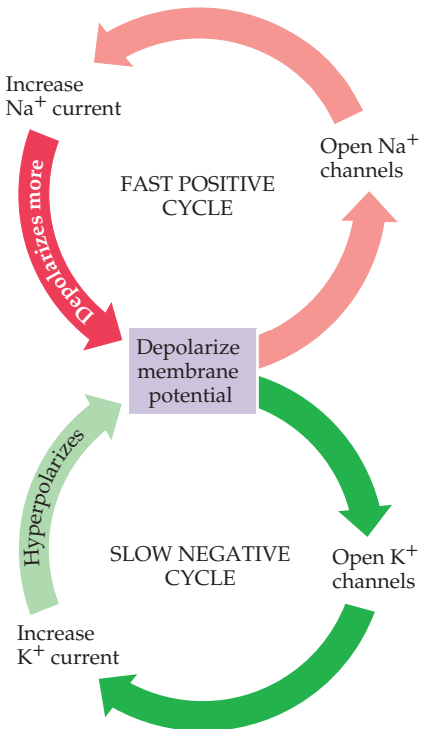


Figure 3.9 Feedback cycles responsible for membrane potential changes during an action potential. Membrane depolarization rapidly activates a positive feedback cycle fueled by the voltage-dependent activation of Na⁺ conductance. This phenomenon is followed by the slower activation of a negative feedback loop as depolarization activates a K⁺ conductance, which helps to repolarize the membrane potential and terminate the action potential.

This mechanism of action potential generation represents a positive feedback loop: Activating the voltage-dependent Na⁺ conductance increases Na⁺ entry into the neuron, which makes the membrane potential depolarize, which leads to the activation of still more Na⁺ conductance, more Na⁺ entry, and still further depolarization (Figure 3.9). Positive feedback continues unabated until Na⁺ conductance inactivation and K⁺ conductance activation restore the membrane potential to the resting level. Because this positive feedback loop, once initiated, is sustained by the intrinsic properties of the neuron—namely, the voltage dependence of the ionic conductances—the action potential is self-supporting, or **regenerative**. This regenerative quality explains why action potentials exhibit all-or-none behavior (see Figure 2.1), and why they have a threshold (Box B). The delayed activation of the K⁺ conductance represents a negative feedback loop that eventually restores the membrane to its resting state.

Hodgkin and Huxley's reconstruction of the action potential and all its features shows that the properties of the voltage-sensitive Na⁺ and K⁺ conductances, together with the electrochemical driving forces created by ion transporters, are sufficient to explain action potentials. Their use of both empirical and theoretical methods brought an unprecedented level of rigor to a long-standing problem, setting a standard of proof that is achieved only rarely in biological research.

Long-Distance Signaling by Means of Action Potentials

The voltage-dependent mechanisms of action potential generation also explain the long-distance transmission of these electrical signals. Recall from Chapter 2 that neurons are relatively poor conductors of electricity, at least compared to a wire. Current conduction by wires, and by neurons in the absence of action potentials, is called **passive current flow** (Box C). The passive electrical properties of a nerve cell axon can be determined by measuring the voltage change resulting from a current pulse passed across the axonal membrane (Figure 3.10A). If this current pulse is not large enough to generate action potentials, the magnitude of the resulting potential change decays exponentially with increasing distance from the site of current injection (Figure 3.10B). Typically, the potential falls to a small fraction of its initial value at a distance of no more than a couple of millimeters away from the site of injection (Figure 3.10C). The progressive decrease in the amplitude of the induced potential change occurs because the injected current leaks out across the axonal membrane; accordingly, less current is available to change the membrane potential farther along the axon. Thus, the leakiness of the axonal membrane prevents effective passive transmission of electrical signals in all but the shortest axons (those 1 mm or less in length). Likewise, the leakiness of the membrane slows the time course of the responses measured at increasing distances from the site where current was injected (Figure 3.10D).

Box B

Threshold

An important—and potentially puzzling—property of the action potential is its initiation at a particular membrane potential, called threshold. Indeed, action potentials never occur without a depolarizing stimulus that brings the membrane to this level. The depolarizing “trigger” can be one of several events: a synaptic input, a receptor potential generated by specialized receptor organs, the endogenous pacemaker activity of cells that generate action potentials spontaneously, or the local current that mediates the spread of the action potential down the axon.

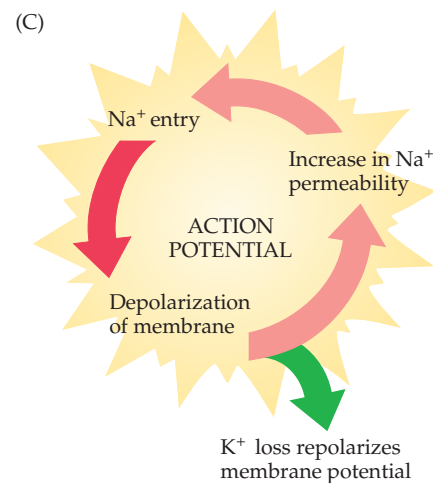
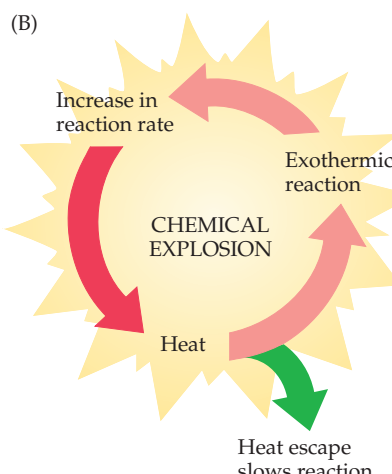
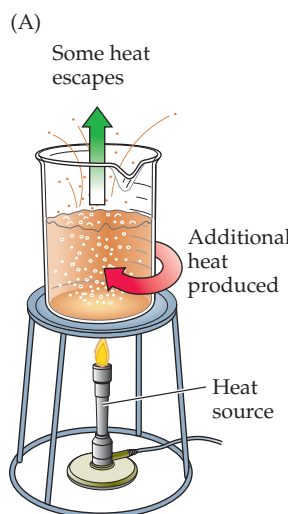
Why the action potential “takes off” at a particular level of depolarization can be understood by comparing the underlying events to a chemical explosion (Figure A). Exogenous heat (analogous to the initial depolarization of the membrane potential) stimulates an exothermic chemical reaction, which produces more heat, which further enhances the reaction (Figure B). As a result of this positive feedback loop, the rate of the reaction builds up exponentially—the definition of an explosion. In any such

process, however, there is a threshold, that is, a point up to which heat can be supplied without resulting in an explosion. The threshold for the chemical explosion diagrammed here is the point at which the amount of heat supplied exogenously is just equal to the amount of heat that can be dissipated by the circumstances of the reaction (such as escape of heat from the beaker).

The threshold of action potential initiation is, in principle, similar (Figure C). There is a range of “subthreshold” depolarization, within which the rate of increased sodium entry is less than the rate of potassium exit (remember that the membrane at rest is highly permeable to K^+ , which therefore flows out as the membrane is depolarized). The point at which Na^+ inflow just equals K^+ outflow represents an unstable equilibrium analogous to the ignition point of an explosive mixture. The behavior of the membrane at threshold reflects this instability: The membrane potential may linger at the threshold level for a variable period before either returning to the resting level or flaring up into a full-blown

action potential. In theory at least, if there is a net internal gain of a single Na^+ ion, an action potential occurs; conversely, the net loss of a single K^+ ion leads to repolarization. A more precise definition of threshold, therefore, is that value of membrane potential, in depolarizing from the resting potential, at which the current carried by Na^+ entering the neuron is exactly equal to the K^+ current that is flowing out. Once the triggering event depolarizes the membrane beyond this point, the positive feedback loop of Na^+ entry on membrane potential closes and the action potential “fires.”

Because the Na^+ and K^+ conductances change dynamically over time, the threshold potential for producing an action potential also varies as a consequence of the previous activity of the neuron. For example, following an action potential, the membrane becomes temporarily refractory to further excitation because the threshold for firing an action potential transiently rises. There is, therefore, no specific value of membrane potential that defines the threshold for a given nerve cell in all circumstances.



A positive feedback loop underlying the action potential explains the phenomenon of threshold.

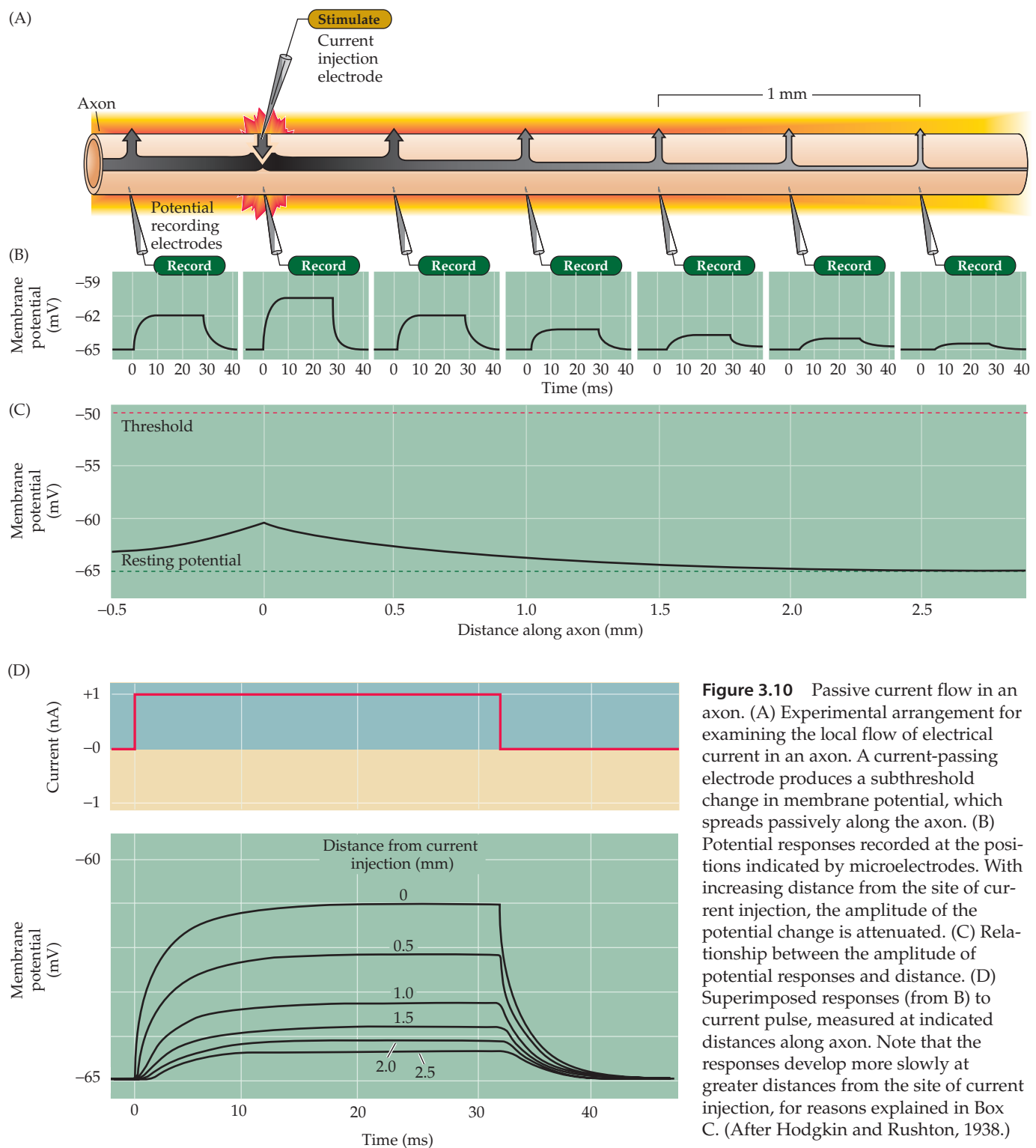
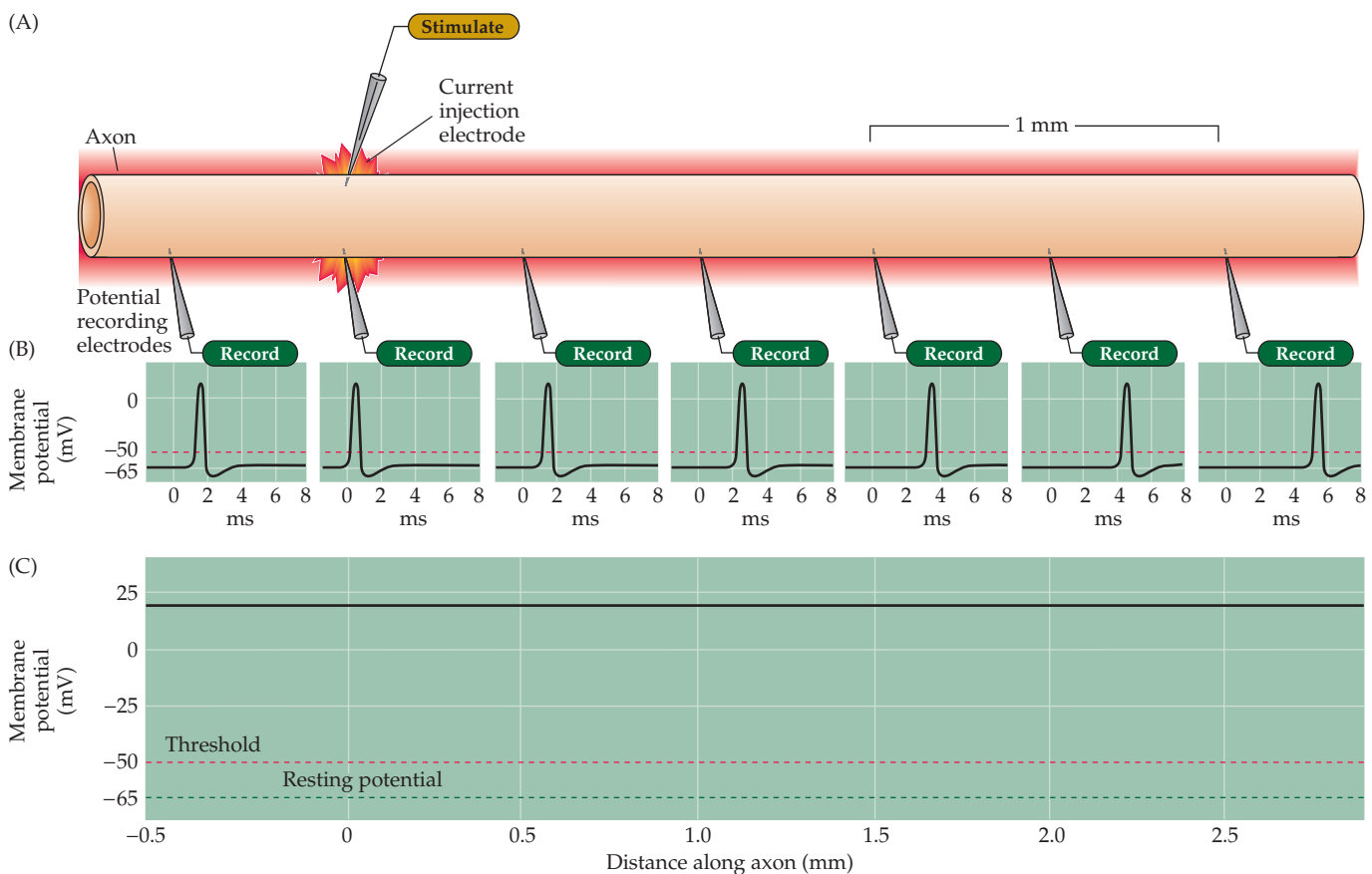


Figure 3.10 Passive current flow in an axon. (A) Experimental arrangement for examining the local flow of electrical current in an axon. A current-passing electrode produces a subthreshold change in membrane potential, which spreads passively along the axon. (B) Potential responses recorded at the positions indicated by microelectrodes. With increasing distance from the site of current injection, the amplitude of the potential change is attenuated. (C) Relationship between the amplitude of potential responses and distance. (D) Superimposed responses (from B) to current pulse, measured at indicated distances along axon. Note that the responses develop more slowly at greater distances from the site of current injection, for reasons explained in Box C. (After Hodgkin and Rushton, 1938.)

If the experiment shown in Figure 3.10 is repeated with a depolarizing current pulse large enough to produce an action potential, the result is dramatically different (Figure 3.11A). In this case, an action potential occurs without decrement along the entire length of the axon, which in humans



may be a distance of a meter or more (Figure 3.11B). Thus, action potentials somehow circumvent the inherent leakiness of neurons.

How, then, do action potentials traverse great distances along such a poor passive conductor? The answer is in part provided by the observation that the amplitude of the action potentials recorded at different distances is constant. This all-or-none behavior indicates that more than simple passive flow of current must be involved in action potential propagation. A second clue comes from examination of the time of occurrence of the action potentials recorded at different distances from the site of stimulation: Action potentials occur later and later at greater distances along the axon (Figure 3.11B). Thus, the action potential has a measurable rate of transmission, called the **conduction velocity**. The delay in the arrival of the action potential at successively more distant points along the axon differs from the case shown in Figure 3.10, in which the electrical changes produced by passive current flow occur at more or less the same time at successive points.

The mechanism of action potential propagation is easy to grasp once one understands how action potentials are generated and how current passively flows along an axon (Figure 3.12). A depolarizing stimulus—a synaptic potential or a receptor potential in an intact neuron, or an injected current pulse in an experiment—locally depolarizes the axon, thus opening the voltage-sensitive Na^+ channels in that region. The opening of Na^+ channels causes inward movement of Na^+ , and the resultant depolarization of the membrane potential generates an action potential at that site. Some of the local current generated by the action potential will then flow passively down

Figure 3.11 Propagation of an action potential. (A) In this experimental arrangement, an electrode evokes an action potential by injecting a suprathreshold current. (B) Potential responses recorded at the positions indicated by microelectrodes. The amplitude of the action potential is constant along the length of the axon, although the time of appearance of the action potential is delayed with increasing distance. (C) The constant amplitude of an action potential (solid black line) measured at different distances.

Box C

Passive Membrane Properties

The passive flow of electrical current plays a central role in action potential propagation, synaptic transmission, and all other forms of electrical signaling in nerve cells. Therefore, it is worthwhile understanding in quantitative terms how passive current flow varies with distance along a neuron. For the case of a cylindrical axon, such as the one depicted in Figure 3.10, subthreshold current injected into one part of the axon spreads passively along the axon until the current is dissipated by leakage out across the axon membrane. The decrement in the current flow with distance (Figure A) is described by a simple exponential function:

$$V_x = V_0 e^{-x/\lambda}$$

where V_x is the voltage response at any distance x along the axon, V_0 is the voltage change at the point where current is injected into the axon, e is the base of natural logarithms (approximately 2.7), and λ is the length constant of the axon. As evident in this relationship, the length constant is the distance where the initial voltage response (V_0) decays to $1/e$ (or 37%) of its value. The length constant is thus a way to characterize how far passive current flow spreads before it leaks out of the axon, with leakier axons having shorter length constants.

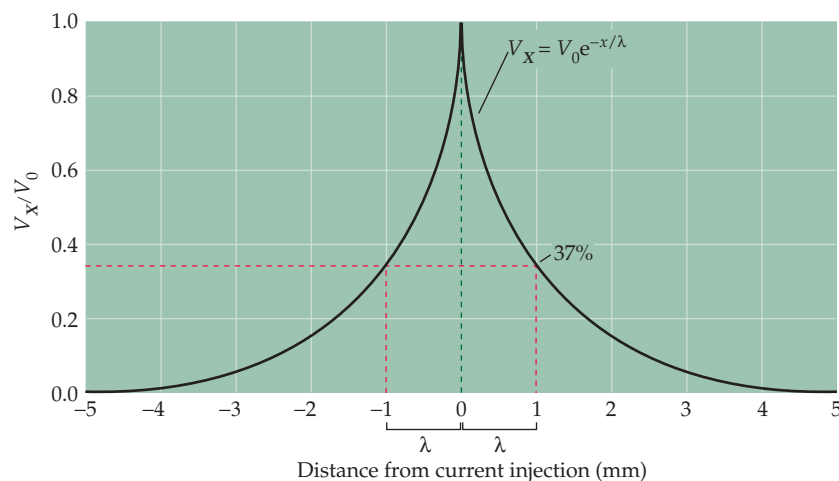
The length constant depends upon the physical properties of the axon, in particular the relative resistances of the

plasma membrane (r_m), the intracellular axoplasm (r_i), and the extracellular medium (r_0). The relationship between these parameters is:

$$\lambda = \sqrt{\frac{r_m}{r_0 + r_i}}$$

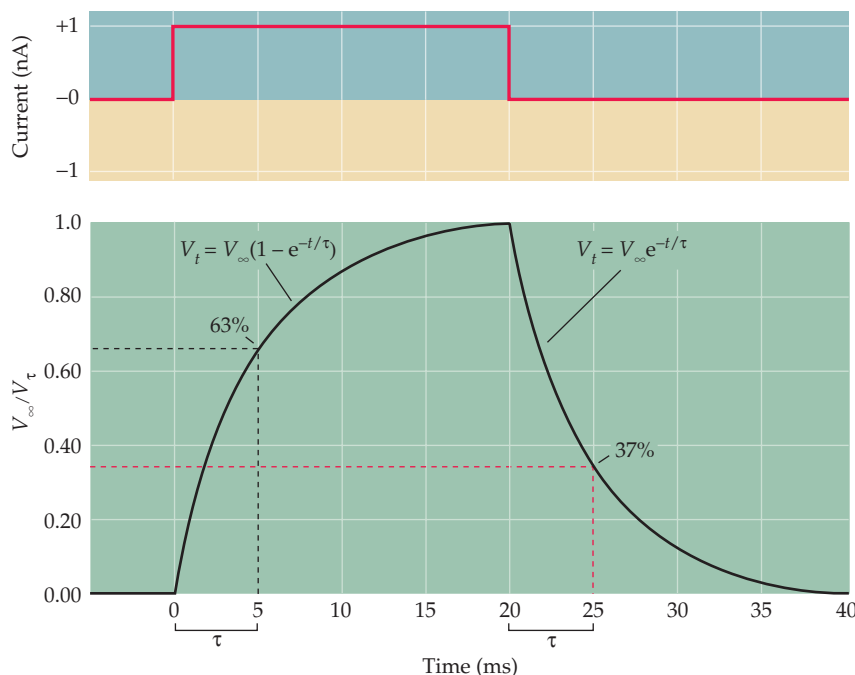
Hence, to improve the passive flow of current along an axon, the resistance of the plasma membrane should be as high as possible and the resistances of the axoplasm and extracellular medium should be low.

Another important consequence of the passive properties of neurons is that currents flowing across a membrane do not immediately change the membrane potential. For example, when a rectangular current pulse is injected into the axon shown in the experiment illustrated in Figure 3.10A, the membrane potential depolarizes slowly over a few milliseconds and then repolarizes over a similar time course when the current pulse ends (see Figure 3.10D). These delays in changing the membrane potential are due to the fact that the plasma mem-



(A) Spatial decay of membrane potential along a cylindrical axon. A current pulse injected at one point in the axon (0 mm) produces voltage responses (V_x) that decay exponentially with distance. The distance where the voltage response is $1/e$ of its initial value (V_0) is the length constant, λ .

the axon, in the same way that subthreshold currents spread along the axon (see Figure 3.10). Note that this passive current flow does not require the movement of Na^+ along the axon but, instead, occurs by a shuttling of charge, somewhat similar to what happens when wires passively conduct electricity by transmission of electron charge. This passive current flow depolarizes the membrane potential in the adjacent region of the axon, thus opening the Na^+ channels in the neighboring membrane. The local depolarization triggers an action potential in this region, which then spreads again in a continuing cycle until the end of the axon is reached. Thus, action potential propagation requires the coordinated action of two forms of current



(B) Time course of potential changes produced in a spatially uniform cell by a current pulse. The rise and fall of the membrane potential (V_t) can be described as exponential functions, with the time constant τ defining the time required for the response to rise to $1 - (1/e)$ of the steady-state value (V_∞), or to decline to $1/e$ of V_∞ .

brane behaves as a capacitor, storing the initial charge that flows at the beginning and end of the current pulse. For the case of a cell whose membrane potential is spatially uniform, the change in the membrane potential at any time, V_t , after beginning the current pulse (Figure B) can also be described by an exponential relationship:

$$V_t = V_\infty(1 - e^{-t/\tau})$$

where V_∞ is the steady-state value of the

membrane potential change, t is the time after the current pulse begins, and τ is the membrane time constant. The time constant is thus defined as the time when the voltage response (V_t) rises to $1 - (1/e)$ (or 63%) of V_∞ . After the current pulse ends, the membrane potential change also declines exponentially according to the relationship

$$V_t = V_\infty e^{-t/\tau}$$

During this decay, the membrane poten-

tial returns to $1/e$ of V_∞ at a time equal to t . For cells with more complex geometries than the axon in Figure 3.10, the time courses of the changes in membrane potential are not simple exponentials, but nonetheless depend on the membrane time constant. Thus, the time constant characterizes how rapidly current flow changes the membrane potential. The membrane time constant also depends on the physical properties of the nerve cell, specifically on the resistance (r_m) and capacitance (c_m) of the plasma membrane such that:

$$\tau = r_m c_m$$

The values of r_m and c_m depend, in part, on the size of the neuron, with larger cells having lower resistances and larger capacitances. In general, small nerve cells tend to have long time constants and large cells brief time constants.

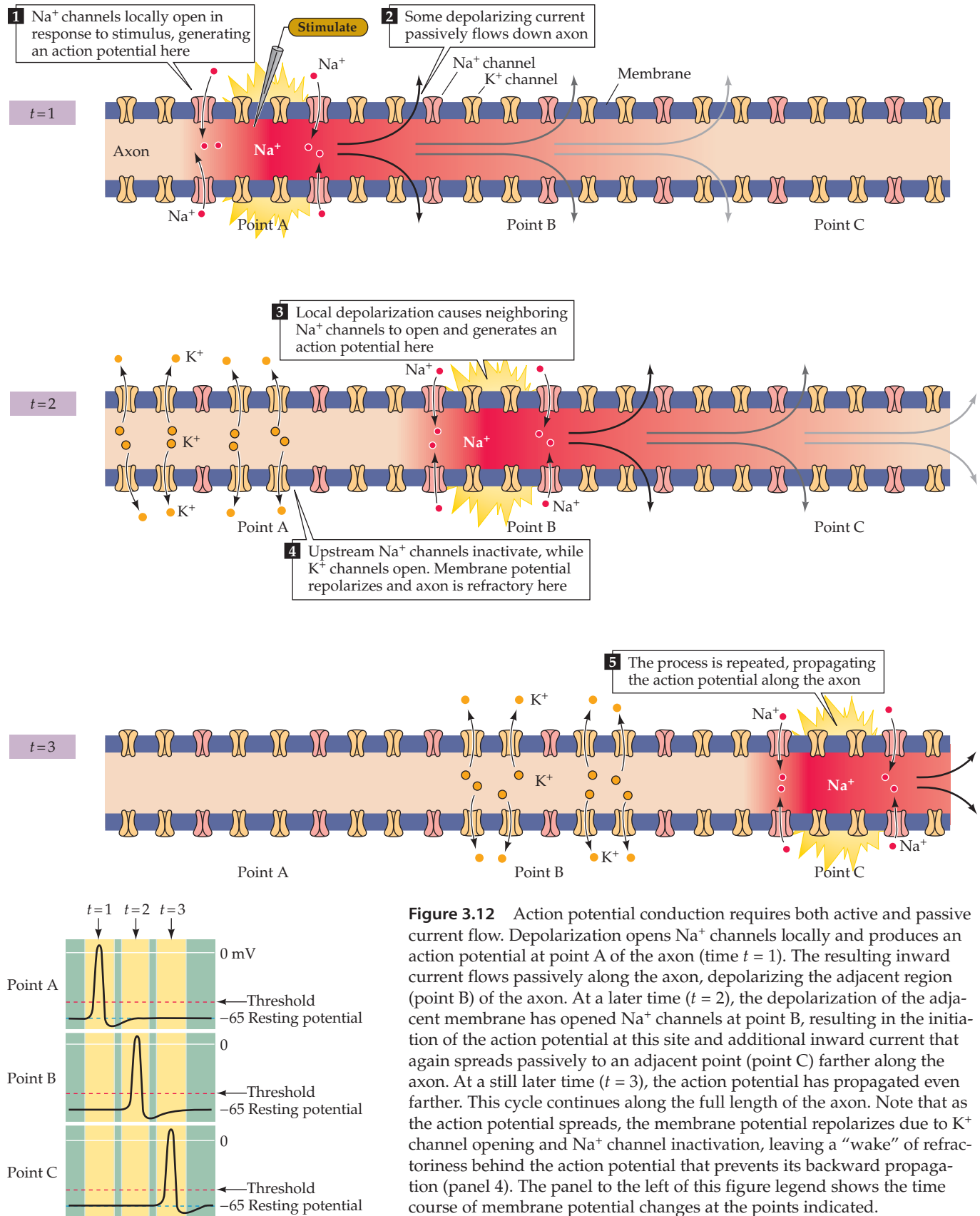
References

- HODGKIN, A. L. AND W. A. H. RUSHTON (1938) The electrical constants of a crustacean nerve fibre. Proc. R. Soc. Lond. 133: 444–479.
- JOHNSTON, D. AND S. M.-S. WU (1995) *Foundations of Cellular Neurophysiology*. Cambridge, MA: MIT Press.
- RAILL, W. (1977) Core conductor theory and cable properties of neurons. In *Handbook of Physiology*, Section 1: *The Nervous System*, Vol. 1: *Cellular Biology of Neurons*. E. R. Kandel (ed.). Bethesda, MD: American Physiological Society, pp. 39–98.

flow—the passive flow of current as well as active currents flowing through voltage-dependent ion channels. The regenerative properties of Na^+ channel opening allow action potentials to propagate in an all-or-none fashion by acting as a booster at each point along the axon, thus ensuring the long-distance transmission of electrical signals.

The Refractory Period

Recall that the depolarization that produces Na^+ channel opening also causes delayed activation of K^+ channels and Na^+ channel inactivation, lead-

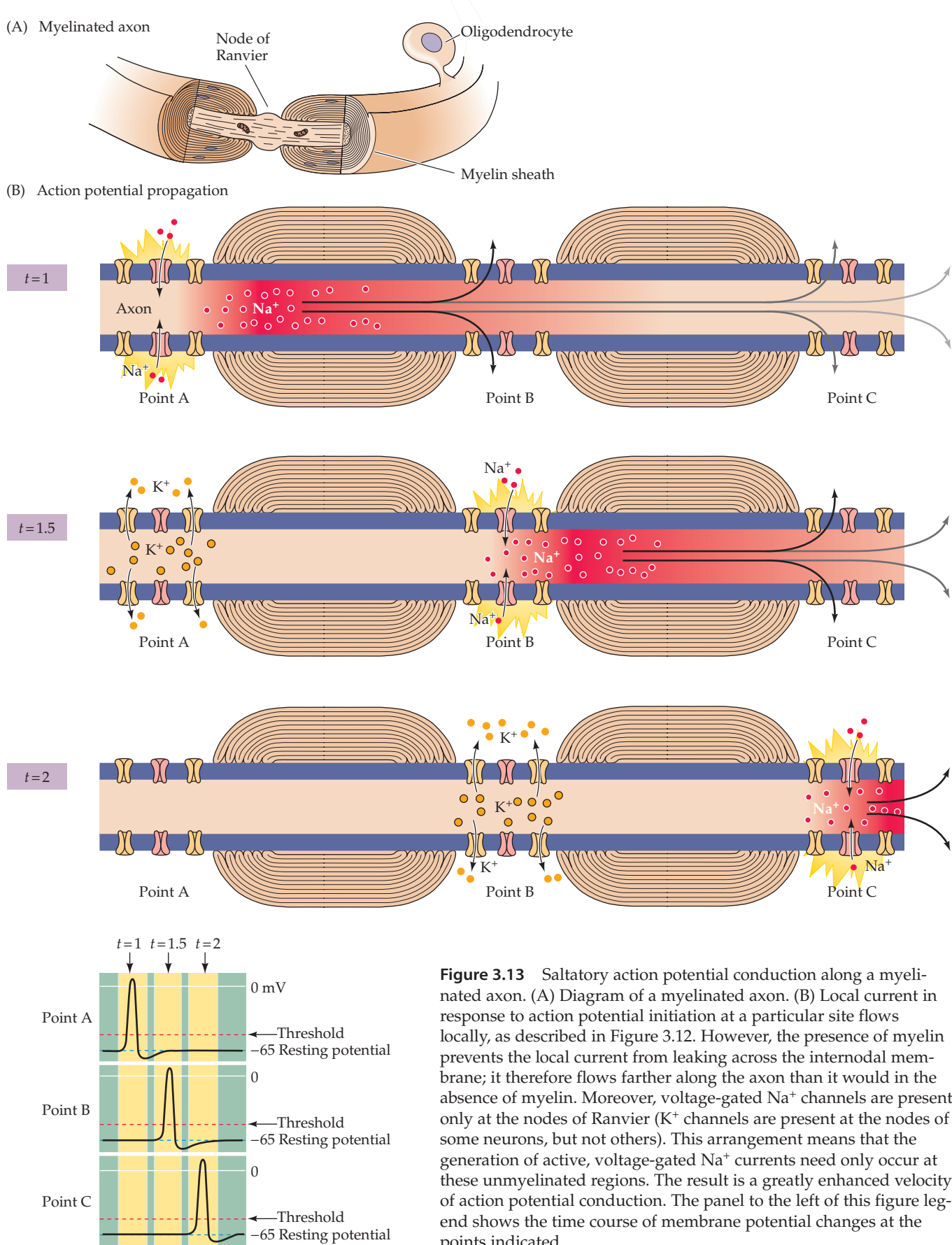


ing to repolarization of the membrane potential as the action potential sweeps along the length of an axon (see Figure 3.12). In its wake, the action potential leaves the Na^+ channels inactivated and K^+ channels activated for a brief time. These transitory changes make it harder for the axon to produce subsequent action potentials during this interval, which is called the **refractory period**. Thus, the refractory period limits the number of action potentials that a given nerve cell can produce per unit time. As might be expected, different types of neurons have different maximum rates of action potential firing due to different types and densities of ion channels. The refractoriness of the membrane in the wake of the action potential also explains why action potentials do not propagate back toward the point of their initiation as they travel along an axon.

Increased Conduction Velocity as a Result of Myelination

The rate of action potential conduction limits the flow of information within the nervous system. It is not surprising, then, that various mechanisms have evolved to optimize the propagation of action potentials along axons. Because action potential conduction requires passive and active flow of current (see Figure 3.12), the rate of action potential propagation is determined by both of these phenomena. One way of improving passive current flow is to increase the diameter of an axon, which effectively decreases the internal resistance to passive current flow (see Box C). The consequent increase in action potential conduction velocity presumably explains why giant axons evolved in invertebrates such as squid, and why rapidly conducting axons in all animals tend to be larger than slowly conducting ones.

Another strategy to improve the passive flow of electrical current is to insulate the axonal membrane, reducing the ability of current to leak out of the axon and thus increasing the distance along the axon that a given local current can flow passively (see Box C). This strategy is evident in the **myelination** of axons, a process by which oligodendrocytes in the central nervous system (and Schwann cells in the peripheral nervous system) wrap the axon in **myelin**, which consists of multiple layers of closely opposed glial membranes (Figure 3.13; see also Chapter 1). By acting as an electrical insulator, myelin greatly speeds up action potential conduction (Figure 3.14). For example, whereas unmyelinated axon conduction velocities range from about 0.5 to 10 m/s, myelinated axons can conduct at velocities of up to 150 m/s. The major reason underlying this marked increase in speed is that the time-consuming process of action potential generation occurs only at specific points along the axon, called **nodes of Ranvier**, where there is a gap in the myelin wrapping (see Figure 1.4F). If the entire surface of an axon were insulated, there would be no place for current to flow out of the axon and action potentials could not be generated. As it happens, an action potential generated at one node of Ranvier elicits current that flows passively within the myelinated segment until the next node is reached. This local current flow then generates an action potential in the neighboring segment, and the cycle is repeated along the length of the axon. Because current flows across the neuronal membrane only at the nodes (see Figure 3.13), this type of propagation is called **saltatory**, meaning that the action potential jumps from node to node. Not surprisingly, loss of myelin, as occurs in diseases such as multiple sclerosis, causes a variety of serious neurological problems (Box D).



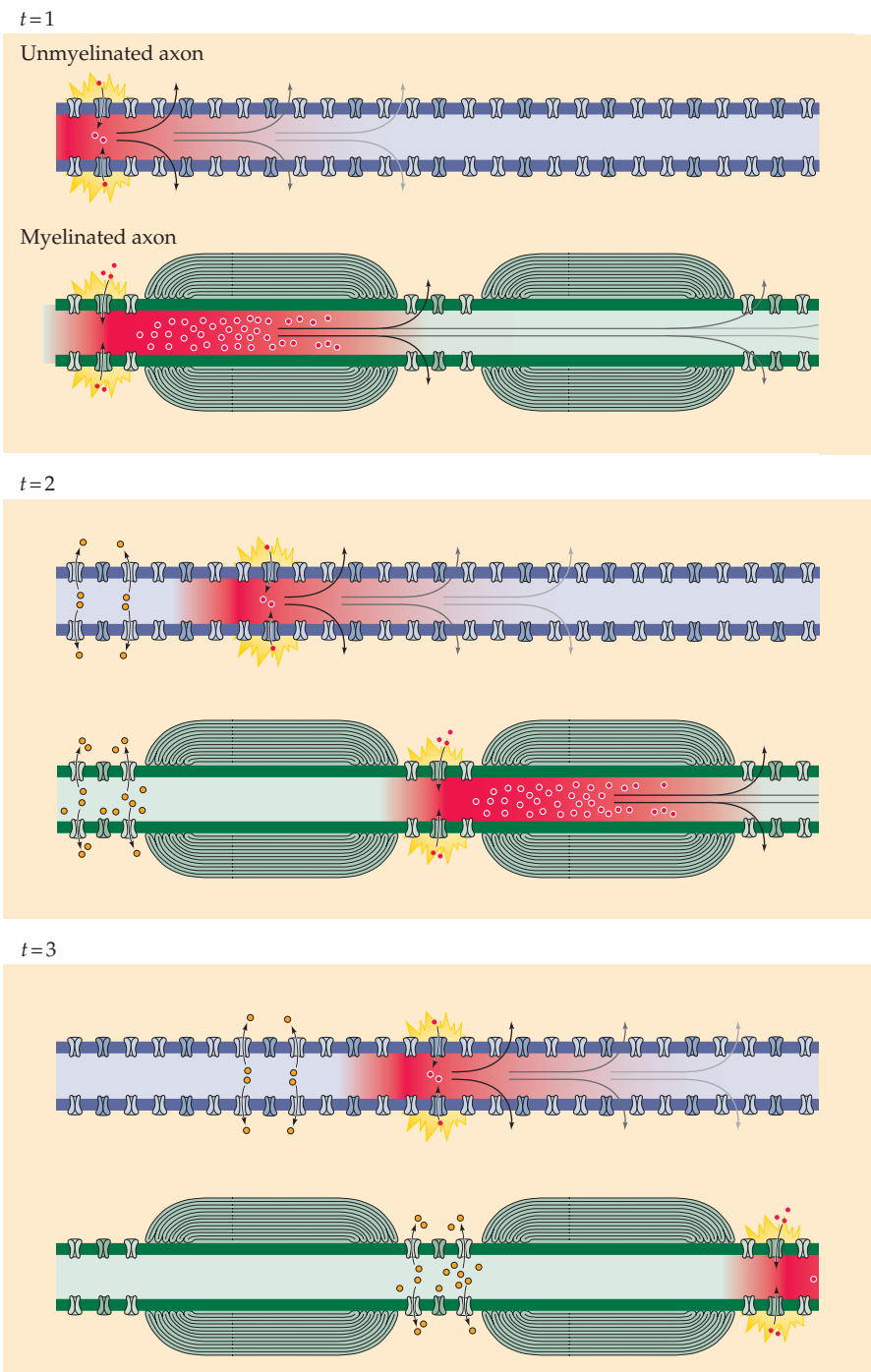


Figure 3.14 Comparison of speed of action potential conduction in unmyelinated (upper) and myelinated (lower) axons.

Summary

The action potential and all its complex properties can be explained by time- and voltage-dependent changes in the Na^+ and K^+ permeabilities of neuronal membranes. This conclusion derives primarily from evidence obtained by a device called the voltage clamp. The voltage clamp technique is an electronic feedback method that allows control of neuronal membrane potential

Box D

Multiple Sclerosis

Multiple sclerosis (MS) is a disease of the central nervous system characterized by a variety of clinical problems arising from multiple regions of demyelination and inflammation along axonal pathways. The disorder commonly begins between ages 20 and 40, characterized by the abrupt onset of neurological deficits that typically persist for days or weeks and then remit. The clinical course ranges from patients with no persistent neurological loss, some of whom experience only occasional later exacerbations, to others who progressively deteriorate as a result of extensive and relentless central nervous system involvement.

The signs and symptoms of MS are determined by the location of the affected regions. Particularly common are monocular blindness (due to lesions of the optic nerve), motor weakness or paralysis (due to lesions of the corticospinal tracts), abnormal somatic sensations (due to lesions of somatic sensory pathways, often in the posterior columns), double vision (due to lesions of medial longitudinal fasciculus), and dizziness (due to lesions of vestibular pathways). Abnormalities are often apparent in the cerebrospinal fluid, which usually contains an abnormal number of cells associated with inflammation and an increased content of antibodies (a sign of an altered immune response). The diagnosis of MS generally relies on the presence of a neurological problem that remits and then returns at an unrelated site. Confirmation can sometimes be obtained from magnetic resonance imaging (MRI), or functional evidence of lesions in a particular pathway by abnormal evoked potentials. The histological hallmark of MS at post-mortem exam is multiple lesions at different sites showing loss of myelin associated with infiltration of inflammatory

cells and, in some instances, loss of axons themselves.

The concept of MS as a demyelinating disease is deeply embedded in the clinical literature, although precisely how the demyelination translates into functional deficits is poorly understood. The loss of the myelin sheath surrounding many axons clearly compromises action potential conduction, and the abnormal patterns of nerve conduction that result presumably produce most of the clinical deficits in the disease. However, MS may have effects that extend beyond loss of the myelin sheath. It is clear that some axons are actually destroyed, probably as a result of inflammatory processes in the overlying myelin and/or loss of trophic support of the axon by oligodendrocytes. Thus, axon loss also contributes to the functional deficits in MS, especially in the chronic, progressive forms of the disease.

The ultimate cause of MS remains unclear. The immune system undoubtedly contributes to the damage and new immunoregulatory therapies provide substantial benefits to many patients. Precisely how the immune system is activated to cause the injury is not known. The most popular hypothesis is that MS is an autoimmune disease (i.e., a disease in which the immune system attacks the body's proper constituents). The fact that immunization of experimental animals with any one of several molecular constituents of the myelin sheath can induce a demyelinating disease (called experimental allergic encephalomyelitis) shows that an autoimmune attack on the myelin membrane is sufficient to produce a picture similar to MS. A possible explanation of the human disease is that a genetically susceptible individual becomes transiently infected (by a minor viral illness, for example) with a microorganism that expresses a molecule struc-

turally similar to a component of myelin. An immune response to this antigen is mounted to attack the invader, but the failure of the immune system to discriminate between the foreign protein and self results in destruction of otherwise normal myelin, a scenario occurring in mice infected with Theiler's virus.

An alternative hypothesis is that MS is caused by a persistent infection by a virus or other microorganism. In this interpretation, the immune system's ongoing efforts to get rid of the pathogen cause the damage to myelin. Tropical spastic paraparesis (TSP) provides a precedent for this idea. TSP is a disease characterized by the gradual progression of weakness of the legs and impaired control of bladder function associated with increased deep tendon reflexes and a positive Babinski sign (see Chapter 16). This clinical picture is similar to that of rapidly advancing MS. TSP is known to be caused by persistent infection with a retrovirus (human T lymphotropic virus-1). This precedent notwithstanding, proving the persistent viral infection hypothesis for MS requires unambiguous demonstration of the presence of a virus. Despite periodic reports of a virus associated with MS, convincing evidence has not been forthcoming. In sum, MS remains a daunting clinical challenge.

References

- ADAMS, R. D. AND M. VICTOR (2001) *Principles of Neurology*, 7th Ed. New York: McGraw-Hill, pp. 954–982.
- MILLER, D. H. AND 9 OTHERS. (2003) A controlled trial of natalizumab for relapsing multiple sclerosis. *N. Engl. J. Med.* 348: 15–23.
- ZANVIL, S. S. AND L. STEINMAN (2003) Diverse targets for intervention during inflammatory and neurodegenerative phases of multiple sclerosis. *Neuron* 38: 685–688.

and, simultaneously, direct measurement of the voltage-dependent fluxes of Na^+ and K^+ that produce the action potential. Voltage clamp experiments show that a transient rise in Na^+ conductance activates rapidly and then inactivates during a sustained depolarization of the membrane potential. Such experiments also demonstrate a rise in K^+ conductance that activates in a delayed fashion and, in contrast to the Na^+ conductance, does not inactivate. Mathematical modeling of the properties of these conductances indicates that they, and they alone, are responsible for the production of all-or-none action potentials in the squid axon. Action potentials propagate along the nerve cell axons initiated by the voltage gradient between the active and inactive regions of the axon by virtue of the local current flow. In this way, action potentials compensate for the relatively poor passive electrical properties of nerve cells and enable neural signaling over long distances. These classical electrophysiological findings provide a solid basis for considering the functional and ultimately molecular variations on neural signaling taken up in the next chapter.

Additional Reading

Reviews

ARMSTRONG, C. M. AND B. HILLE (1998) Voltage-gated ion channels and electrical excitability. *Neuron* 20: 371–80.

NEHER, E. (1992) Ion channels for communication between and within cells. *Science* 256: 498–502.

Important Original Papers

ARMSTRONG, C. M. AND L. BINSTOCK (1965) Anomalous rectification in the squid giant axon injected with tetraethylammonium chloride. *J. Gen. Physiol.* 48: 859–872.

HODGKIN, A. L. AND A. F. HUXLEY (1952a) Currents carried by sodium and potassium ions through the membrane of the giant axon of *Loligo*. *J. Physiol.* 116: 449–472.

HODGKIN, A. L. AND A. F. HUXLEY (1952b) The components of membrane conductance in the giant axon of *Loligo*. *J. Physiol.* 116: 473–496.

HODGKIN, A. L. AND A. F. HUXLEY (1952c) The dual effect of membrane potential on sodium conductance in the giant axon of *Loligo*. *J. Physiol.* 116: 497–506.

HODGKIN, A. L. AND A. F. HUXLEY (1952d) A quantitative description of membrane current and its application to conduction and excitation in nerve. *J. Physiol.* 116: 507–544.

HODGKIN, A. L. AND W. A. H. RUSHTON (1938) The electrical constants of a crustacean nerve fibre. *Proc. R. Soc. Lond.* 133: 444–479.

HODGKIN, A. L., A. F. HUXLEY AND B. KATZ (1952) Measurements of current–voltage relations in the membrane of the giant axon of *Loligo*. *J. Physiol.* 116: 424–448.

MOORE, J. W., M. P. BLAUSTEIN, N. C. ANDERSON AND T. NARAHASHI (1967) Basis of tetrodotoxin's selectivity in blockage of squid axons. *J. Gen. Physiol.* 50: 1401–1411.

Books

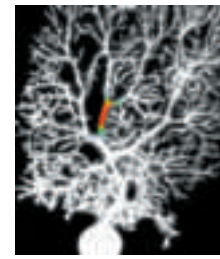
AIDLEY, D. J. AND P. R. STANFIELD (1996) *Ion Channels: Molecules in Action*. Cambridge: Cambridge University Press.

HILLE, B. (2001) *Ion Channels of Excitable Membranes*, 3rd Ed. Sunderland, MA: Sinauer Associates.

JOHNSTON, D. AND S. M.-S. WU (1995) *Foundations of Cellular Neurophysiology*. Cambridge, MA: MIT Press.

JUNGE, D. (1992) *Nerve and Muscle Excitation*, 3rd Ed. Sunderland, MA: Sinauer Associates.

Chapter 4



Channels and Transporters

Overview

The generation of electrical signals in neurons requires that plasma membranes establish concentration gradients for specific ions and that these membranes undergo rapid and selective changes in the membrane permeability to these ions. The membrane proteins that create and maintain ion gradients are called active transporters, whereas other proteins called ion channels give rise to selective ion permeability changes. As their name implies, ion channels are transmembrane proteins that contain a specialized structure, called a pore, that permits particular ions to cross the neuronal membrane. Some of these channels also contain other structures that are able to sense the electrical potential across the membrane. Such voltage-gated channels open or close in response to the magnitude of the membrane potential, allowing the membrane permeability to be regulated by changes in this potential. Other types of ion channels are gated by extracellular chemical signals such as neurotransmitters, and some by intracellular signals such as second messengers. Still others respond to mechanical stimuli, temperature changes, or a combination of such effects. Many types of ion channels have now been characterized at both the gene and protein level, resulting in the identification of a large number of ion channel subtypes that are expressed differentially in neuronal and non-neuronal cells. The specific expression pattern of ion channels in each cell type can generate a wide spectrum of electrical characteristics. In contrast to ion channels, active transporters are membrane proteins that produce and maintain ion concentration gradients. The most important of these is the Na^+ pump, which hydrolyzes ATP to regulate the intracellular concentrations of both Na^+ and K^+ . Other active transporters produce concentration gradients for the full range of physiologically important ions, including Cl^- , Ca^{2+} , and H^+ . From the perspective of electrical signaling, active transporters and ion channels are complementary: Transporters create the concentration gradients that help drive ion fluxes through open ion channels, thus generating electrical signals.

Ion Channels Underlying Action Potentials

Although Hodgkin and Huxley had no knowledge of the physical nature of the conductance mechanisms underlying action potentials, they nonetheless proposed that nerve cell membranes have channels that allow ions to pass selectively from one side of the membrane to the other (see Chapter 3). Based on the ionic conductances and currents measured in voltage clamp experiments, the postulated channels had to have several properties. First, because the ionic currents are quite large, the channels had to be capable of allowing ions to move across the membrane at high rates. Second, because

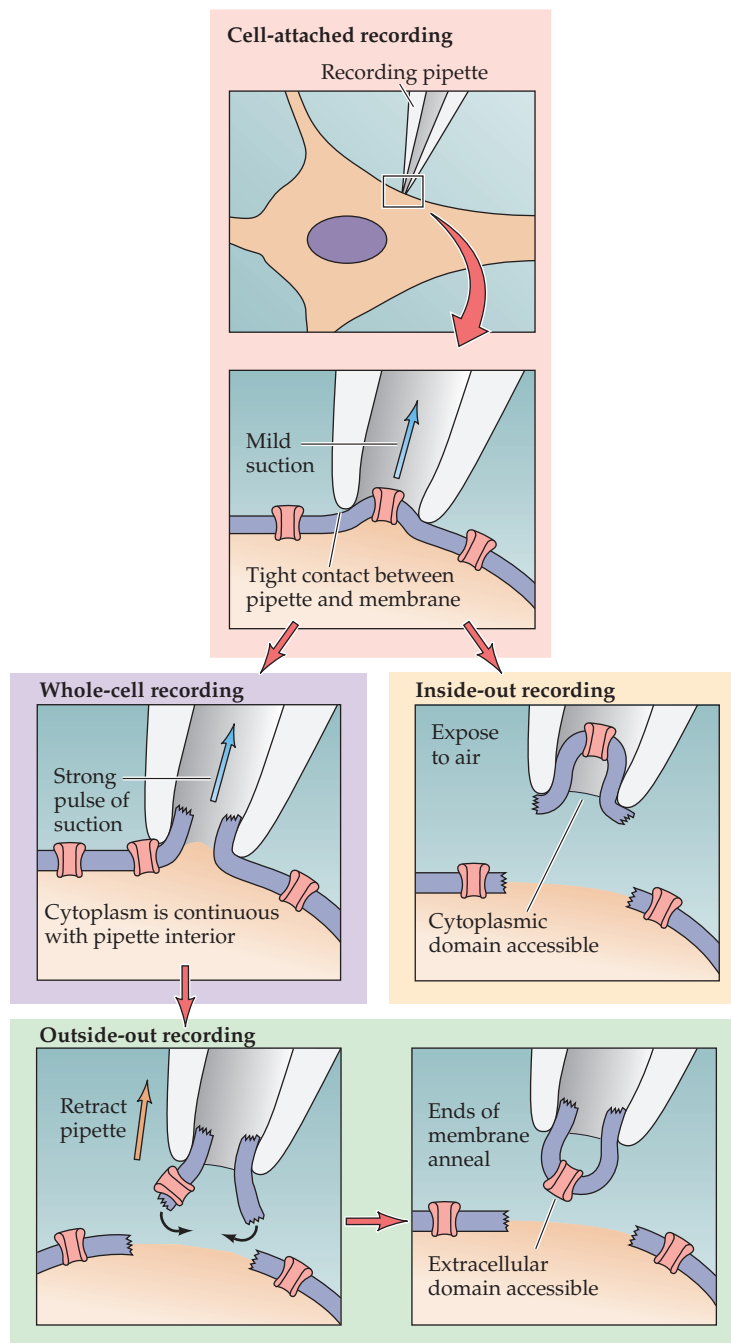
Box A

The Patch Clamp Method

A wealth of new information about ion channels resulted from the invention of the patch clamp method in the 1970s. This technique is based on a very simple idea. A glass pipette with a very small opening is used to make tight contact with a tiny area, or patch, of neuronal membrane. After the application of a small amount of suction to the back of the pipette, the seal between pipette and membrane becomes so tight that no ions can flow between the pipette and the membrane. Thus, all the ions that flow when a single ion channel opens must flow into the pipette. The resulting electrical current, though small, can be measured with an ultrasensitive electronic amplifier connected to the pipette. Based on the geometry involved, this arrangement usually is called the *cell-attached patch clamp recording method*. As with the conventional voltage clamp method, the patch clamp method allows experimental control of the membrane potential to characterize the voltage dependence of membrane currents.

Although the ability to record currents flowing through single ion channels is an important advantage of the cell-attached patch clamp method, minor technical modifications yield still other advantages. For example, if the membrane patch within the pipette is disrupted by briefly applying strong suction, the interior of the pipette becomes continuous with the cytoplasm of the cell. This arrangement allows measurements of electrical potentials and currents from the entire cell and is therefore called the *whole-cell recording method*. The whole-cell configuration also allows diffusional exchange between the pipette and the cytoplasm, producing a convenient way to inject substances into the interior of a “patched” cell.

Two other variants of the patch clamp method originate from the finding that once a tight seal has formed between the



Four configurations in patch clamp measurements of ionic currents.

membrane and the glass pipette, small pieces of membrane can be pulled away from the cell without disrupting the seal; this yields a preparation that is free of the complications imposed by the rest of the cell. Simply retracting a pipette that

is in the cell-attached configuration causes a small vesicle of membrane to remain attached to the pipette. By exposing the tip of the pipette to air, the vesicle opens to yield a small patch of membrane with its (former) intracellular sur-

face exposed. This arrangement, called the inside-out patch recording configuration, allows the measurement of single-channel currents with the added benefit of making it possible to change the medium to which the intracellular surface of the membrane is exposed. Thus, the inside-out configuration is particularly valuable when studying the influence of intracellular molecules on ion channel function. Alternatively, if the pipette is retracted while it is in the

whole-cell configuration, a membrane patch is produced that has its extracellular surface exposed. This arrangement, called the outside-out recording configuration, is optimal for studying how channel activity is influenced by extracellular chemical signals, such as neurotransmitters (see Chapter 5). This range of possible configurations makes the patch clamp method an unusually versatile technique for studies of ion channel function.

References

- HAMILL, O. P., A. MARTY, E. NEHER, B. SAKMANN AND F. J. SIGWORTH (1981) Improved patch-clamp techniques for high-resolution current recording from cells and cell-free membrane patches. *Pflügers Arch.* 391: 85–100.
- LEOIS, R. A. AND J. L. RAE (1998) Low-noise patch-clamp techniques. *Meth. Enzym.* 293: 218–266.
- SIGWORTH, F. J. (1986) The patch clamp is more useful than anyone had expected. *Fed. Proc.* 45: 2673–2677.

the ionic currents depend on the electrochemical gradient across the membrane, the channels had to make use of these gradients. Third, because Na^+ and K^+ flow across the membrane independently of each other, different channel types had to be capable of discriminating between Na^+ and K^+ , allowing only one of these ions to flow across the membrane under the relevant conditions. Finally, given that the conductances are voltage-dependent, the channels had to be able to sense the voltage drop across the membrane, opening only when the voltage reached appropriate levels. While this concept of channels was highly speculative in the 1950s, later experimental work established beyond any doubt that transmembrane proteins called voltage-sensitive ion channels indeed exist and are responsible for all of the ionic conductance phenomena described in Chapter 3.

The first direct evidence for the presence of voltage-sensitive, ion-selective channels in nerve cell membranes came from measurements of the ionic currents flowing through individual ion channels. The voltage-clamp apparatus used by Hodgkin and Huxley could only resolve the *aggregate* current resulting from the flow of ions through many thousands of channels. A technique capable of measuring the currents flowing through single channels was devised in 1976 by Erwin Neher and Bert Sakmann at the Max Planck Institute in Goettingen. This remarkable approach, called patch clamping (Box A), revolutionized the study of membrane currents. In particular, the patch clamp method provided the means to test directly Hodgkin and Huxley's proposals about the characteristics of ion channels.

Currents flowing through Na^+ channels are best examined in experimental circumstances that prevent the flow of current through other types of channels that are present in the membrane (e.g., K^+ channels). Under such conditions, depolarizing a patch of membrane from a squid giant axon causes tiny inward currents to flow, but only occasionally (Figure 4.1). The size of these currents is minuscule—approximately 1–2 pA (i.e., 10^{-12} ampere), which is orders of magnitude smaller than the Na^+ currents measured by voltage clamping the entire axon. The currents flowing through single channels are called **microscopic currents** to distinguish them from the **macroscopic currents** flowing through a large number of channels distributed over a much more extensive region of surface membrane. Although microscopic currents are certainly small, a current of 1 pA nonetheless reflects the flow of thousands of ions per millisecond. Thus, as predicted, a single channel can let many ions pass through the membrane in a very short time.

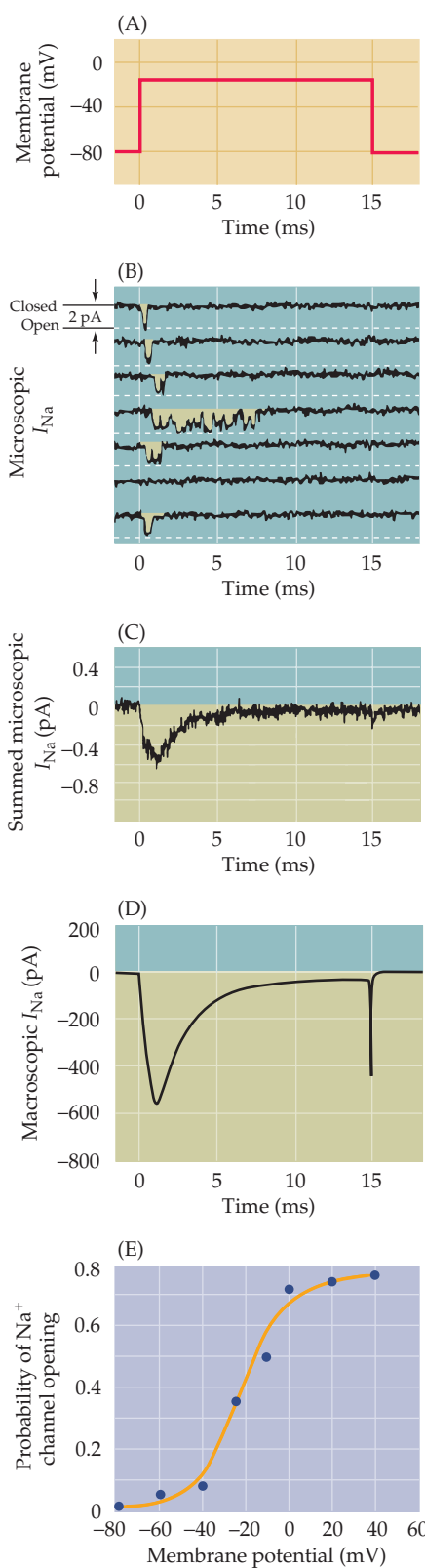


Figure 4.1 Patch clamp measurements of ionic currents flowing through single Na^+ channels in a squid giant axon. In these experiments, Cs^+ was applied to the axon to block voltage-gated K^+ channels. Depolarizing voltage pulses (A) applied to a patch of membrane containing a single Na^+ channel result in brief currents (B, downward deflections) in the seven successive recordings of membrane current (I_{Na}). (C) The sum of many such current records shows that most channels open in the initial 1–2 ms following depolarization of the membrane, after which the probability of channel openings diminishes because of channel inactivation. (D) A macroscopic current measured from another axon shows the close correlation between the time courses of microscopic and macroscopic Na^+ currents. (E) The probability of an Na^+ channel opening depends on the membrane potential, increasing as the membrane is depolarized. (B,C after Bezanilla and Correa, 1995; D after Vandenberg and Bezanilla, 1991; E after Correa and Bezanilla, 1994.)

Several observations further proved that the microscopic currents in Figure 4.1B are due to the opening of single, voltage-activated Na^+ channels. First, the currents are carried by Na^+ ; thus, they are directed inward when the membrane potential is more negative than E_{Na} , reverse their polarity at E_{Na} , are outward at more positive potentials, and are reduced in size when the Na^+ concentration of the external medium is decreased. This behavior exactly parallels that of the macroscopic Na^+ currents described in Chapter 3. Second, the channels have a time course of opening, closing, and inactivating that matches the kinetics of macroscopic Na^+ currents. This correspondence is difficult to appreciate in the measurement of microscopic currents flowing through a single open channel, because individual channels open and close in a stochastic (random) manner, as can be seen by examining the individual traces in Figure 4.1B. However, repeated depolarization of the membrane potential causes each Na^+ channel to open and close many times. When the current responses to a large number of such stimuli are averaged together, the collective response has a time course that looks much like the macroscopic Na^+ current (Figure 4.1C). In particular, the channels open mostly at the beginning of a prolonged depolarization, showing that they subsequently inactivate, as predicted from the macroscopic Na^+ current (compare Figures 4.1C and 4.1D). Third, both the opening and closing of the channels are voltage-dependent; thus, the channels are closed at -80 mV but open when the membrane potential is depolarized. In fact, the probability that any given channel will be open varies with membrane potential (Figure 4.1E), again as predicted from the macroscopic Na^+ conductance (see Figure 3.7). Finally, tetrodotoxin, which blocks the macroscopic Na^+ current (see Box C), also blocks microscopic Na^+ currents. Taken together, these results show that the macroscopic Na^+ current measured by Hodgkin and Huxley does indeed arise from the aggregate effect of many thousands of microscopic Na^+ currents, each representing the opening of a single voltage-sensitive Na^+ channel.

Patch clamp experiments have also revealed the properties of the channels responsible for the macroscopic K^+ currents associated with action potentials. When the membrane potential is depolarized (Figure 4.2A), microscopic outward currents (Figure 4.2B) can be observed under conditions that block Na^+ channels. The microscopic outward currents exhibit all the features expected for currents flowing through action-potential-related K^+ channels. Thus, the microscopic currents (Figure 4.2C), like their macroscopic counterparts (Figure 4.2D), fail to inactivate during brief depolarizations. Moreover, these single-channel currents are sensitive to ionic manipu-

Figure 4.2 Patch clamp measurements of ionic currents flowing through single K⁺ channels in a squid giant axon. In these experiments, tetrodotoxin was applied to the axon to block voltage-gated Na⁺ channels. Depolarizing voltage pulses (A) applied to a patch of membrane containing a single K⁺ channel results in brief currents (B, upward deflections) whenever the channel opens. (C) The sum of such current records shows that most channels open with a delay, but remain open for the duration of the depolarization. (D) A macroscopic current measured from another axon shows the correlation between the time courses of microscopic and macroscopic K⁺ currents. (E) The probability of a K⁺ channel opening depends on the membrane potential, increasing as the membrane is depolarized. (B and C after Augustine and Bezanilla, in Hille 1992; D after Augustine and Bezanilla, 1990; E after Perozo et al., 1991.)

lations and drugs that affect the macroscopic K⁺ currents and, like the macroscopic K⁺ currents, are voltage-dependent (Figure 4.2E). This and other evidence shows that macroscopic K⁺ currents associated with action potentials arise from the opening of many voltage-sensitive K⁺ channels.

In summary, patch clamping has allowed direct observation of microscopic ionic currents flowing through single ion channels, confirming that voltage sensitive Na⁺ and K⁺ channels are responsible for the macroscopic conductances and currents that underlie the action potential. Measurements of the behavior of single ion channels has also provided some insight into the molecular attributes of these channels. For example, single channel studies show that the membrane of the squid axon contains at least two types of channels—one selectively permeable to Na⁺ and a second selectively permeable to K⁺. Both channel types are **voltage-gated**, meaning that their opening is influenced by membrane potential (Figure 4.3). For each channel, depolarization increases the probability of channel opening, whereas hyperpolarization closes them (see Figures 4.1E and 4.2E). Thus, both channel types must have a **voltage sensor** that detects the potential across the membrane (Figure 4.3). However, these channels differ in important respects. In addition to their different ion selectivities, depolarization also inactivates the Na⁺ channel but not the K⁺ channel, causing Na⁺ channels to pass into a nonconducting state. The Na⁺ channel must therefore have an additional molecular mechanism responsible for **inactivation**. And, as expected from the macroscopic behavior of the Na⁺ and K⁺ currents described in Chapter 3, the kinetic properties of the gating of the two channels differs. This information about the physiology of single channels set the stage for subsequent studies of the molecular diversity of ion channels in various cell types, and of their detailed functional characteristics.

The Diversity of Ion Channels

Molecular genetic studies, in conjunction with the patch clamp method and other techniques, have led to many additional advances in understanding ion channels. Genes encoding Na⁺ and K⁺ channels, as well as many other channel types, have now been identified and cloned. A surprising fact that has emerged from these molecular studies is the diversity of genes that code for ion channels. Well over 100 ion channel genes have now been discovered, a number that could not have been anticipated from early studies of ion channel function. To understand the functional significance of this multitude of ion channel genes, the channels can be selectively expressed in well-

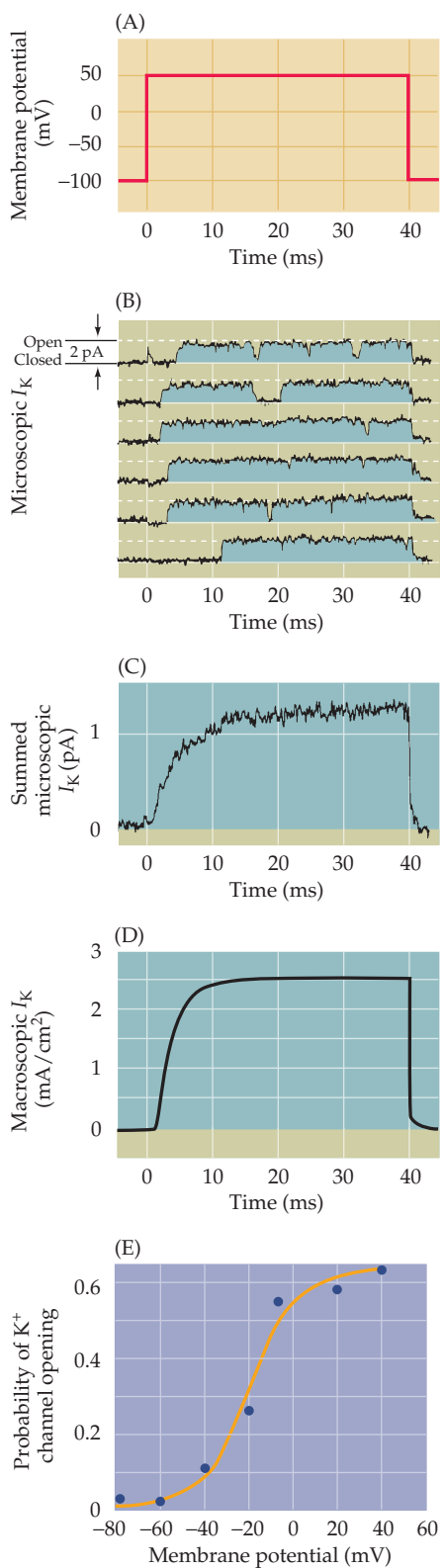
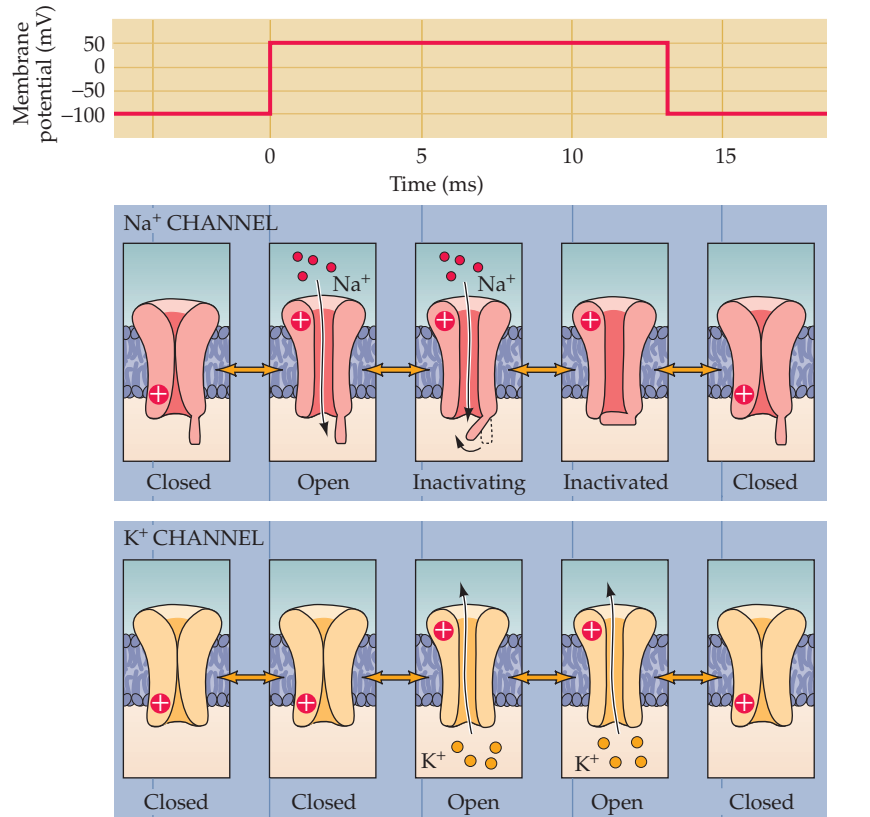


Figure 4.3 Functional states of voltage-gated Na^+ and K^+ channels. The gates of both channels are closed when the membrane potential is hyperpolarized. When the potential is depolarized, voltage sensors (indicated by +) allow the channel gates to open—first the Na^+ channels and then the K^+ channels. Na^+ channels also inactivate during prolonged depolarization, whereas many types of K^+ channels do not.



defined experimental systems, such as in cultured cells or frog oocytes (Box B), and then studied with patch clamping and other physiological techniques. Such studies have found many voltage-gated channels that respond to membrane potential in much the same way as the Na^+ and K^+ channels that underlie the action potential. Other channels, however, are gated by chemical signals that bind to extracellular or intracellular domains on these proteins and are insensitive to membrane voltage. Still others are sensitive to mechanical displacement, or to changes in temperature.

Further magnifying this diversity of ion channels are a number of mechanisms that can produce functionally different types of ion channels from a single gene. Ion channel genes contain a large number of coding regions that can be spliced together in different ways, giving rise to channel proteins that can have dramatically different functional properties. RNAs encoding ion channels also can be edited, modifying their base composition after transcription from the gene. For example, editing the RNA encoding of some receptors for the neurotransmitter glutamate (Chapter 6) changes a single amino acid within the receptor, which in turn gives rise to channels that differ in their selectivity for cations and in their conductance. Channel proteins can also undergo posttranslational modifications, such as phosphorylation by protein kinases (see Chapter 7), which can further change their functional characteristics. Thus, although the basic electrical signals of the nervous system are relatively stereotyped, the proteins responsible for generating these signals are remarkably diverse, conferring specialized signaling properties to many of the neuronal cell types that populate the nervous system. These channels also are involved in a broad range of neurological diseases.

Box B

Expression of Ion Channels in *Xenopus* Oocytes

Bridging the gap between the sequence of an ion channel gene and understanding channel function is a challenge. To meet this challenge, it is essential to have an experimental system in which the gene product can be expressed efficiently, and in which the function of the resulting channel can be studied with methods such as the patch clamp technique. Ideally, the vehicle for expression should be readily available, have few endogenous channels, and be large enough to permit mRNA and DNA to be microinjected with ease. Oocytes (immature eggs) from the clawed African frog, *Xenopus laevis* (Figure A), fulfill all these demands. These huge cells (approximately 1 mm in diameter; Figure B) are easily harvested from the female

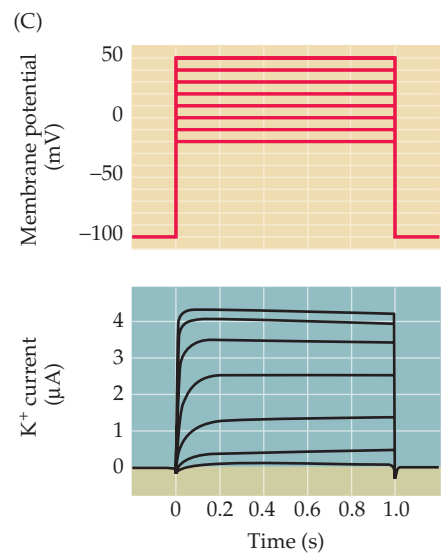
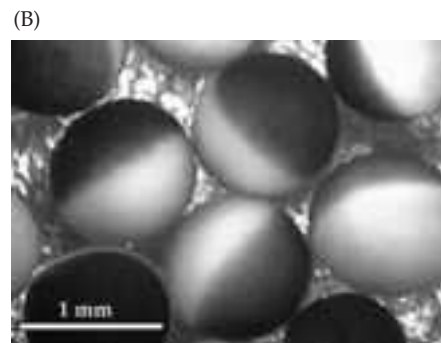
Xenopus. Work performed in the 1970s by John Gurdon, a developmental biologist, showed that injection of exogenous mRNA into frog oocytes causes them to synthesize foreign protein in prodigious quantities. In the early 1980s, Ricardo Miledi, Eric Barnard, and other neurobiologists demonstrated that *Xenopus* oocytes could express exogenous ion channels, and that physiological methods could be used to study the ionic currents generated by the newly-synthesized channels (Figure C).

As a result of these pioneering studies, heterologous expression experiments have now become a standard way of studying ion channels. The approach has been especially valuable in deciphering the relationship between channel structure and function. In such experiments, defined mutations (often affecting a single nucleotide) are made in the part of the channel gene that encodes a structure of interest; the resulting channel proteins are then expressed in oocytes to assess the functional consequences of the mutation.

The ability to combine molecular and physiological methods in a single cell system has made *Xenopus* oocytes a powerful experimental tool. Indeed, this system has been as valuable to contemporary studies of voltage-gated ion channels as the squid axon was to such studies in the 1950s and 1960s.

References

- GUNDERSEN, C. B., R. MILEDI AND I. PARKER (1984) Slowly inactivating potassium channels induced in *Xenopus* oocytes by messenger ribonucleic acid from *Torpedo* brain. *J. Physiol. (Lond.)* 353: 231–248.
 GURDON, J. B., C. D. LANE, H. R. WOODLAND AND G. MARBAIX (1971) Use of frog eggs and oocytes for the study of messenger RNA and its translation in living cells. *Nature* 233: 177–182.
 STÜHMER, W. (1998) Electrophysiological recordings from *Xenopus* oocytes. *Meth. Enzym.* 293: 280–300.
 SUMIKAWA, K., M. HOUGHTON, J. S. EMTAGE, B. M. RICHARDS AND E. A. BARNARD (1981) Active multi-subunit ACh receptor assembled by translation of heterologous mRNA in *Xenopus* oocytes. *Nature* 292: 862–864.



(A) The clawed African frog, *Xenopus laevis*. (B) Several oocytes from *Xenopus* highlighting the dark coloration of the original pole and the lighter coloration of the vegetal pole. (Courtesy of P. Reinhart.) (C) Results of a voltage clamp experiment showing K⁺ currents produced following injection of K⁺-channel mRNA into an oocyte. (After Gundersen et al., 1984.)

Voltage-Gated Ion Channels

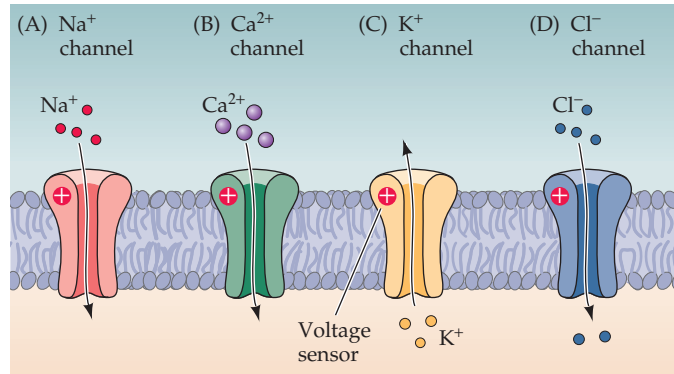
Voltage-gated ion channels that are selectively permeable to each of the major physiological ions— Na^+ , K^+ , Ca^{2+} , and Cl^- —have now been discovered (Figure 4.4 A–D). Indeed, many different genes have been discovered for each type of voltage-gated ion channel. An example is the identification of 10 human Na^+ channel genes. This finding was unexpected because Na^+ channels from many different cell types have similar functional properties, consistent with their origin from a single gene. It is now clear, however, that all of these Na^+ channel genes (called SCN genes) produce proteins that differ in their structure, function, and distribution in specific tissues. For instance, in addition to the rapidly inactivating Na^+ channels discovered by Hodgkin and Huxley in squid axon, a voltage-sensitive Na^+ channel that does *not* inactivate has been identified in mammalian axons. As might be expected, this channel gives rise to action potentials of long duration and is a target of local anesthetics such as benzocaine and lidocaine.

Other electrical responses in neurons entail the activation of voltage-gated Ca^{2+} channels (Figure 4.4B). In some neurons, voltage-gated Ca^{2+} channels give rise to action potentials in much the same way as voltage-sensitive Na^+ channels. In other neurons, Ca^{2+} channels control the shape of action potentials generated primarily by Na^+ conductance changes. More generally, by affecting intracellular Ca^{2+} concentrations, the activity of Ca^{2+} channels regulates an enormous range of biochemical processes within cells (see Chapter 7). Perhaps the most important of the processes regulated by voltage-sensitive Ca^{2+} channels is the release of neurotransmitters at synapses (see Chapter 5). Given these crucial functions, it is perhaps not surprising that 16 different Ca^{2+} channel genes (called CACNA genes) have been identified. Like Na^+ channels, Ca^{2+} channels differ in their activation and inactivation properties, allowing subtle variations in both electrical and chemical signaling processes mediated by Ca^{2+} . As a result, drugs that block voltage-gated Ca^{2+} channels are especially valuable in treating a variety of conditions ranging from heart disease to anxiety disorders.

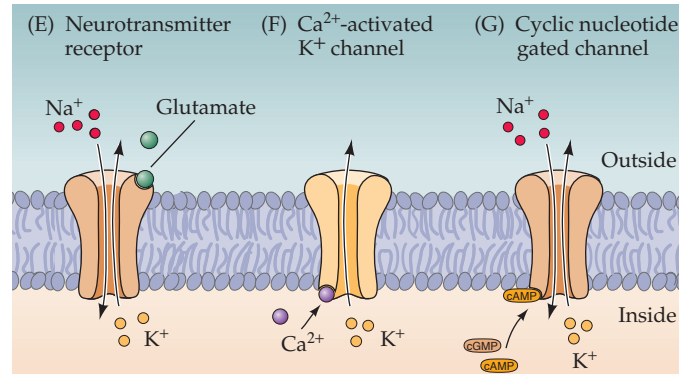
By far the largest and most diverse class of voltage-gated ion channels are the K^+ channels (Figure 4.4C). Nearly 100 K^+ channel genes are now known, and these fall into several distinct groups that differ substantially in their activation, gating, and inactivation properties. Some take minutes to inactivate, as in the case of squid axon K^+ channels studied by Hodgkin and Huxley (Figure 4.5A). Others inactivate within milliseconds, as is typical of most voltage-gated Na^+ channels (Figure 4.5B). These properties influence the

Figure 4.4 Types of voltage-gated ion channels. Examples of voltage-gated channels include those selectively permeable to Na^+ (A), Ca^{2+} (B), K^+ (C), and Cl^- (D). Ligand-gated ion channels include those activated by the extracellular presence of neurotransmitters, such as glutamate (E). Other ligand-gated channels are activated by intracellular second messengers, such as Ca^{2+} (F) or the cyclic nucleotides, cAMP and cGMP (G).

VOLTAGE-GATED CHANNELS



LIGAND-GATED CHANNELS



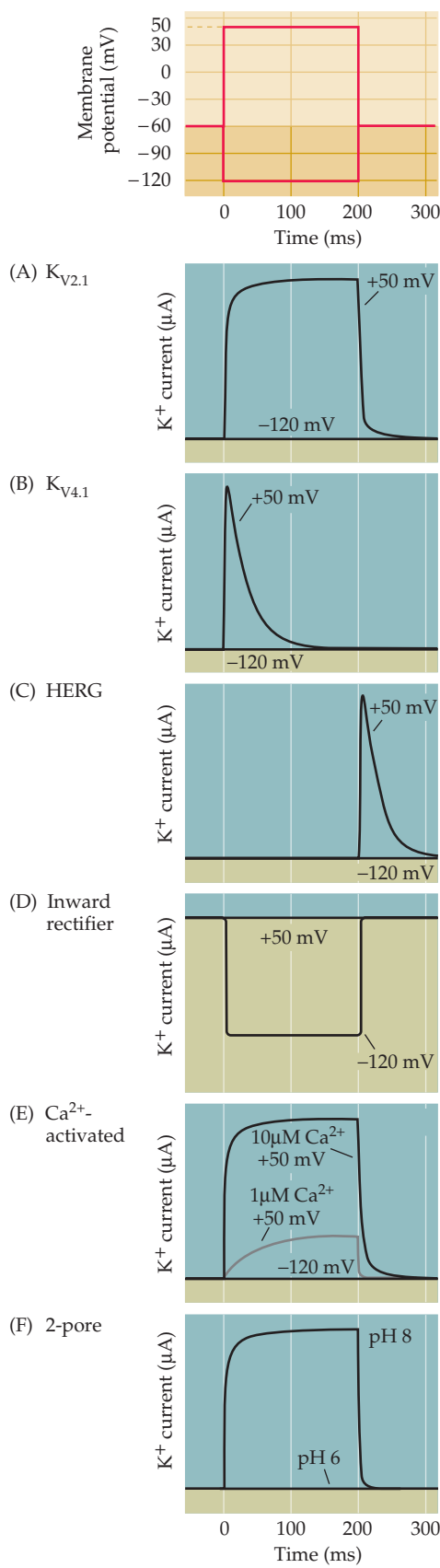


Figure 4.5 Diverse properties of K^+ channels. Different types of K^+ channels were expressed in *Xenopus* oocytes (see Box B), and the voltage clamp method was used to change the membrane potential (top) and measure the resulting currents flowing through each type of channel. These K^+ channels vary markedly in their gating properties, as evident in their currents (left) and conductances (right). (A) $K_{V2.1}$ channels show little inactivation and are closely related to the delayed rectifier K^+ channels involved in action potential repolarization. (B) $K_{V4.1}$ channels inactivate during a depolarization. (C) HERG channels inactivate so rapidly that current flows only when inactivation is rapidly removed at the end of a depolarization. (D) Inward rectifying K^+ channels allow more K^+ current to flow at hyperpolarized potentials than at depolarized potentials. (E) Ca^{2+} -activated K^+ channels open in response to intracellular Ca^{2+} ions and, in some cases, membrane depolarization. (F) K^+ channels with two pores usually respond to chemical signals, such as pH, rather than changes in membrane potential.

duration and rate of action potential firing, with important consequences for axonal conduction and synaptic transmission. Perhaps the most important function of K⁺ channels is the role they play in generating the resting membrane potential (see Chapter 2). At least two families of K⁺ channels that are open at substantially negative membrane voltage levels contribute to setting the resting membrane potential (Figure 4.5D).

Finally, several types of voltage-gated Cl⁻ channel have been identified (see Figure 4.4D). These channels are present in every type of neuron, where they control excitability, contribute to the resting membrane potential, and help regulate cell volume.

Ligand-Gated Ion Channels

Many types of ion channels respond to chemical signals (ligands) rather than to changes in the membrane potential (Figure 4.4E–G). The most important of these **ligand-gated ion channels** in the nervous system is the class activated by binding neurotransmitters (Figure 4.4E). These channels are essential for synaptic transmission and other forms of cell-cell signaling phenomena discussed in Chapters 5–7. Whereas the voltage-gated ion channels underlying the action potential typically allow only one type of ion to permeate, channels activated by extracellular ligands are usually less selective, allowing two or more types of ions to pass through the channel pore.

Other ligand-gated channels are sensitive to chemical signals arising within the cytoplasm of neurons (see Chapter 7), and can be selective for specific ions such as K⁺ or Cl⁻, or permeable to all physiological cations. Such channels are distinguished by ligand-binding domains on their *intracellular* surfaces that interact with second messengers such as Ca²⁺, the cyclic nucleotides cAMP and cGMP, or protons. Examples of channels that respond to intracellular cues include Ca²⁺-activated K⁺ channels (Figure 4.4F), the cyclic nucleotide gated cation channel (Figure 4.4G), or acid-sensing ion channels (ASICs). The main function of these channels is to convert intracellular chemical signals into electrical information. This process is particularly important in sensory transduction, where channels gated by cyclic nucleotides convert odors and light, for example, into electrical signals. Although many of these ligand-gated ion channels are located in the cell surface membrane, others are in membranes of intracellular organelles such as mitochondria or the endoplasmic reticulum. Some of these latter channels are selectively permeable to Ca²⁺ and regulate the release of Ca²⁺ from the lumen of the endoplasmic reticulum into the cytoplasm, where this second messenger can then trigger a spectrum of cellular responses such as described in Chapter 7.

Stretch- and Heat-Activated Channels

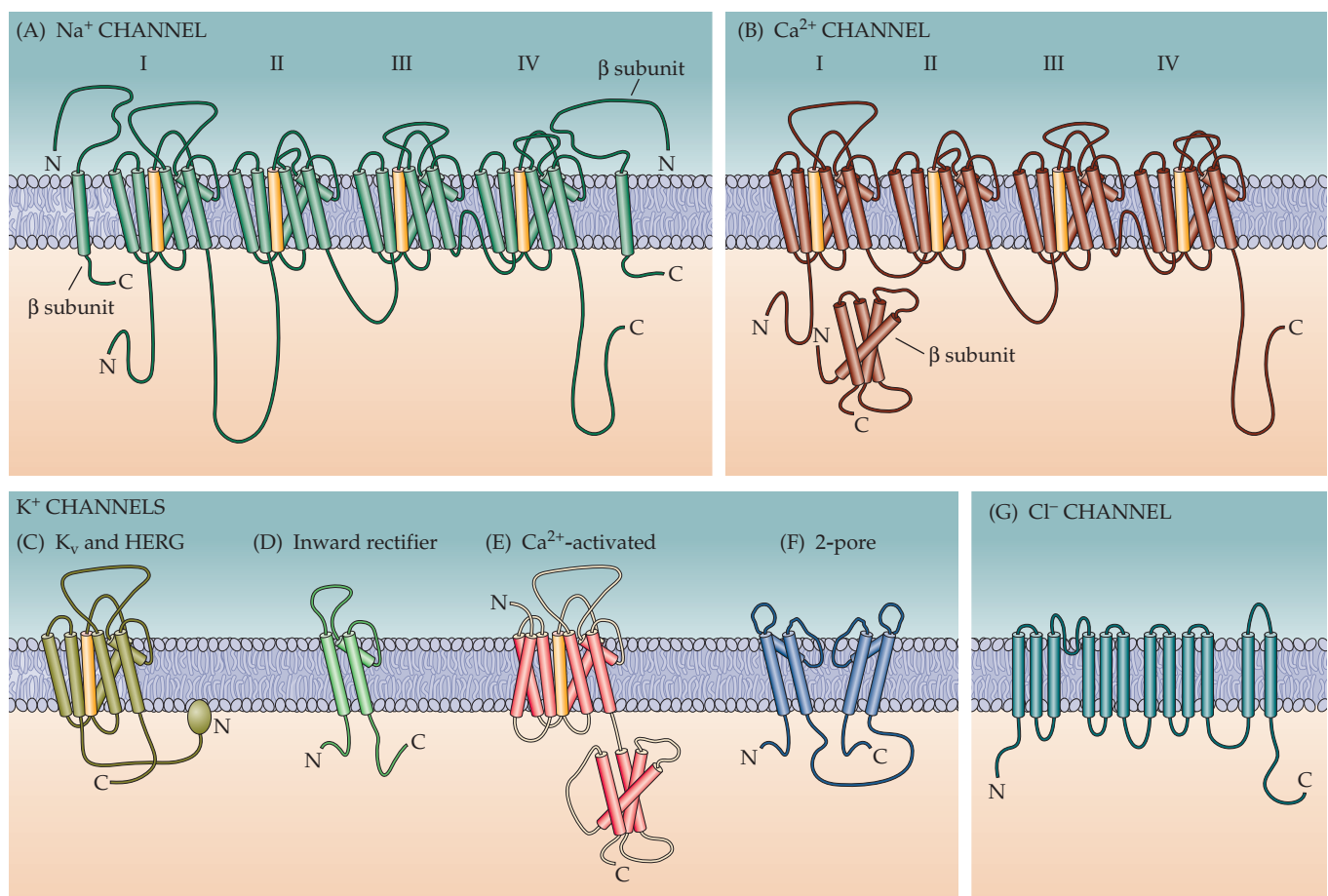
Still other ion channels respond to heat or membrane deformation. Heat-activated ion channels, such as some members of the transient receptor potential (TRP) gene family, contribute to the sensations of pain and temperature and help mediate inflammation (see Chapter 9). These channels are often specialized to detect specific temperature ranges, and some are even activated by cold. Other ion channels respond to mechanical distortion of the plasma membrane and are the basis of stretch receptors and neuromuscular stretch reflexes (see Chapters 8, 15 and 16). A specialized form of these channels enables hearing by allowing auditory hair cells to respond to sound waves (see Chapter 12).

In summary, this tremendous variety of ion channels allows neurons to generate electrical signals in response to changes in membrane potential, synaptic input, intracellular second messengers, light, odors, heat, sound, touch, and many other stimuli.

The Molecular Structure of Ion Channels

Understanding the physical structure of ion channels is obviously the key to sorting out how they actually work. Until recently, most information about channel structure was derived indirectly from studies of the amino acid composition and physiological properties of these proteins. For example, a great deal has been learned by exploring the functions of particular amino acids within the proteins using **mutagenesis** and the expression of such channels in *Xenopus* oocytes (see Box B). Such studies have discovered a general transmembrane architecture common to all the major ion channel families. Thus, these molecules are all integral membrane proteins that span the plasma membrane repeatedly. Na^+ (and Ca^{2+}) channel proteins, consist of repeating motifs of 6 membrane-spanning regions that are repeated 4 times, for a total of 24 transmembrane regions (Figure 4.6A,B). Na^+ (or Ca^{2+}) channels can be produced by just one of these proteins, although other accessory proteins, called β subunits, can regulate the function of these channels. K^+ channel proteins typically span the membrane six times (Figure 4.6C),

Figure 4.6 Topology of the principal subunits of voltage-gated Na^+ , Ca^{2+} , K^+ , and Cl^- channels. Repeating motifs of Na^+ (A) and Ca^{2+} (B) channels are labeled I, II, III, and IV; (C–F) K^+ channels are more diverse. In all cases, four subunits combine to form a functional channel. (G) Chloride channels are structurally distinct from all other voltage-gated channels.



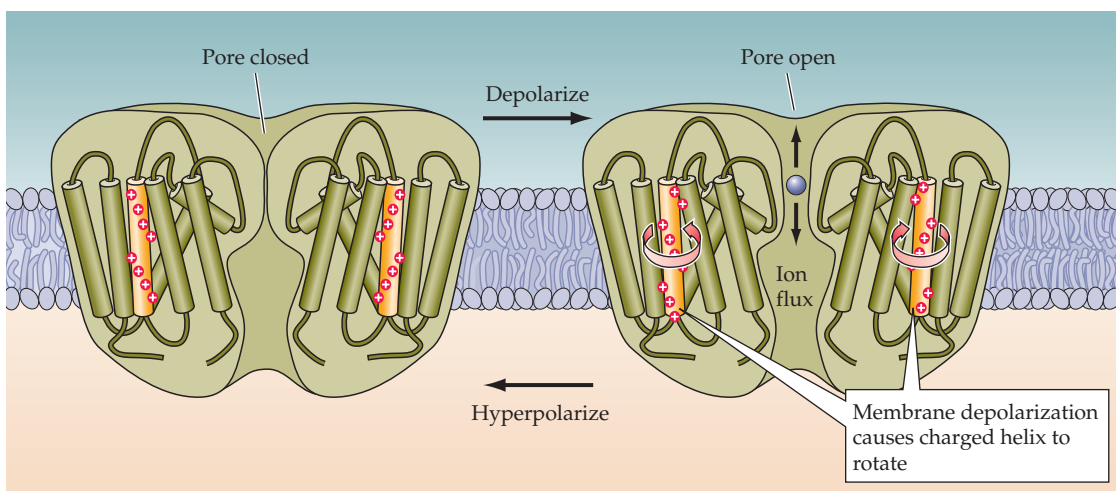
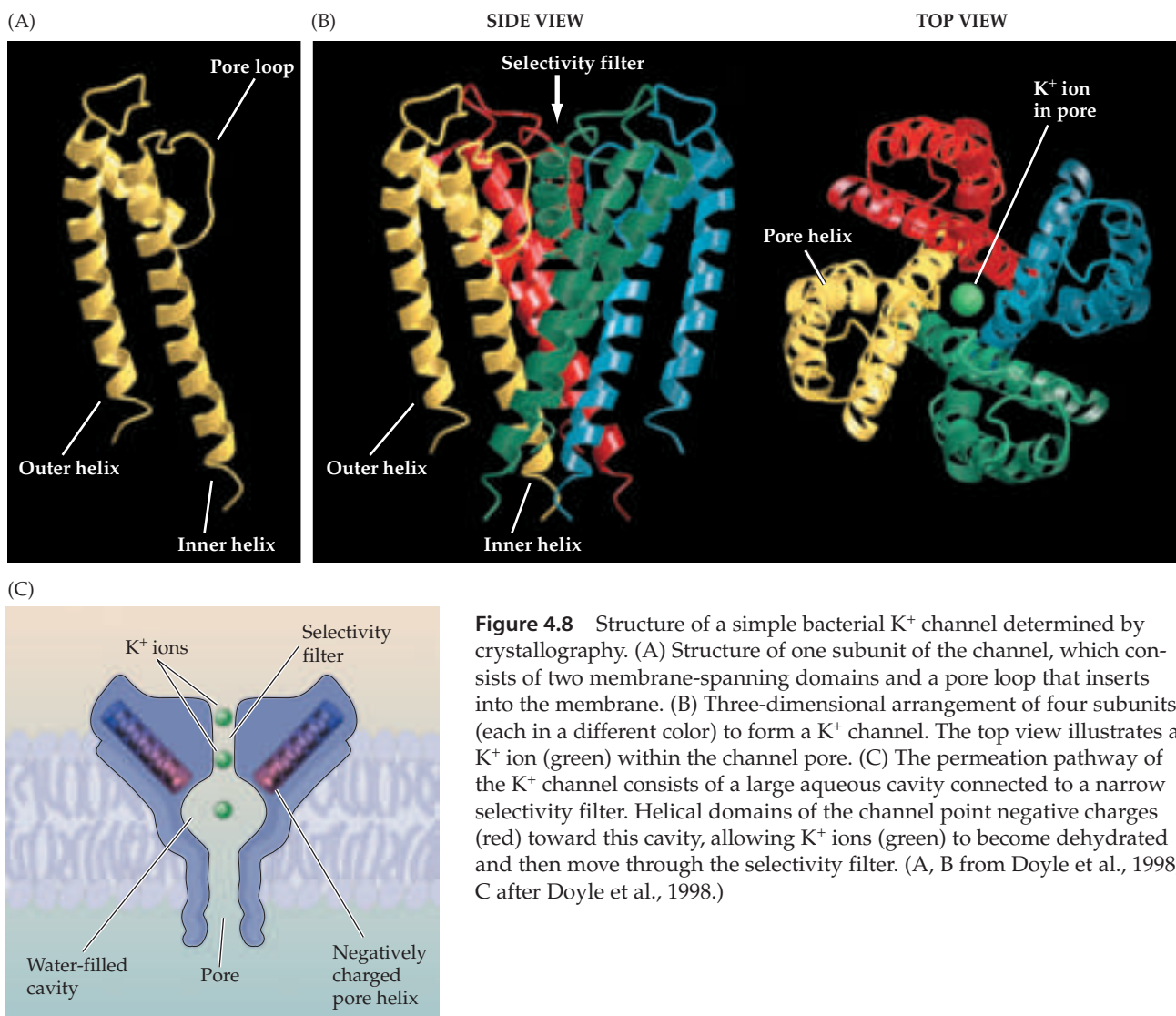


Figure 4.7 A charged voltage sensor permits voltage-dependent gating of ion channels. The process of voltage activation may involve the rotation of a positively charged transmembrane domain. This movement causes a change in the conformation of the pore loop, enabling the channel to conduct specific ions.

though there are some K^+ channels, such as a bacterial channel and some mammalian channels, that span the membrane only twice (Figure 4.6D), and others that span the membrane four times (Figure 4.6F) or seven times (Figure 4.6E). Each of these K^+ channel proteins serves as a channel subunit, with 4 of these subunits typically aggregating to form a single functional ion channel.

Other imaginative mutagenesis experiments have provided information about how these proteins function. Two membrane-spanning domains of all ion channels appear to form a central **pore** through which ions can diffuse, and one of these domains contains a protein loop that confers an ability to selectively allow certain ions to diffuse through the channel pore (Figure 4.7). As might be expected, the amino acid composition of the pore loop differs among channels that conduct different ions. These distinct structural features of channel proteins also provide unique binding sites for drugs and for various neurotoxins known to block specific subclasses of ion channels (Box C). Furthermore, many voltage gated ion channels contain a distinct type of transmembrane helix containing a number of positively charged amino acids along one face of the helix (Figures 4.6 and 4.7). This structure evidently serves as a sensor that detects changes in the electrical potential across the membrane. Membrane depolarization influences the charged amino acids such that the helix undergoes a conformational change, which in turn allows the channel pore to open. One suggestion is that the helix rotates to cause the pore to open (Figure 4.7). Other types of mutagenesis experiments have demonstrated that one end of certain K^+ channels plays a key role in channel inactivation. This intracellular structure (labeled "N" in Figure 4.6C) can plug the channel pore during prolonged depolarization.

More recently, very direct information about the structural underpinnings of ion channel function has come from **X-ray crystallography** studies of bacterial K^+ channels (Figure 4.8). This molecule was chosen for analysis because the large quantity of channel protein needed for crystallography could be obtained by growing large numbers of bacteria expressing this molecule. The results of such studies showed that the channel is formed by subunits that each cross the plasma membrane twice; between these two membrane-spanning structures is a loop that inserts into the plasma membrane (Figure 4.8A). Four of these subunits are assembled together to form a chan-



nel (Figure 4.8B). In the center of the assembled channel is a narrow opening through the protein that allows K^+ to flow across the membrane. This opening is the channel pore and is formed by the protein loop, as well as by the membrane-spanning domains. The structure of the pore is well suited for conducting K^+ ions (Figure 4.8C). The narrowest part is near the outside mouth of the channel and is so constricted that only a non-hydrated K^+ ion can fit through the bottleneck. Larger cations, such as Cs^+ , cannot traverse this region of the pore, and smaller cations such as Na^+ cannot enter the pore because the “walls” of the pore are too far apart to stabilize a dehydrated Na^+ ion. This part of the channel complex is responsible for the selective permeability to K^+ and is therefore called the **selectivity filter**. The sequence of amino acids making up part of this selectivity filter is often referred to as the K^+ channel “signature sequence”. Deeper within the channel is a water-filled cavity that connects to the interior of the cell. This cavity evidently collects K^+ from the cytoplasm and, utilizing negative charges from the protein,

Box C

Toxins That Poison Ion Channels

Given the importance of Na^+ and K^+ channels for neuronal excitation, it is not surprising that a number of organisms have evolved channel-specific toxins as mechanisms for self-defense or for capturing prey. A rich collection of natural toxins selectively target the ion channels of neurons and other cells. These toxins are valuable not only for survival, but for studying the function of cellular ion channels. The best-known channel toxin is *tetrodotoxin*, which is produced by certain puffer fish and other animals.

Tetrodotoxin produces a potent and specific obstruction of the Na^+ channels responsible for action potential generation, thereby paralyzing the animals unfortunate enough to ingest it.

Saxitoxin, a chemical homologue of tetrodotoxin produced by dinoflagellates, has a similar action on Na^+ channels. The potentially lethal effects of eating shellfish that have ingested these “red tide” dinoflagellates are due to the potent neuronal actions of saxitoxin.

Scorpions paralyze their prey by injecting a potent mix of peptide toxins that also affect ion channels. Among these are the α -toxins, which slow the inactivation of Na^+ channels (Figure A1); exposure of neurons to these toxins prolongs the action potential (Figure A2),

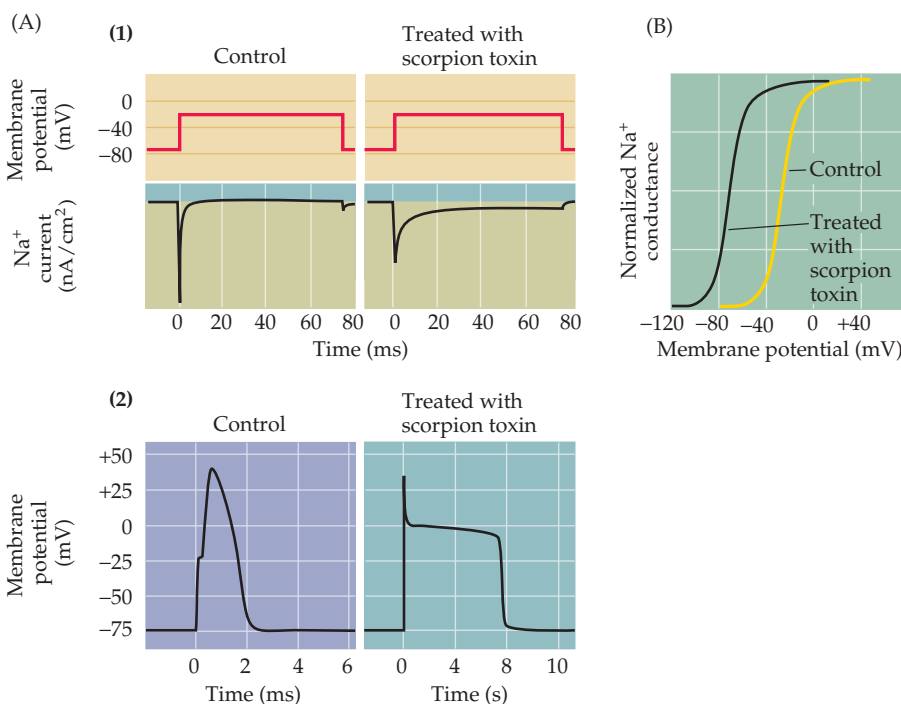
thereby scrambling information flow within the nervous system of the soon-to-be-devoured victim. Other peptides in scorpion venom, called β -toxins, shift the voltage dependence of Na^+ channel activation (Figure B). These toxins cause Na^+ channels to open at potentials much more negative than normal, disrupting action potential generation. Some alkaloid toxins combine these actions, both removing inactivation and shifting activation of Na^+ channels. One such toxin is *batrachotoxin*, produced by a species of frog; some tribes of South American Indians use this poison on their arrow tips. A number of plants produce similar toxins, including *aconitine*, from buttercups; *veratridine*, from lilies; and a number of insecticidal toxins produced by plants such as chrysanthemums and rhododendrons.

Potassium channels have also been targeted by toxin-producing organisms.

Peptide toxins affecting K^+ channels include *dendrotoxin*, from wasps; *apamin*, from bees; and *charybdotoxin*, yet another toxin produced by scorpions. All of these toxins block K^+ channels as their primary action; no toxin is known to affect the activation or inactivation of these channels, although such agents may simply be awaiting discovery.

References

- CAHALAN, M. (1975) Modification of sodium channel gating in frog myelinated nerve fibers by *Centruroides sculpturatus* scorpion venom. *J. Physiol. (Lond.)* 244: 511–534.
- NARAHASHI, T. (2000) Neuroreceptors and ion channels as the basis for drug action: Present and future. *J. Pharmacol. Exptl. Therapeutics* 294: 1–26.
- SCHMIDT, O. AND H. SCHMIDT (1972) Influence of calcium ions on the ionic currents of nodes of Ranvier treated with scorpion venom. *Pflügers Arch. 333: 51–61.*



(A) Effects of toxin treatment on frog axons. (1) α -Toxin from the scorpion *Leiurus quinquestriatus* prolongs Na^+ currents recorded with the voltage clamp method. (2) As a result of the increased Na^+ current, α -toxin greatly prolongs the duration of the axonal action potential. Note the change in timescale after treating with toxin. (B) Treatment of a frog axon with β -toxin from another scorpion, *Centruroides sculpturatus*, shifts the activation of Na^+ channels, so that Na^+ conductance begins to increase at potentials much more negative than usual. (A after Schmidt and Schmidt, 1972; B after Cahalan, 1975.)

allows K^+ ions to become dehydrated so they can enter the selectivity filter. These “naked” ions are then able to move through four K^+ binding sites within the selectivity filter to eventually reach the extracellular space (recall that the normal concentration gradient drives K^+ out of cells). On average, two K^+ ions reside within the selectivity filter at any moment, with electrostatic repulsion between the two ions helping to speed their transit through the selectivity filter, thereby permitting rapid ion flux through the channel.

Crystallographic studies have also determined the structure of the **voltage sensor** in another type of bacterial K^+ channel. Such studies indicate that the sensor is at the interface between proteins and lipid on the cytoplasmic surface of the channel, leading to the suggestion that the sensor is a paddle-like structure that moves through the membrane to gate the opening of the channel pore (Figure 4.9A), rather than being a rotating helix buried within the ion channel protein (as in Figure 4.7). Crystallographic work has also revealed the molecular basis of the rapid transitions between the closed and the open state of the channel during channel gating. By comparing data from K^+ channels crystallized in what is believed to be closed and open conformations (Figure 4.9B), it appears that channels gate by a conformational change in one of the transmembrane helices lining the channel pore. Producing a “kink” in one of these helices increases the opening from the central water-filled pore to the intracellular space, thereby permitting ion fluxes.

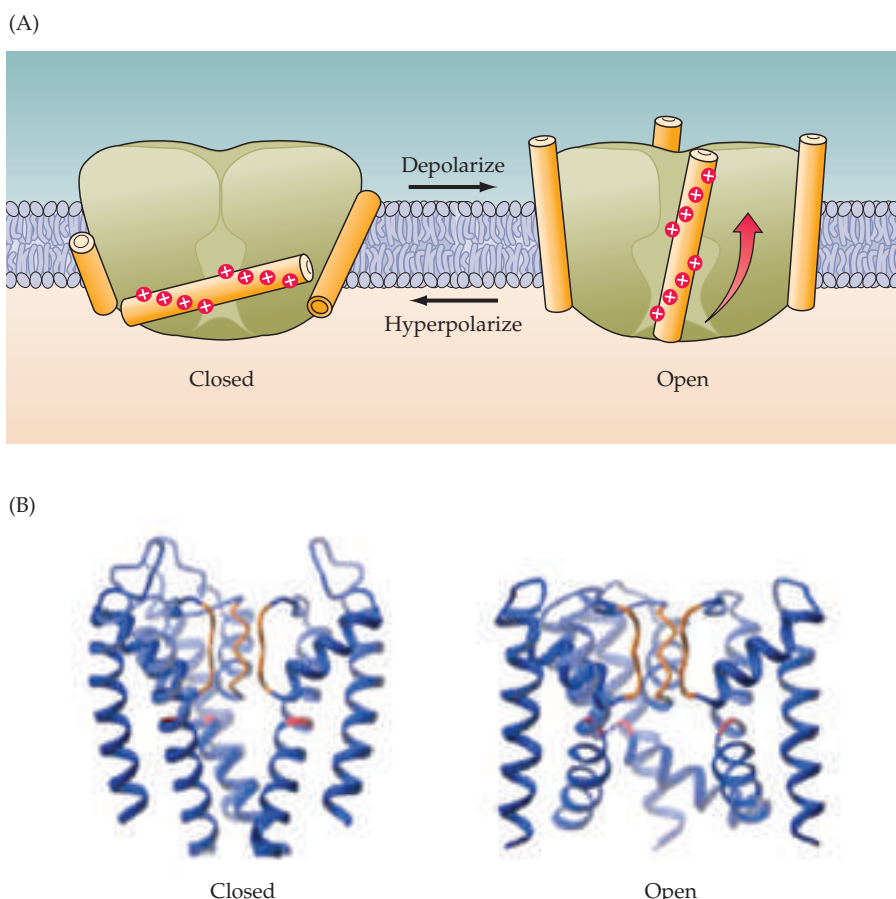


Figure 4.9 Structural features of K^+ channel gating. (A) Voltage sensing may involve paddle-like structures of the channel. These paddles reside within the lipid bilayer of the plasma membrane and may respond to changes in membrane potential by moving through the membrane. The gating charges that sense membrane potential are indicated by red “plus” signs. (B) Structure of K^+ channels in closed (left) and open (right) conformations. Three of the four channel subunits are shown. Opening of the pore of the channel involves kinking of a transmembrane domain at the point indicated in red, which then dilates the pore. (A after Jiang et al., 2003; B after MacKinnon, 2003).

Box D

Diseases Caused by Altered Ion Channels

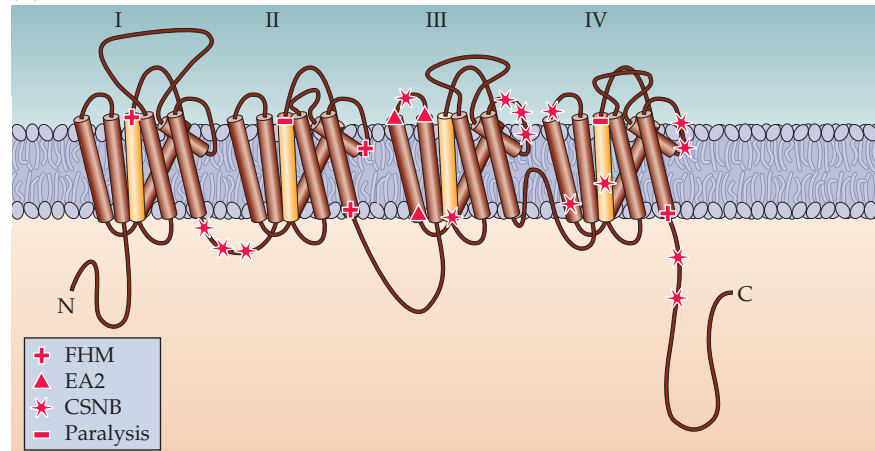
Several genetic diseases, collectively called *channelopathies*, result from small but critical alterations in ion channel genes. The best-characterized of these diseases are those that affect skeletal muscle cells. In these disorders, alterations in ion channel proteins produce either myotonia (muscle stiffness due to excessive electrical excitability) or paralysis (due to insufficient muscle excitability). Other disorders arise from ion channel defects in heart, kidney, and the inner ear.

Channelopathies associated with ion channels localized in brain are much more difficult to study. Nonetheless, voltage-gated Ca^{2+} channels have recently been implicated in a range of neurological diseases. These include episodic ataxia, spinocerebellar degeneration, night blindness, and migraine headaches. *Familial hemiplegic migraine* (FHM) is characterized by migraine attacks that typically last one to three days. During such episodes, patients experience severe headaches and vomiting. Several mutations in a human Ca^{2+} channel have been identified in families with FHM, each having different clinical symptoms. For example, a mutation in the pore-forming region of the channel produces hemiplegic migraine with progressive cerebellar ataxia, whereas other mutations cause only the usual FHM symptoms. How these altered Ca^{2+} channel properties lead to migraine attacks is not known.

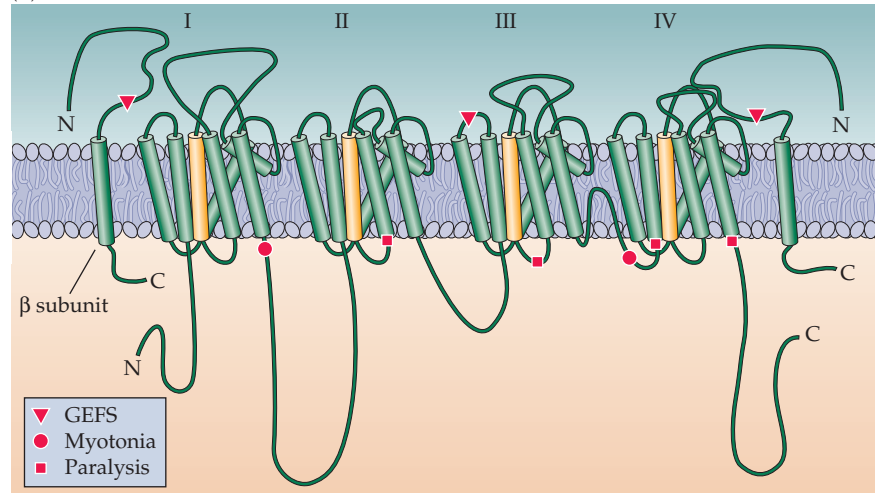
Episodic ataxia type 2 (EA2) is a neurological disorder in which affected individuals suffer recurrent attacks of abnormal limb movements and severe ataxia. These problems are sometimes accompa-

Genetic mutations in (A) Ca^{2+} channels, (B) Na^+ channels, (C) K^+ channels, and (D) Cl^- channels that result in diseases. Red regions indicate the sites of these mutations; the red circles indicate mutations. (After Lehmann-Horn and Jurkat-Kott, 1999.)

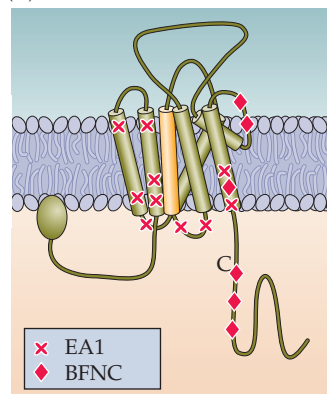
(A) Ca^{2+} CHANNEL



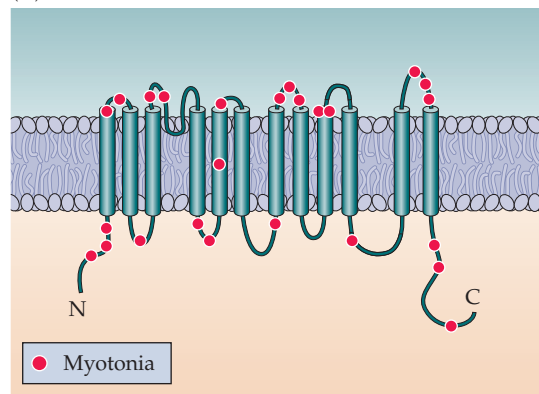
(B) Na^+ CHANNEL

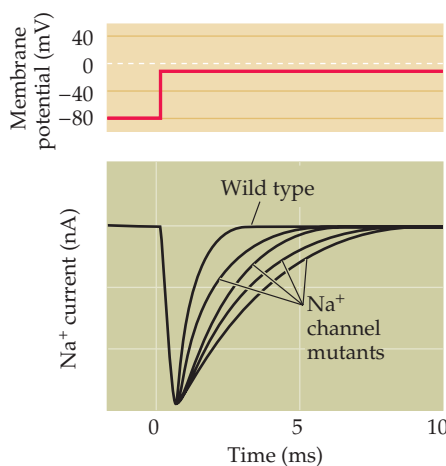


(C) K^+ CHANNEL



(D) Cl^- CHANNEL





Mutations in Na^+ channels slow the rate of inactivation of Na^+ currents. (After Barchi, 1995.)

nied by vertigo, nausea, and headache. Usually, attacks are precipitated by emotional stress, exercise, or alcohol and last for a few hours. The mutations in EA2 cause Ca^{2+} channels to be truncated at various sites, which may cause the clinical manifestations of the disease by preventing the normal assembly of Ca^{2+} channels in the membrane.

X-linked *congenital stationary night blindness* (CSNB) is a recessive retinal disorder that causes night blindness, decreased visual acuity, myopia, nystagmus, and strabismus. Complete CSNB causes retinal rod photoreceptors to be nonfunctional. Incomplete CSNB causes subnormal (but measurable) functioning

of both rod and cone photoreceptors. Like EA2, the incomplete type of CSNB is caused by mutations producing truncated Ca^{2+} channels. Abnormal retinal function may arise from decreased Ca^{2+} currents and neurotransmitter release from photoreceptors (see Chapter 11).

A defect in brain Na^+ channels causes *generalized epilepsy with febrile seizures* (GEFS) that begins in infancy and usually continues through early puberty. This defect has been mapped to two mutations: one on chromosome 2 that encodes an α subunit for a voltage-gated Na^+ channel, and the other on chromosome 19 that encodes a Na^+ channel β subunit. These mutations cause a slowing of Na^+ channel inactivation (see figure above), which may explain the neuronal hyperexcitability underlying GEFS.

Another type of seizure, *benign familial neonatal convulsion* (BFNC), is due to K^+ channel mutations. This disease is characterized by frequent brief seizures commencing within the first week of life and disappearing spontaneously within a few months. The mutation has been mapped to at least two voltage-gated K^+ channel genes. A reduction in K^+ current flow through the mutated channels probably accounts for the hyperexcitability associated with this defect. A related disease, episodic ataxia type 1 (EA1), has been linked to a defect in another type of voltage-gated K^+ channel. EA1 is characterized by brief episodes of ataxia. Mu-

tant channels inhibit the function of other, non-mutant K^+ channels and may produce clinical symptoms by impairing action potential repolarization. Mutations in the K^+ channels of cardiac muscle are responsible for the irregular heartbeat of patients with long Q-T syndrome. Numerous genetic disorders affect the voltage-gated channels of skeletal muscle and are responsible for a host of muscle diseases that either cause muscle weakness (*paralysis*) or muscle contraction (*myotonia*).

References

- BARCHI, R. L. (1995) Molecular pathology of the skeletal muscle sodium channel. *Ann. Rev. Physiol.* 57: 355–385.
- BERKOVIC, S. F. AND I. E. SCHEFFER (1997) Epilepsies with single gene inheritance. *Brain Develop.* 19: 13–28.
- COOPER, E. C. AND L. Y. JAN (1999) Ion channel genes and human neurological disease: Recent progress, prospects, and challenges. *Proc. Natl. Acad. Sci. USA* 96: 4759–4766.
- DAVIES, N. P. AND M. G. HANNA (1999) Neurological channelopathies: Diagnosis and therapy in the new millennium. *Ann. Med.* 31: 406–420.
- JEN, J. (1999) Calcium channelopathies in the central nervous system. *Curr. Op. Neurobiol.* 9: 274–280.
- LEHMANN-HORN, F. AND K. JURKAT-ROTT (1999) Voltage-gated ion channels and hereditary disease. *Physiol. Rev.* 79: 1317–1372.
- OPHOFF, R. A., G. M. TERWINDT, R. R. FRANTS AND M. D. FERRARI (1998) P/Q-type Ca^{2+} channel defects in migraine, ataxia and epilepsy. *Trends Pharm. Sci.* 19: 121–127.

In short, ion channels are integral membrane proteins with characteristic features that allow them to assemble into multimolecular aggregates. Collectively, these structures allow channels to conduct ions, sense the transmembrane potential, to inactivate, and to bind to various neurotoxins. A combination of physiological, molecular biological and crystallographic studies has begun to provide a detailed physical picture of K^+ channels. This work has now provided considerable insight into how ions are conducted from one side of the plasma membrane to the other, how a channel can be selectively permeable to a single type of ion, how they are able to sense changes in membrane voltage, and how they gate the opening of their pores. It is likely that other types of ion channels will be similar in their functional architecture. Finally, this sort of work has illuminated how mutations in ion channel genes can lead to a variety of neurological disorders (Box D).

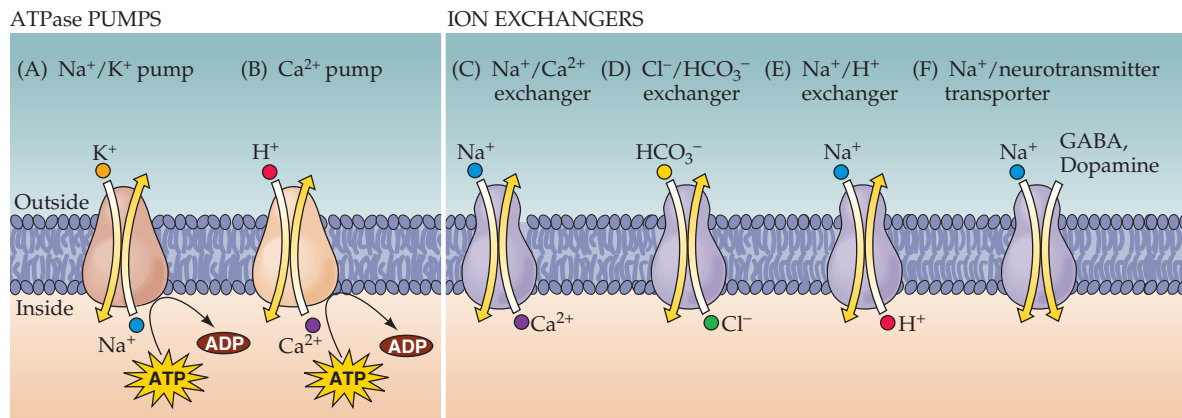
Active Transporters Create and Maintain Ion Gradients

Up to this point, the discussion of the molecular basis of electrical signaling has taken for granted the fact that nerve cells maintain ion concentration gradients across their surface membranes. However, none of the ions of physiological importance (Na^+ , K^+ , Cl^- , and Ca^{2+}) are in electrochemical equilibrium. Because channels produce electrical effects by allowing one or more of these ions to diffuse down their electrochemical gradients, there would be a gradual dissipation of these concentration gradients unless nerve cells could restore ions displaced during the current flow that occurs as a result of both neural signaling and the continual ionic leakage that occurs at rest. The work of generating and maintaining ionic concentration gradients for particular ions is carried out by a group of plasma membrane proteins known as **active transporters**.

Active transporters carry out this task by forming complexes with the ions that they are translocating. The process of ion binding and unbinding for transport typically requires several milliseconds. As a result, ion translocation by active transporters is much slower than ion movement through channels: Recall that ion channels can conduct thousands of ions across a membrane each millisecond. In short, active transporters gradually store energy in the form of ion concentration gradients, whereas the opening of ion channels rapidly dissipates this stored energy during relatively brief electrical signaling events.

Several types of active transporter have now been identified (Figure 4.10). Although the specific jobs of these transporters differ, all must translocate ions against their electrochemical gradients. Moving ions uphill requires the consumption of energy, and neuronal transporters fall into two classes based on their energy sources. Some transporters acquire energy directly from the hydrolysis of ATP and are called **ATPase pumps** (Figure 4.10, left). The most prominent example of an ATPase pump is the Na^+ pump (or, more properly, the Na^+/K^+ ATPase pump), which is responsible for maintaining transmembrane concentration gradients for both Na^+ and K^+ (Figure 4.10A). Another is the Ca^{2+} pump, which provides one of the main mechanisms for removing Ca^{2+} from cells (Figure 4.10B). The second class of active transporter does not use ATP directly, but depends instead on the electrochemical gradients of other ions as an energy source. This type of transporter carries one or more ions *up* its electrochemical gradient while simultaneously taking another ion (most often Na^+) *down* its gradient. Because at least two species of ions are

Figure 4.10 Examples of ion transporters found in cell membranes. (A,B) Some transporters are powered by the hydrolysis of ATP (ATPase pumps), whereas others (C–F) use the electrochemical gradients of co-transported ions as a source of energy (ion exchangers).



involved in such transactions, these transporters are usually called **ion exchangers** (Figure 4.10, right). An example of such a transporter is the $\text{Na}^+/\text{Ca}^{2+}$ exchanger, which shares with the Ca^{2+} pump the important job of keeping intracellular Ca^{2+} concentrations low (Figure 4.10C). Another exchanger in this category regulates both intracellular Cl^- concentration and pH by swapping intracellular Cl^- for another extracellular anion, bicarbonate (Figure 4.10D). Other ion exchangers, such as the Na^+/H^+ exchanger (Figure 4.10E), also regulate intracellular pH, in this case by acting directly on the concentration of H^+ . Yet other ion exchangers are involved in transporting neurotransmitters into synaptic terminals (Figure 4.10F), as described in Chapter 6. Although the electrochemical gradient of Na^+ (or other counter ions) is the proximate source of energy for ion exchangers, these gradients ultimately depend on the hydrolysis of ATP by ATPase pumps, such as the Na^+/K^+ ATPase pump.

Functional Properties of the Na^+/K^+ Pump

Of these various transporters, the best understood is the Na^+/K^+ pump. The activity of this pump is estimated to account for 20–40% of the brain's energy consumption, indicating its importance for brain function. The Na^+ pump was first discovered in neurons in the 1950s, when Richard Keynes at Cambridge University used radioactive Na^+ to demonstrate the energy-dependent efflux of Na^+ from squid giant axons. Keynes and his collaborators found that this efflux ceased when the supply of ATP in the axon was interrupted by treatment with metabolic poisons (Figure 4.11A, point 4). Other conditions that lower intracellular ATP also prevent Na^+ efflux. These experiments showed that removing intracellular Na^+ requires cellular metabolism. Further studies with radioactive K^+ demonstrated that Na^+ efflux is associated with simultaneous, ATP-dependent influx of K^+ . These opposing fluxes of Na^+ and K^+ are operationally inseparable: Removal of external K^+ greatly reduces Na^+ efflux (Figure 4.11, point 2), and vice versa. These energy-dependent movements of Na^+ and K^+ implicated an ATP-hydrolyzing Na^+/K^+ pump in the generation of the transmembrane gradients of both Na^+ and K^+ . The exact mechanism responsible for these fluxes of Na^+ and K^+ is still not entirely clear, but the pump is thought to alternately shuttle these ions across the membranes in a cycle fueled by the transfer of a phosphate group from ATP to the pump protein (Figure 4.11B).

Additional quantitative studies of the movements of Na^+ and K^+ indicate that the two ions are not pumped at identical rates: The K^+ influx is only about two-thirds the Na^+ efflux. Thus, the pump apparently transports two K^+ into the cell for every three Na^+ that are removed (see Figure 4.11B). This stoichiometry causes a net loss of one positively charged ion from inside of the cell during each round of pumping, meaning that the pump generates an electrical current that can hyperpolarize the membrane potential. For this reason, the Na^+/K^+ pump is said to be **electrogenic**. Because pumps act much more slowly than ion channels, the current produced by the Na^+/K^+ pump is quite small. For example, in the squid axon, the net current generated by the pump is less than 1% of the current flowing through voltage-gated Na^+ channels and affects the resting membrane potential by only a millivolt or less.

Although the electrical current generated by the activity of the Na^+/K^+ pump is small, under special circumstances the pump can significantly influence the membrane potential. For instance, prolonged stimulation of

Figure 4.11 Ionic movements due to the Na^+/K^+ pump. (A) Measurement of radioactive Na^+ efflux from a squid giant axon. This efflux depends on external K^+ and intracellular ATP. (B) A model for the movement of ions by the Na^+/K^+ pump. Uphill movements of Na^+ and K^+ are driven by ATP, which phosphorylates the pump. These fluxes are asymmetrical, with three Na^+ carried out for every two K^+ brought in. (A after Hodgkin and Keynes, 1955; B after Lingrel et al., 1994.)

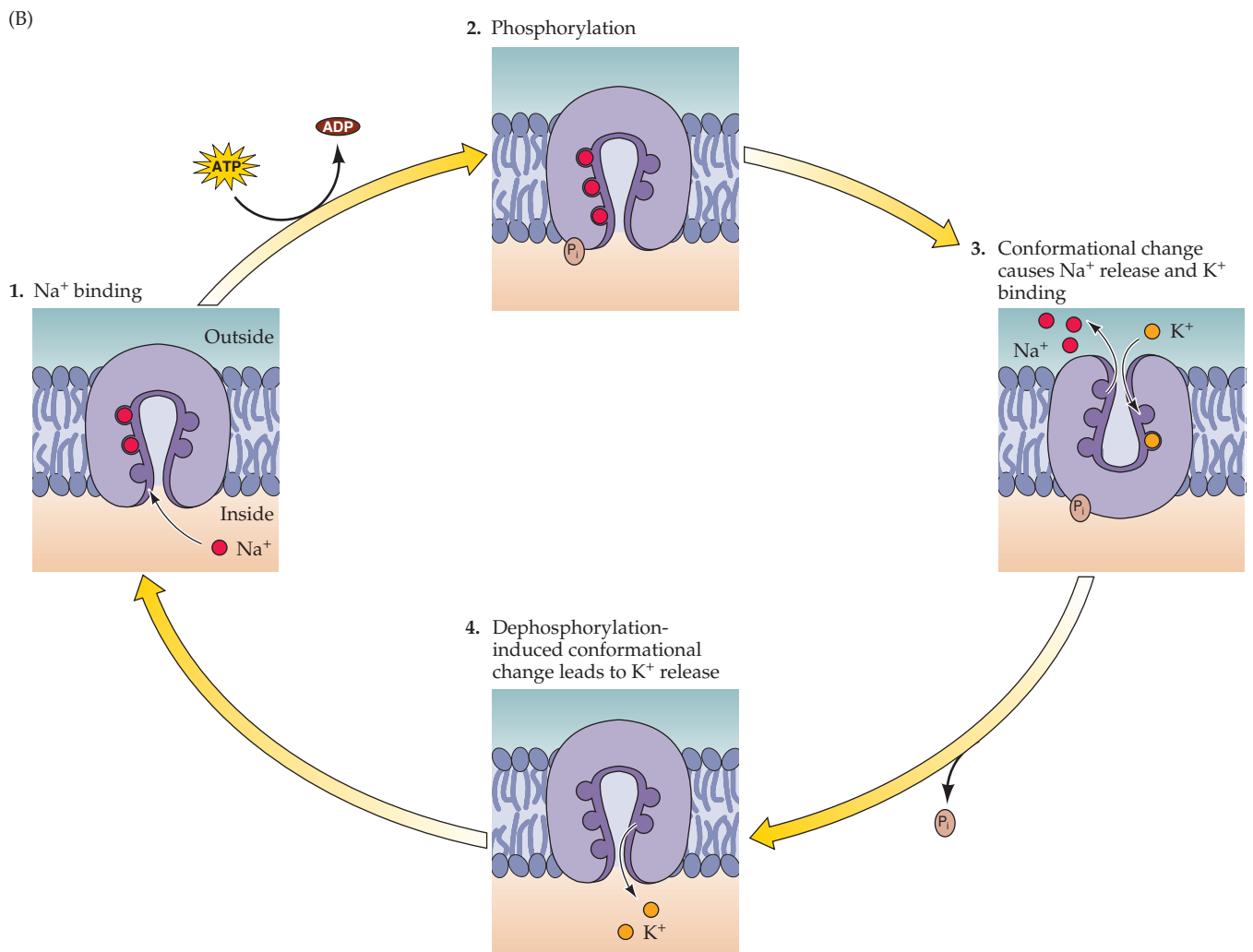
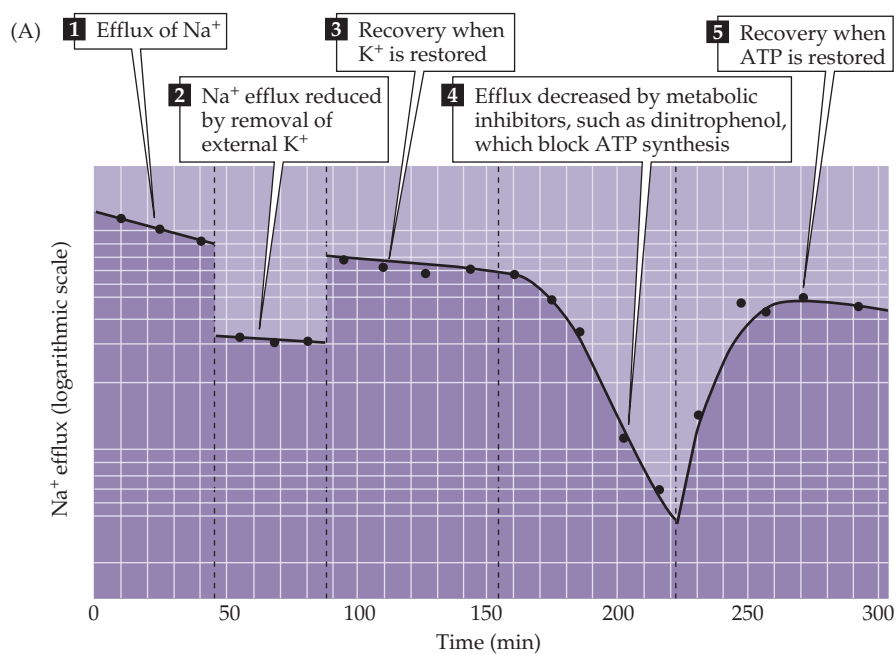


Figure 4.12 The electrogenic transport of ions by the Na^+/K^+ pump can influence membrane potential. Measurements of the membrane potential of a small unmyelinated axon show that a train of action potentials is followed by a long-lasting hyperpolarization. This hyperpolarization is blocked by ouabain, indicating that it results from the activity of the Na^+/K^+ pump. (After Rang and Ritchie, 1968.)

small unmyelinated axons produces a substantial hyperpolarization (Figure 4.12). During the period of stimulation, Na^+ enters through voltage-gated channels and accumulates within the axons. As the pump removes this extra Na^+ , the resulting current generates a long-lasting hyperpolarization. Support for this interpretation comes from the observation that conditions that block the Na^+/K^+ pump—for example, treatment with ouabain, a plant glycoside that specifically inhibits the pump—prevent the hyperpolarization. The electrical contribution of the Na^+/K^+ pump is particularly significant in these small-diameter axons because their large surface-to-volume ratio causes intracellular Na^+ concentration to rise to higher levels than it would in other cells. Nonetheless, it is important to emphasize that, in most circumstances, the Na^+/K^+ pump plays no part in generating the action potential and has very little *direct* effect on the resting potential.

The Molecular Structure of the Na^+/K^+ Pump

These observations imply that the Na^+ and K^+ pump must exhibit several molecular properties: (1) It must bind both Na^+ and K^+ ; (2) it must possess sites that bind ATP and receive a phosphate group from this ATP; and (3) it must bind ouabain, the toxin that blocks this pump (Figure 4.13A). A variety of studies have now identified the aspects of the protein that account for these properties of the Na^+/K^+ pump. This pump is a large, integral membrane protein made up of at least two subunits, called α and β . The primary sequence shows that the α subunit spans the membrane 10 times, with most of the molecule found on the cytoplasmic side, whereas the β subunit spans the membrane once and is predominantly extracellular. Although a detailed account of the functional domains of the Na^+/K^+ pump is not yet available, some parts of the amino acid sequence have identified functions (Figure 4.13B). One intracellular domain of the protein is required for ATP binding

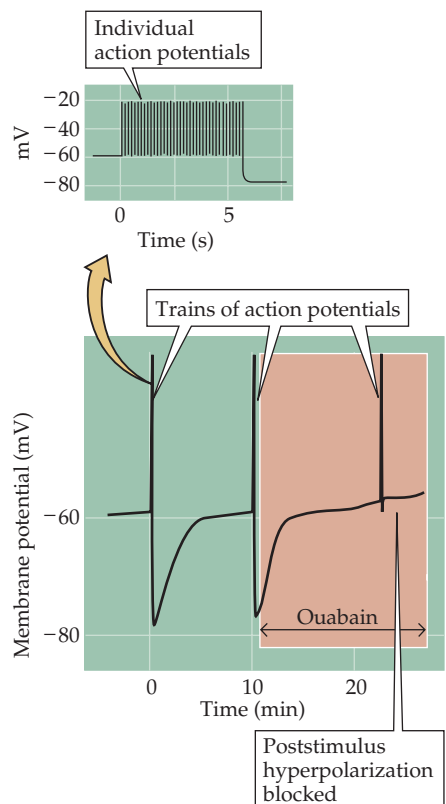
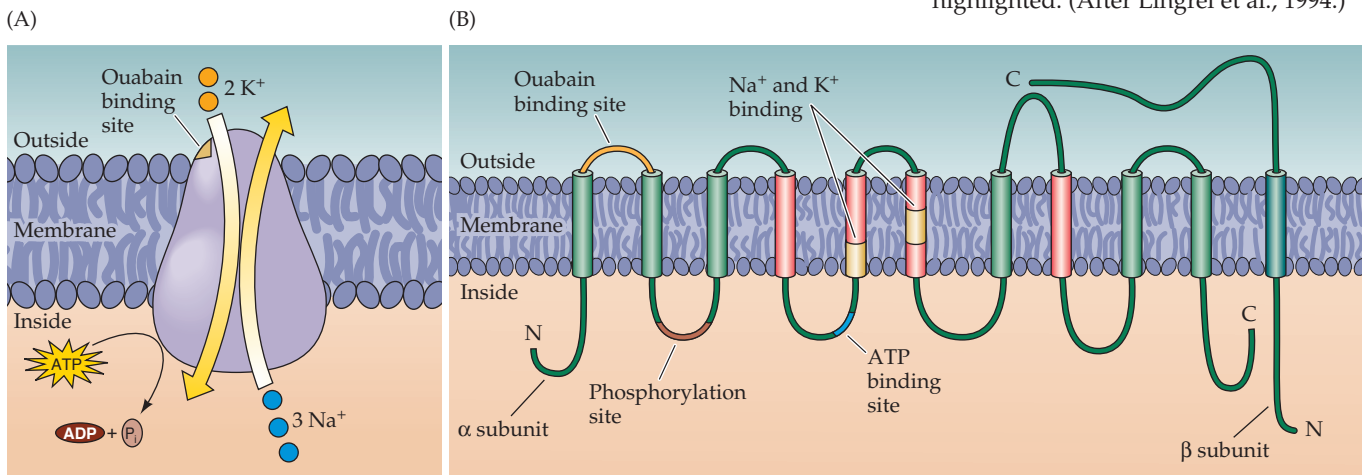


Figure 4.13 Molecular structure of the Na^+/K^+ pump. (A) General features of the pump. (B) The molecule spans the membrane 10 times. Amino acid residues thought to be important for binding of ATP, K^+ , and ouabain are highlighted. (After Lingrel et al., 1994.)



and hydrolysis, and the amino acid phosphorylated by ATP has been identified. Another extracellular domain may represent the binding site for ouabain. However, the sites involved in the most critical function of the pump—the movement of Na^+ and K^+ —have not yet been defined. Nonetheless, altering certain membrane-spanning domains (red in Figure 4.13B) impairs ion translocation; moreover, kinetic studies indicate that both ions bind to the pump at the same site. Because these ions move across the membrane, it is likely that this site traverses the plasma membrane; it is also likely that the site has a negative charge, since both Na^+ and K^+ are positively charged. The observation that removing negatively charged residues in a membrane-spanning domain of the protein (pale yellow in Figure 4.13B) greatly reduces Na^+ and K^+ binding provides at least a hint about the ion-translocating domain of the transporter molecule.

Summary

Ion transporters and channels have complementary functions. The primary purpose of transporters is to generate transmembrane concentration gradients, which are then exploited by ion channels to generate electrical signals. Ion channels are responsible for the voltage-dependent conductances of nerve cell membranes. The channels underlying the action potential are integral membrane proteins that open or close ion-selective pores in response to the membrane potential, allowing specific ions to diffuse across the membrane. The flow of ions through single open channels can be detected as tiny electrical currents, and the synchronous opening of many such channels generates the macroscopic currents that produce action potentials. Molecular studies show that such voltage-gated channels have highly conserved structures that are responsible for features such as ion permeation and voltage sensing, as well as the features that specify ion selectivity and toxin sensitivity. Other types of channels are sensitive to chemical signals, such as neurotransmitters or second messengers, or to heat or membrane deformation. A large number of ion channel genes create channels with a correspondingly wide range of functional characteristics, thus allowing different types of neurons to have a remarkable spectrum of electrical properties. Ion transporter proteins are quite different in both structure and function. The energy needed for ion movement against a concentration gradient (e.g., in maintaining the resting potential) is provided either by the hydrolysis of ATP or by the electrochemical gradient of co-transported ions. The Na^+/K^+ pump produces and maintains the transmembrane gradients of Na^+ and K^+ , while other transporters are responsible for the electrochemical gradients for other physiologically important ions, such as Cl^- , Ca^{2+} , and H^+ . Together, transporters and channels provide a reasonably comprehensive molecular explanation for the ability of neurons to generate electrical signals.

Additional Reading

Reviews

ARMSTRONG, C. M. AND B. HILLE (1998) Voltage-gated ion channels and electrical excitability. *Neuron* 20: 371–380.

BEZANILLA, F. AND A. M. CORREA (1995) Single-channel properties and gating of Na^+ and K^+ channels in the squid giant axon. In *Cephalopod Neurobiology*, N. J. Abbott, R. Williamson and L. Maddock (eds.). New York: Oxford University Press, pp. 131–151.

CATTERALL, W. A. (1988) Structure and function of voltage-sensitive ion channels. *Science* 242: 50–61.

ISOM, L. L., K. S. DE JONGH AND W. A. CATTERALL (1994) Auxiliary subunits of voltage-gated ion channels. *Neuron* 12: 1183–1194.

JAN, L. Y. AND Y. N. JAN (1997) Voltage-gated and inwardly rectifying potassium channels. *J. Physiol.* 505: 267–282.

JENTSCH, T. J., T. FRIEDRICH, A. SCHRIEVER AND H. YAMADA (1999) The CLC chloride channel family. *Pflügers Archiv* 437: 783–795.

KAPLAN, J. H. (2002) Biochemistry of Na,K -ATPase. *Annu. Rev. Biochem.* 71: 511–535.

KRISHNAL, O. (2003). The ASICs: Signaling molecules? Modulators? *Trends Neurosci.* 26: 477–483.

LINGREL, J. B., J. VAN HUYSSE, W. O'BRIEN, E. JEWELL-MOTZ, R. ASKEW AND P. SCHULTHEIS (1994) Structure-function studies of the Na,K -ATPase. *Kidney Internat.* 45: S32–S39.

MACKINNON, R. (2003) Potassium channels. *FEBS Lett.* 555: 62–65.

NEHER, E. (1992) Nobel lecture: Ion channels for communication between and within cells. *Neuron* 8: 605–612.

PATAPOUTIAN, A., A. M. PEIER, G. M. STORY AND V. VISWANATH (2003). ThermoTRP channels and beyond: Mechanisms of temperature sensation. *Nat. Rev. Neurosci.* 4: 529–539.

SEEBURG, P. H. (2002). A-to-I editing: New and old sites, functions and speculations. *Neuron* 35: 17–20.

SKOU, J. C. (1988) Overview: The Na,K pump. *Meth. Enzymol.* 156: 1–25.

Important Original Papers

ANTZ, C. AND 7 OTHERS (1997) NMR structure of inactivation gates from mammalian voltage-dependent potassium channels. *Nature* 385: 272–275.

BEZANILLA, F., E. PEROZO, D. M. PAPAZIAN AND

E. STEFANI (1991) Molecular basis of gating charge immobilization in Shaker potassium channels. *Science* 254: 679–683.

BOULTER, J. AND 6 OTHERS (1990) Molecular cloning and functional expression of glutamate receptor subunit genes. *Science* 249: 1033–1037.

CATERINA, M. J., M. A. SCHUMACHER, M. TOMINAGA, T. A. ROSEN, J. D. LEVINE AND D. JULIUS (1997) The capsaicin receptor: A heat-activated ion channel in the pain pathway. *Nature* 389: 816–824.

CHA, A., G. E. SNYDER, P. R. SELVIN AND F. BEZANILLA (1999) Atomic scale movement of the voltage-sensing region in a potassium channel measured via spectroscopy. *Nature* 402: 809–813.

DOYLE, D. A. AND 7 OTHERS (1998) The structure of the potassium channel: Molecular basis of K^+ conduction and selectivity. *Science* 280: 69–77.

FAHLKE, C., H. T. YU, C. L. BECK, T. H. RHODES AND A. L. GEORGE JR. (1997) Pore-forming segments in voltage-gated chloride channels. *Nature* 390: 529–532.

HO, K. AND 6 OTHERS (1993) Cloning and expression of an inwardly rectifying ATP-regulated potassium channel. *Nature* 362: 31–38.

HODGKIN, A. L. AND R. D. KEYNES (1955) Active transport of cations in giant axons from *Sepia* and *Loligo*. *J. Physiol.* 128: 28–60.

HOSHI, T., W. N. ZAGOTTA AND R. W. ALDRICH (1990) Biophysical and molecular mechanisms of *Shaker* potassium channel inactivation. *Science* 250: 533–538.

JIANG, Y. AND 6 OTHERS (2003) X-ray structure of a voltage-dependent K^+ channel. *Nature* 423: 33–41.

LLANO, I., C. K. WEBB AND F. BEZANILLA (1988) Potassium conductance of squid giant axon. Single-channel studies. *J. Gen. Physiol.* 92: 179–196.

MIKAMI, A. AND 7 OTHERS (1989) Primary structure and functional expression of the cardiac dihydropyridine-sensitive calcium channel. *Nature* 340: 230–233.

NODA, M. AND 6 OTHERS (1986) Expression of functional sodium channels from cloned cDNA. *Nature* 322: 826–828.

NOWICKY, M. C., A. P. FOX AND R. W. TSIEN (1985) Three types of neuronal calcium channel with different calcium agonist sensitivity. *Nature* 316: 440–443.

PAPAZIAN, D. M., T. L. SCHWARZ, B. L. TEMPET, Y. N. JAN AND L. Y. JAN (1987) Cloning of

genomic and complementary DNA from *Shaker*, a putative potassium channel gene from *Drosophila*. *Science* 237: 749–753.

RANG, H. P. AND J. M. RITCHIE (1968) On the electrogenic sodium pump in mammalian non-myelinated nerve fibres and its activation by various external cations. *J. Physiol.* 196: 183–221.

SIGWORTH, F. J. AND E. NEHER (1980) Single Na^+ channel currents observed in cultured rat muscle cells. *Nature* 287: 447–449.

THOMAS, R. C. (1969) Membrane current and intracellular sodium changes in a snail neurone during extrusion of injected sodium. *J. Physiol.* 201: 495–514.

TOYOSHIMA, C., M. NAKASAKO, H. NOMURA AND H. OGAWA (2000) Crystal structure of the calcium pump of sarcoplasmic reticulum at 2.6 Å resolution. *Nature* 405: 647–655.

VANDERBERG, C. A. AND F. BEZANILLA (1991) A sodium channel model based on single channel, macroscopic ionic, and gating currents in the squid giant axon. *Biophys. J.* 60: 1511–1533.

WALDMANN, R., G. CHAMPIGNY, F. BASSILANA, C. HEURTEAUX AND M. LAZDUNSKI (1997) A proton-gated cation channel involved in acid-sensing. *Nature* 386: 173–177.

WEI, A. M., A. COVARUBIAS, A. BUTLER, K. BAKER, M. PAK AND L. SALKOFF (1990) K^+ current diversity is produced by an extended gene family conserved in *Drosophila* and mouse. *Science* 248: 599–603.

YANG, N., A. L. GEORGE JR. AND R. HORN (1996) Molecular basis of charge movement in voltage-gated sodium channels. *Neuron* 16: 113–22.

Books

AIDLEY, D. J. AND P. R. STANFIELD (1996) *Ion Channels: Molecules in Action*. Cambridge: Cambridge University Press.

ASHCROFT, F. M. (2000) *Ion Channels and Disease*. Boston: Academic Press.

HILLE, B. (2001) *Ion Channels of Excitable Membranes*, 3rd Ed. Sunderland, MA: Sinauer Associates.

JUNGE, D. (1992) *Nerve and Muscle Excitation*, 3rd Ed. Sunderland, MA: Sinauer Associates.

NICHOLLS, D. G. (1994) *Proteins, Transmitters and Synapses*. Oxford: Blackwell Scientific

SIEGEL, G. J., B. W. AGRANOFF, R. W. ALBERS, S. K. FISHER AND M. D. UHLER (1999) *Basic Neurochemistry*. Philadelphia: Lippincott-Raven.

